SYNTHESIS AND CHARACTERIZATION OF L-LYSINE BASED SEMIORGANIC NONLINEAR OPTICAL SINGLE CRYSTALS



Thesis of research work submitted to

Bharathidasan University, Tiruchirappalli in partial fulfillment of the requirements for the award of the degree of

DOCTOR OF PHILOSOPHY

IN

PHYSICS

By

Mrs. S. VARADARAJAN, M.Sc., B.Ed., M.Phil.,

(Ref.No.40357/Ph.D.K2/ Physics/Part-Time/January-2017/Date:28.12.2016.)

Under the Supervision of

Dr. M. SENTHILKUMAR, Ph.D.,

Assistant Professor of Physics



POSTGRADUATE & RESEARCH DEPARTMENT OF PHYSICS
GOVERNMENT ARTS COLLEGE (AUTONOMOUS)
KUMBAKONAM - 612002
TAMIL NADU, INDIA

MARCH -2022

Dr. M. SENTHILKUMAR

Assistant Professor

Department of Physics

Government Arts College(Autonomous)

Kumbakonam – 612 002, Tamil Nadu,India.

Phone: +91 4352412143 Cell: +91 9443411143

 ${\bf Email: msenthilprof@gmail.com}$

CERTIFICATE

This is to certify that the thesis work entitled "SYNTHESIS AND CHARACTERIZATION OF L-LYSINE **BASED** SEMIORGANIC **NONLINEAR OPTICAL SINGLE CRYSTALS"** submitted to Bharathidasan University, Tiruchirappalli, for the award of the degree of DOCTOR OF PHILOSOPHY IN PHYSICS, embodies the results of the bona fide research work carried out by Mr. S. VARADARAJAN under my guidance and supervision in the Department of Physics, Government Arts College (Autonomous), Kumbakonam – 612 002, Tamil Nadu, India, during the period 2017- 2022. I further certify that no part of the thesis has been submitted anywhere else for the award of any degree, diploma, associateship, fellowship or other similar titles to any candidate.

Place: Kumbakonam Dr. M. SENTHILKUMAR

(Research Supervisor)

Date:

Dr. M. SENTHILKUMAR

Date:

Assistant Professor
Department of Physics
Government Arts College(Autonomous)
Kumbakonam – 612 002, Tamil Nadu,India.

Phone: +91 4352412143 Cell: +91 9443411143 Email:msenthilprof@gmail.com

(Research Supervisor)

PLAGIARISM FREE CERTIFICATE

It is certified that the thesis "SYNTHESIS AND CHARACTERIZATION OF L-LYSINE BASED SEMIORGANIC NONLINEAR OPTICAL SINGLE CRYSTALS" submitted by Mr. S. VARADARAJAN, has been subjected to plagiarism check in the URKUND(CURIGINAL) software and found 9% significance, which is accepted 15% limit of Bharathidasan University guidelines(Under section 10.3). So, this is a plagiarism free thesis.

Place: Kumbakonam Dr. M. SENTHILKUMAR

S. VARADARAJAN

(Ref.No.40357/Ph.D. K2/ Physics/Part-Time/January-2017/Date:28.12.2016.)

Part-Time Research Scholar

Department of Physics

Government Arts

College (Autonomous)

Kumbakonam – 612 002

DECLARATION

I do hereby declare that the work presented in this thesis entitled as "SYNTHESIS AND CHARACTERIZATION OF L-LYSINE BASED SEMIORGANIC NONLINEAR OPTICAL SINGLE CRYSTALS" has been originally carried out by me under the guidance and supervision of Dr.M.SENTHILKUMAR, Assistant Professor, Department of Physics, Government Arts College (Autonomous), Kumbakonam – 612 002, affiliated to Bharathidasan University, Tiruchirappalli - 620 024and this work has not been submitted either in whole or in part for any other degree or diploma at any universities or research institutes.

Place: Kumbakonam (S. VARADARAJAN)

Date:

ACKNOWLEDGEMENTS

I would like to take this opportunity to express my thanks and gratitude to the many people who have in so many ways helped and supported me throughout my research work.

First and foremost I would like to express my profound gratitude to my research supervisor, **Dr. M. SENTHIL KUMAR, M.Sc., M.Phil., M.Ed., PGDCA., Ph.D.,** has been invaluable on both an academic and a personal level for which I am extremely grateful. I owe my deepest gratitude to my thesis supervisor for his constant and invaluable guidance during my research work. I am deeply indebted to him for his immense help, suggestions and the inspiring discussions during writing and completion of this thesis work. I am very much thankful to my supervisors for putting me in the track of this research.

I am very grateful to **Dr. K. DURAIARASAN**, Principal, Government Arts College (Autonomous), Kumbakonam – 612 002, for their encouragement and interest in carrying out the research.

I express my sincere thanks to **Dr.R.S.SUNDARARAJAN**, **M.Sc.**, **M.Phil.**, **Ph.D.**, **PGDCA.**, HOD of Physics, Government Arts College (Autonomous), Kumbakonam – 612 002, for their constant support, encouragement and providing the opportunity.

I sincerely acknowledge the suggestions and support given by my doctoral committee members **Dr. C. RAMACHANDRA RAJA, M.Sc.,M.Phil., M.Sc. (I.T), Ph.D.,** Associate Professor of Physics, Government Arts College (Autonomous), Kumbakonam – 612 002. **Dr. V. KARUNAKARAN, Ph.D.,** Assistant Professor of Physics PG & Research Department of Physics, Government Arts College Ariyalur.

I express my sincere thanks to **Dr. S. SHANMUGAN, M.Sc., M. Tech., Ph.D.,** Associate Professor of Physics, Koneru Lakshmaiah Education Foundation, Vijayawada, Andhra Pradesh, India, for his constant support, encouragement and providing the opportunity.

At this moment, I would like to express my special thanks to **Dr. S. SEKAR, Ph.D** Principal, Meenaakshi Ramasamy Arts and Science College, Thathanur for hir valuable suggestion, immense motivation and guidance for my research career.

I am very grateful to **Mr. M.R.RAHUNATHAN M.A.,ML., Correspondent**, Meenakshi Ramasamy Institution, Thathanur, Ariyalur - 621804, for his encouragement and interest in carrying out the research.

I thank **Dr.K.SUNDARESAN**, **M.Sc.,B.Ed.,Ph.D.**, Assistant Professor, PG Department of Chemistry, Meenaakshi Ramasamy Arts & Science College, Thathanur for his suggestions and, encouragement.

I am gratefully acknowledging the authorities of IIT Madras, SAIF Chennai for providing single crystal EDXRD, TEM, and Koneru Lakshmaiah Education Foundation, Vijayawada, Andhra Pradesh, for provide single crystalXRD, UV, FTIR, Raman characterization facilities. I sincere thanks to NIT, Trichy for extent to powder XRD facilities and Z-scan test, St. Joseph's College, Tiruchirappalli for permitting to spectral and optical studies. I would like to thank the Prof. P. K. Das, IISc, Bangalore for providing SHG testing facility, I express my sincere gratitude to SASTRA University, Thanjavur for giving me the opportunity to utilizing the TG/DTA facilities. I extend my sincere thanks to all the teaching and non-teaching staff members of the Department of Physics, Government Arts College, Kumbakonam for their support.

Lastly and most importantly my wholehearted thanks to my **parents**, **families** and my **friends** without whom's encouragement for their co-operation and blessings which gave me a super natural power to face the problems and solve them with confidence.

CONTENTS

Chapter		Page No
No.	Title	
I	Principles of Crystal Growth - Iintroduction	1
	1.1 Introduction	1
	1.2 General classification of crystal Growth Methods	2
	1.2.1 Melt growth	2
	1.2.2 Bridgman technique	2
	1.2.3 Czochralski Technique	3
	1.2.4 Kyropoulos Technique	3
	1.2.5 Zone melting Technique	3
	1.2.6 Verneuil Technique	4
	1.2.7 Vapour Growth	4
	1.2.8 Growth by slow cooling	5
	1.2.9 Top Seeded Solution Growth	5
	1.2.10 Hydrothermal Growth	5
	1.2.11 Low Temperature Solution Growth	6
	1.2.12 Slow Cooling Method	6
	1.2.13 Slow Evaporated Method	6
	1.2.14 Temperature gradient Method	7
	1.2.15 Growth from Solution	7
	1.2.16 Gel Growth	8
	1.3 Importance of non-linear optical crystals	8
	1.4 Definition of the Problem	Q

	Based on recent review articles of l-lysine materials:	11
	1.6 Scope of the Research Work	12
	1.7 Methodology	13
	Reference	15
II	A new class single crystal L-lysine hydrogen chloride(LLHC)	17
	for optoelectronic applications	
	2.1 Introduction	17
	2.2 Experimental Techniques	18
	2.2.1 Solubility test	18
	2.3 LLHC single crystals Growing process	19
	2.4 Results and discussion	20
	2.4.1 LLHC characterization studies on X-ray powder	20
	diffraction Evaluation	
	. 2.4.2 LLHC analysis of FTIR-FT-Raman spectra	21
	2.4.3 LLHC crystal analysis of NMR process	24
	2.4.4 LLHC crystal analysis of thermal process	25
	2.4.5 LLHC crystal analysis of Vicker's micro hardness	26
	2.4.6 LLHC crystal analysis of transmission spectra	27
	2.4.7 LLHC crystal analysis of NLO assessment	28
	2.5 Conclusion	28
	Reference	29

III	Growth and investigation on novel single crystal of	31
	β-cyclodextrin 2, 4- dinitrophenylhydrazine for optical	
	sensors applications	
	3.1 Introduction	31
	3.2 Result and Discussion	32
	3.2.1. Single crystal X-ray Diffraction	32
	3.2.2 Powder X-ray Diffraction Analysis	32
	3.3. Results and discussion	33
	3.3.1 Single Crystal X-ray diffraction	33
	3.4 Nonlinear optical studies	37
	3.5. Conclusions	39
	Reference	41
IV	Growing, Characteristics on L-Lysine hydrogen chloride -	45
	Tartaric Acid (LHCTA), single crystal for optoelectronic	
	applications	
	4.1 Introduction	45
	4.2 Experimental Technique	46
	4.2.1 Solubility test	46
	4. 3. Result and Discussion	48
	4. 3.1 LLHC Characterization studies on X-ray powder	48
	diffraction evaluation	
	4.3.2 LLHC analysis of FTIR-FT- Raman Spectra	48
	4.3.3 LLHC crystal analysis of NMR process	51
	4.3.4 LLHC crystal analysis of thermal process	52
	4.3.5 LLHC crystal analysis of Vicker's micro hardness	53

	4.3.6 LLHC crystal analysis of transmission spectra	54
	4.3.7 LLHC crystal analysis of NLO assessment	55
	4.4 Conclusion	55
	Reference	56
V	Synthesis and Characterization of L-Lysine - Lithium sulfate	60
	- Citric Acid (LLCA)grown on single crystal for NLO	
	materials: An Experimental for slow evaporation techniques	
	5.1 Introduction	60
	5.2 Materials and Experimental Methodology	61
	5.2.1 Characterization of L-Lysine single crystal	63
	5.3 Results and Discussion	63
	5.3.1 The analysis of X-ray diffraction	63
	5.3.2 Solubility test of doped LMOL single crystals:	64
	5.3.3 FTIR analysis of LMOL single crystals	65
	5.3.4 LMOL Crystals analysis of Optical Transmission	66
	5.3.5 Assessment of optical Energy	67
	5.3.6 LMOL crystal analysis of Vicker's microhardness:	68
	5.3.7 Z-scan Studies	70
	5.3.8 Optical limiting studies	72
	5.3.9 LMOL Crystals analysis of Nonlinear optical	74
	5.3.10 LMOL Crystals analysis of TG - DTA	74
	5.4 Conclusion	76
	Reference	78

VI	Growth and characterization of L-Lysine Doping with effect	80
	of hydrochloride Citric Acid - Glycine Barium Chloride	
	(LHCAGBC)on the grown single crystals for optical sensor	
	applications	
	6.1 Introduction	80
	6.2. Materials and Experimental Methodology	81
	6.2.1 Synthesized of the L-Lysine doped crystal growth	81
	6.2.2 Characterization analysis of pure L-Lysine and Co-Doped	82
	with effect of single crystals	83
	6.3 Results and Discussion	83
	6.3.1 Pure L-Lysine and Co-Doped Single Crystal Powder XRD analysis	
	6.3.2. Pure L-Lysine and doped samples analysis of FTIR studies	84
	6.3.3. Pure L-Lysine and doped samples analysis of Optical	85
	Transmission studies	
	6.3.4 Pure L-Lysine and doped samples analysis of Nonlinear	87
	optical studies	
	6.3.5 Pure L-Lysine and doped samples analysis of TG - DTA	88
	studies	00
	6.4 Conclusion	00
	Reference	90
		91
	Overall Conclusion	93
	Bibliography	95

PREFACE

The development of the science in the field of solid state and material scienceneeds a good quality single crystal. There is an ever increasing demand of crystals due to its potential application in many fields. As per the demand, a large variety of crystalsare grown from various techniques. In general, semi-organic crystals have great focus due to the design flexibility in molecular compounds, possessing nonlinear optical behavior of the materials. L-Lysine with organic compounds have nonlinear optical applications, and are widely used in the area of laser technology, optical communications, harmonic generators and data storage technology. The thesis aims at growing organic, semiorganic and L-Lysine crystals for optical applications. The dissertation contains Six chapters.

Chapter – I

Principles of Crystal Growth - Introduction

Introduces the crystal growth methods in different types of crystal growth methods with a brief discussion on slow evaprotation solution technique. This chapter ends with aim and scope of the research work.

The deals with nonlinear optical phenomenon, organic, inorganic and semiorganic crystals. This chapter also includes the L-Lysine based crystals and applications of NLO crystals are given in this chapter.

Chapter - II

A new class single crystal L-lysine hydrogen chloride (LLHC) for optoelectronic applications

Growth and characterization of L-Lysine hydrogen chloride (LLHC) crystal have been studied. The Molecular geometry shows good agreement with Experimental and Theoretical (HF and DFT) bond lengths and bond angles. From X-ray diffraction studies it is observed that TGA and DTA have been approved out in nitrogen atmosphere at a heating rate of 20°C/min from 0°C to 1000°C. Vibrational assignments of TDA crystal is discussed by FT-IR and FT-Raman spectroscopic studies.

Chapter – III

Growth and investigation on novel single crystal of b-cyclodextrin 2, 4-dinitrophenylhydrazine for optical sensors applications

Nonlinear optical (NLO) 2, 4-Dinitrophenylhydrazine (DNPH) single crystal has been grown by Slow Evaporation Solution Technique. The experiments are carried out to study the structural, optical, thermal and nonlinear optical properties of the grown crystals.

The XRD grades are in good covenant with the described values. The good quality grown of LYTAPB single crystals have been exposed to various characterization study in direction to assess the mechanical, structural and optical, thermal, dielectric properties of the material. FTIR, Optical properties, UV–Vis NIR, from EDAX analysis, micro hardness structure, SEM, SHG and involved by an optical microscope.

Chapters – IV

Growing, Characteristics on L-Lysine hydrogen chloride (LLHC) single crystal for optoelectronic applications

Growing, Characteristics on L-Lysine hydrogen chloride grown on single crystal for optoelectronic materials: An Experimental for slow evaporation techniques. FT-IR, FT-Raman, NMR spectra, UV-Vis absorption spectra, TG-DTA and X-ray diffraction is reported. The chemical formula for L-LMHClCA is C₁₃H₂₅N₂O₁₀. The results showed no significant geometrical differences like distances Thermal, Dielectric, Micro hardness, SEM.

Chapter – V

Growth and characterization of L-Lysine Doping with effect of hydrochloride Citric Acid - Glycine Barium Chloride (LHCAGBC) on the grown single crystals for optical sensor applications

Single crystals of L-Lysine Doping with effect of hydrochloride Citric Acid - Glycine Barium Chloride (LHCAGBC) have been grown by slow evaporation solution growth method. Harsh environments to control through the L-Lysine single crystal has arranged of the crystalline advantages of good performance of the structure, compact, convenient to investigation of results following in crystal XRD, FTIR, UV-vis-NIR, TGA and DTA.

Chapter – VI

Synthesis and Characterization of L-Lysine - Lithium sulfate - Citric Acid (LLCA) grown on single crystal for NLO materials: An Experimental for slow evaporation techniques

L-Lysine -Lithium sulfate - Citric Acid (LLCA)single crystal has been developed by the novel organic nonlinear optical (NLO) materials. The L-Lysine with CA has been grown of the crystal by the controlled for the solution to slow evaporation techniques. It is used in XRD, FTIR spectrum to conform with the crystal structure. The morphology studies are doped solutions to varying rates of reflected in form of XRD values

Chapter - VII

To summarizes the results obtained from various characterizationstudies carried out on the grown crystals. It also includes the comparison of these results and discusses the suggestion for future work.

CHAPTER - 1

PRINCIPLES OF CRYSTAL GROWTH

1.1 Introduction

Crystal growth is one of the frontier areas of today's science and technology. In recent years the research in crystal growth has proved the commercial importance of crystals and their significance. Today's modern technology is largely based on semiconductors, ferrites, magnetic garnets, solid state laser materials, ultraviolet and infrared sensitive crystals and crystalline films. In health sciences crystals play an important role since some of the diseases are mainly due to crystal depositions in kidney, urinary bladder and gallbladder as shown in

Fig.1.1

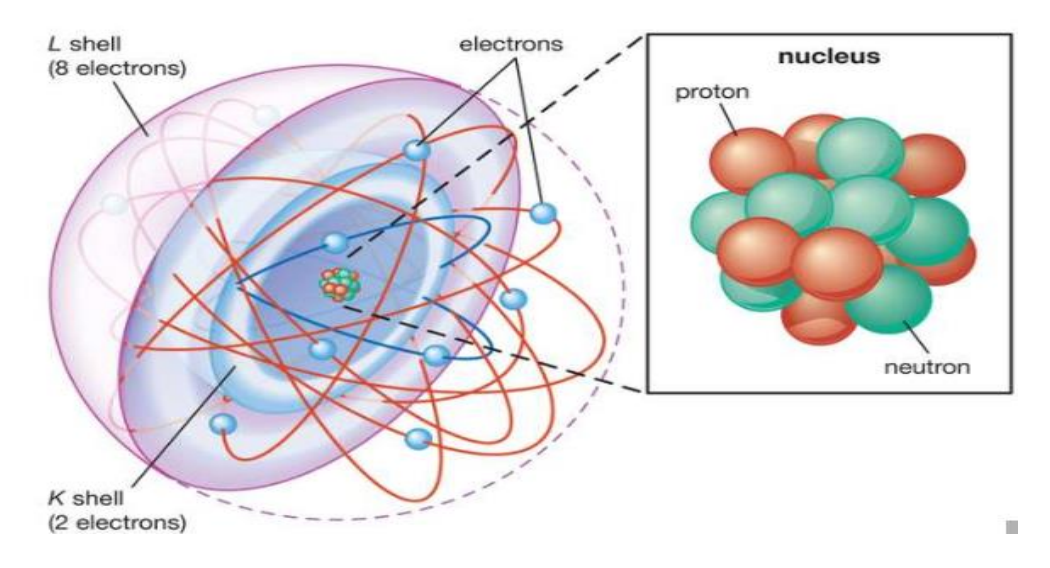


Fig. 1.1 Show the crystals play an important role.

The single crystals take part in the development of electronic industry, solid state technology, laser and electro optical engineering, communication systems and computer industries. They are also much useful in our daily life such as electronic devices in telecommunication network, frequency controlling devices for electromagnetic waves, solar cells, radiation detectors and devices in semiconductor applications. So, the understanding of crystallization process in essential both in modern technology and in medicine. A crystal is the regular

polyhedral form, bounded by smooth surfaces, which is assumed by a chemical compound, under the action of its inter atomic forces, when passing from the state of a liquid or gas to that of a solid under suitable conditions or a crystal is a homogeneous, anisotropic body having natural shape of polyhedron.

1.2 General classification of crystal Growth Methods

Depends upon the nature of the starting material the growing methods are generally classified into different methods. The techniques involved in different methods are explained as follows:

1.2.1 Melt growth

Melt growth can be applied to solids which can be melted and crystallized by the change in phase from liquid to solid. Growth from the melt is the fastest of growth methods as its rate does not depend on the mass transport processes. In this method, apart from possible contamination from crucible materials and the surrounding atmosphere, no impurities and introduced in the growing crystal.

1.2.2 Bridgman technique

The easiest and inexpensive melt growth technique is normal freezing a molten in got is gradually frozen from one end to the other. When this is achieved by the use of a two Zone furnace, it is called Bridgman - stock Barger technique. The usual configuration is vertical with the melt is an ampoule being lowered slowly from the hot zone to the cooler zone which is below the melting point. Large metal single crystals as well as Optical quality alkali halide crystals fro prisms and lenses were grown by the technique. For fast growth, the materials to be grown should melt congruently, i.e. the melt and crystal should have the same composition. A crystal which adheres strongly to the crucible is undesirable. To keep the technology simple, materials with high vapour pressures should be avoided by systems

capable of withstanding internal pressure of 200 atmospheres at 180^{0} c have been used. Neither the liquid not its vapour must attack the crucible significantly.

1.2.3 Czochralski Technique

Among the many crystal growth methods are in sue today, one method which can produce crystal weighing from several grams to many kilograms is the crystal pulling technique. All crystal pulling processes are based upon a technique developed by Czochralski in 1918. This technique and its various modifications have become in the dominant processes used in the industry today for the production of semiconductor and oxide single crystals. The standard materials² which are Si, Al₂O₃, GaP, GaAs, InP, Ge and LiNbO₃.

1.2.4 Kyropoulos Technique

In this technique, the crystal can be grown to a larger diameter. So this method is more suitable for the growth of crystals with longer diameter used in the fabrication of windows, prisms, lenses and other optical components. Same as that in Czochralski growth here also the seed is brought into contact with the melt, and is not raised much during the growth period, i.e. the part of the seed is allowed to melt and a short narrow neck is grown. After this, the vertical motion of the seed is stopped and growth continues by decreasing the lower input to the melt. This technique is mainly useful for the growth of alkali halides used in many optical devices, mostly for long wavelength application.

1.2.5 Zone melting Technique

In the zone melting techniques, a liquid zone is created by melting small amount of materials in a relatively large or long solid charge. Then it is made to traverse through a part of the whole of the charge. This is the more advantageous method than other methods due to the removal or addition of impurities from or to the crystal as the crystal is growing. In this method, the rate of zone movement depends of the orientation of the two solids binding the liquid zone as well as the thickness and temperature of the zone.

1.2.6 Verneuil Technique

Verneuil announced this technique in 1902 and gave a full description. In the technique, an Oxy hydrogen flame is produced and it is used to heat the seed crystal. The powder to be crystallized is allowed to fall on to this flame through sleeve, using the vibrator at a low amplitude. The powder melts in the flame, and if the condition have been set correctly, a film of melt forms on the surface of the sleeve. During growth the sleeve is lowered. The volume of the growth rate depends on the rate of lowering. By appropriate adjustments, the crystal diameter can be changed. A large number of materials with his melting points and for example ZrO₂ (2700°C) etc., have been grown as single crystals by this method.

1.2.7 Vapour Growth

Single crystals of high perfection can be grown from the vapour growth method by sublimation and chemical vapour deposition techniques. The crystals like Cds. Al₂O₂ and Hgl₂ can be grown by this technique. This vapour growth is subdivided into two methods.

- * Physical Vapour Transport (PVT)
- * Chemical Vapour Transport (CVT)

(i) Physical Vapour Transport

This is the simplest and only pure vapour growth method. It has been used recently for the production of high-quality bulk crystals of materials like Cds and HgI₂.

(ii) Chemical Vapor Transport

Chemical Vapour Transport methods are widely used in the growth of new semi conducting, insulation and magnetic crystals. For example, small crystals of adamantine were grown in sealed quartz ampoules when about 5 mg/cc if I₂ are added to a powered charge of the compound in Vacuum. Crystals grow at the cold end of the tube.

1.2.8 Growth by slow cooling

A saturated solution prepared by keeping the crucible containing flux and the crystal constituents are maintained just above the saturation temperature as far as to ensure the total dissolution of the solute. After that the crucible is cooled by the rate of 0.5 C/hour to 5 C/hour through a long temperature range, where the desired crystal is known to precipitate, the crucible is cooled to room temperature. The crystals like BaTiO₃, KTP and KTN are being grown by this technique.

1.2.9 Top Seeded Solution Growth

In this method, the crystal is grown at the surface of the melt when the temperature at the surface is lower than the temperature at the bottom. The temperature gradient should be maintained as small and the growth temperature has to be continuously lowered by slow cooling of the melt.

1.2.10 Hydrothermal Growth

Hydrothermal growth is the growth of crystal from aqueous solution at high temperature and pressure. A number of metals, metal oxides and the compounds which are practically insoluble in water up to its boiling point, show an appreciable solubility when the temperature and pressure are increased well above 100°C and one atmosphere respectively. Growth is usually carried out in steel autoclaves with Gold or Silver linings the liquids from which the process starts are typically in the range 400°C to 600°C and the pressure in involved in the range of hundreds or thousands of the atmosphere. The requirements of high pressure present practical difficulties and there are only few crystals of good quality and large size can be grown by the technique. Quartz is the crystal being grown industrially by this technique.

1.2.11 Low Temperature Solution Growth

At least 90% of all crystals produced by low temperature solution methods are soluble in water. In its commercial from, low temperature solution growth⁴ involves run time measured in weeks or months. Low temperature solution growth can be subdivided into three following categories.

- * Slow Cooling Method
- * Slow Evaporation Method
- * Temperature Gradient Method

1.2.12 Slow Cooling Method

The use of slow cooling is the earliest method for the growth of crystals from solution. Its main disadvantage is the need to use a range of temperature. The possible range is usually small so that much of the solute remains in the solution at the end of a growth run. To compensate this effect, large volumes of solution are required. The use of a range of temperature may also not be desirable, because the properties of the grown material may vary with temperature and the amount of solute incorporated will almost certainly vary. Though this method has the technical difficulty of requiring a programmed temperature control, it is widely used with great success.

1.2.13 Slow Evaporated Method

This method is similar to the slow cooling method in view of the apparatus requirements as shown in Fig.1.2. The temperatures are fixed constant and provision is made for evaporation with nontoxic solvents like water, it is permissible to allow evaporation into the atmosphere. Typical growth condition involves temperature stabilization to about plus or minus 0.001°C and rate of evaporation of a few mm³/hr. The evaporation techniques of crystal growth have the advantage that the crystals grow at a fixed temperature, but inadequacies of the temperature control system still have a major effect on the growth rate.

This method is the only one which can be used with material having very small temperature coefficient of solubility. (5)

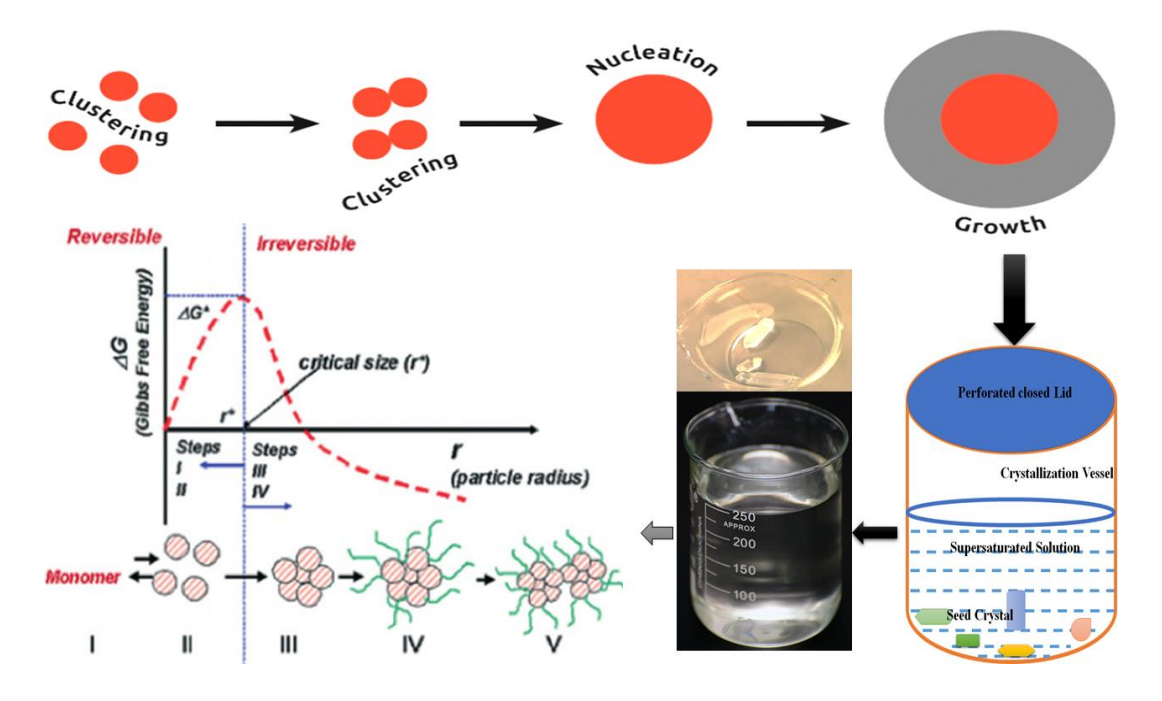


Fig. 1.2 show slow evaporation growth on single crystal method.

1.2.14 Temperature gradient Method:

In this method the process which involves is transport of the materials from a hot region containing the source material to be grown to a cooler region where the solution is supersaturated and the crystal grows. The main advantageous of this method are economy of solvent and solute, Crystal grows at fixed temperature. This method is insensitive to change in temperature provided both the source and the growing crystal undergo the same change. On the other hand, changes in the small temperature difference between the source and the crystal zones have a large effect on the growth rate of crystal. In general, there are two methods of crystal growth coming under this category.

1.2.15 Growth from Solution:

It is the simple and oldest method and it has many advantages over the melt growth, through the rate of crystallization is very slow. Crystals will be grown from solution, if the solution is supersaturated. i.e. if the solvent contains more of the solute than it can be in

equilibrium that are used to produce the required supersaturation. By using this method of growth, organic inorganic, sugar and excellent quality crystals of Ferro - electric and piezo-electric materials such as Potassium Dihydrogen Phosphate (KDP) Ammonium Dihydrogen Phosphate (ADP) and Semi organic crystals like potassium Acid Phathalate (KAP), Triglycine Sulphate (TGS) and important organic nonlinear crystals such as NMBA, MNA, etc., are commercially grown. This method of crystal growth will be discussed elaborately n chapter III.

1.2.16 Gel Growth:

Crystal growth is gels are an intermediate process between growth from solid and growth from solutions. This method relied on reaction and precipitation of species diffusing in gels. Gel growth technique is a simple and elegant method of growth of single crystals under controlled growth at room temperature. Growth in this method is limited by diffusion process. By using this method of growth, crystals, or organic inorganic Ferro electric and Piezo electric materials can be grown.

1.3 IMPORTANCE OF NON-LINEAR OPTICAL CRYSTALS

Lysine is one of nine essential amino acids in humans required for growth and tissue repair, Lysine is supplied by many foods, especially red meats, fish, and dairy products. Lysine seems to be active against herpes simplex viruses and present in many forms of diet supplements. Over the past three decades, Nonlinear optics (NLO) has emerged as one of the most attractive fields of current research in view of its vital applications in areas like optical modulation, optical switching, optical logic, frequency shifting and optical data storage for developing technologies in telecommunications and signal processing. Organic materials have been demonstrated in recent years to possess superior second and third order NLO properties compared to the more traditional inorganic materials. Organic materials have attracted much attention because the NLO responses in this broad class of materials is

microscopic in origin, offering an opportunity to use theoretical modeling coupled with extremely synthetic flexibility to design and breed new materials. The properties of organic compounds can be refined using molecular engineering and chemical synthesis. The complex sympathetic of the structural, electronic reply to the properties of NLO materials are developed in expansively to equally from theoretically and experimentally improving the quantum chemical density functional theory (DFT) method through the vibrational spectroscopy.

The art research goal, L-Lysine crystals have been grown to observer the optical nature and depending on the optical property the grown L-Lysine crystal can be subjected for its application-oriented means. The grown L-Lysine crystal in subjected to linear and nonlinear optical studies to find its absorbance or transmittance property. The same is checked by the nonlinear study, which confirms whether the L-Lysine crystal possesses the nonlinear nature. This property L-Lysine crystals can be used for long distance communication and transfer of energy without any loss.

1.4 Definition of the Problem

The technological development to a larger extent is dependent on the development of crystal growth. Crystal growth, which had been a relatively small area in the field of material science, now enjoys a unique status owing to recent development of novel materials with user defined properties. Crystal growth, demands collaboration of physicists, chemists, chemical and process engineers, electrical and mechanical engineers, instrumentation engineers, material scientists, crystallographers, etc. The growth of single crystals has become inevitable for any further developments in materials science research. Non-linear materials such as Urea, KTP, BBO, KDP, ADP and LAP are investigated widely for their potential application and devices. Among the various methods of crystal growth, low temperature solution growth is practiced next to melt growth. The solution growth can be considered as a superior method

because good optical transparency of crystals and uniform mixing of dopant in the lattice are achievable easily. However, the disadvantages are due to the slow growth rate and container problem. In order to grow good quality large single crystals by solution growth method, the materials should have high solubility and variation in solubility with temperature.

In the present investigation, some organic nonlinear optical crystals have been grown by slow evaporation solution growth technique at room temperature. Single crystal X- ray diffraction analysis has been done to determine the structure properties like cell parameters, Molecular geometry, Intra & Intermolecular properties. Hirshfeld surfaces analysis has been performed to reveal the nature of intermolecular interactions. The positions and the strengths of intermolecular interactions were visualized. UV-Vis-NIR spectra have been recorded for the grown crystals in the range from 190 nm to 1100 nm to know the transparency and UV cut-off wavelength of the crystals. Fourier transform infrared spectrum (FT-IR) and Fourier transform Raman spectrum (FT-Raman) has been recorded to analyze the vibrations of functional groups present in the grown organic crystalline material. The thermogravimetric analysis (TGA), differential thermal gravimetric (DTG) and differential scanning calorimetric (DSC) studies show the thermal stability and decomposition behavior of the crystals. The third-order nonlinear optical properties of the grown crystal were studied by Z-scan technique. The nonlinear refractive index (n₂), nonlinear absorption coefficient (β) and nonlinear susceptibility (χ^3) were evaluated. The Quantum chemical calculations are done to compute the molecular geometry like bond length and bond angle values, HOMO-LUMO calculations are carried out to find the energy gap value of all organic crystal studied in the present investigation and TD-DFT calculations are done to get the Theoretical UV-Vis spectrum with Gaussian-09W program using the TD-DFT/6-31++G(d,p) basis set.

1.1 Table BASED ON RECENT REVIEW ARTICLES OF L-LYSINE MATERIALS

S. No.	Name of the Authors	Year	Materials	Inferences
1	Mahadevan <i>et al</i> . [1]	2014	L-Lysine 4- nitrophenolate monohydrate	wavelength - 481 nm and SHG efficiency is 4.45 and 1.4 time shigher than of KDP
2	Aneeba et al. [2]	2020	Pure and K+ ion doped L- Lysine monohydrochl oride (L- LMHCL)	Highest dielectric constant an antibacterial activity against certain bacteria
3	Gnanaraj <i>et al</i> . [3]	2018	L-Lysine doped Oxalic acid	Optical Constants, phase matchable and exhibit self-defocusing behavior.
4	Khan et al. [4]	2018	L-lysine (LL) influenced cadmium thiourea acetate (CTA)	Improved optical quality, transmittance, dielectric properties, SHG efficiency of LL-CTA is 2.18×(KDP) and 1.78×(CTA).
5	Ramya et al., [5]	2017	L-Lysine adipate - Liquid diffusion method	The material possesses a wide transparent range, FTIR, FT Raman spectra, optical property, and thermal property up to 205°C.
6	Febena et al., [6]	2019	Glycine Lithium Sulphate (GLS)	A single crystal with dimension is 10 x 11 x 12 mm ³ . A strong intermolecular hydrogen bonding in the molecule is confirmed. Nonlinear optical absorption is 633 nm and Z-scan technique.
7	Alexandar and Rameshkumar [7]	2018	Nicotinium tartrate (NT) and L-tartaric acid nicotinamide (LTN)	Optical microscope, dielectric constant, polarizability values are higher. The third order NLO parameters such as nonlinear refractive index (n_2) , nonlinear absorption coefficient (β) , and third order susceptibility (χ^3) closed aperture Z-scan techniques using He-Ne laser for the first time.

8	Jayaprakash <i>et al.</i> , [8]	2018	4- chloroaniliniu m-l-tartrate monohydrate (4CALTM)	The SHG was 1.5 times greater than that of KDP, phase-matchable. which is used of 65% transparency with visible region and soft material.
9	Sun et al., [9]	2008	L-Lysine acetate	structure analysis space group P21, with cell parameters: a=5.420(2) Å, b=7.542(4) Å, c=12.653(1) Å, β=91.73(1)°, Z=2 and V=516.8 Å3 and thermal properties also is good acts.
10	Wang et al., [10]	2016	L-Lysine (Lly) and p-toluene sulfonic acid (pTS) (LLTS)	Slow cool technique, Good transparency, melting point of fairly high, at around 259 °C.
11	Helen and Kanchana [11]	2014	pure and metal ions (K+, Na+ and Li+) doped l-serine	EDAX, ICP-OES, XRD studies are good results.FTIR and FT-RAMAN analyses, TGA,DSC, thermal stability, mechanical properties of lithium doped l-serine crystal are enhanced. The percentage of transmission is increased in lithium doped l-serine crystals.
12	Neelam Rani et al., [12]	2013	L-lysine acetate	The monoclinic system is space group of P ₂₁ . It is high of HRXRD. The 13C NMR, 1H NMR and FTIR, Optical studies are wavelength of 236 nm and band gap was 5.29 eV. The electrical properties, an optical band gap is 5.29 eV. The thermal properties were studied in photopyroelectric technique. Vickers micro hardness studies were used in Vickers hardness.

1.6 Scope of the Research Work

Product concentration, drying and grown by slow evaporation techniques. The L-Lysine doped from the ion-exchange columns is mixed with different acid from the product-filtration step and concentrated by slow evaporation. The concentrated L-Lysine solution is doped Tartaric Acid-Potassium Bromide, Citric Acid, hydrochloride Citric Acid, Malic acid - Oxalic acid - Lithium sulfate, Glycine Barium Chloride and free L-Lysine is

grown to L-lysine single crystals. The doped L-Lysine solution is then sent to the crystallizer and low temperature grown on L-Lysine single crystal.

Opinion of the possible to concentration in nonlinear optical crystals, the contemporary study has been designed at the

- 1.6.1 Synthesis and growth of single crystals of
 - (a) L-Lysine Monohydrochloride Dihydrate (LMHCl)
 - (b) L-Lysine Tartaric Acid-Potassium Bromide (LTAPB),
 - (c)L-Lysine monohydrochloride Citric Acid (LMCA),
 - (d)L-lysine Malic acid ($C_4H_6O_5$) /Oxalic acid ($C_2H_2O_4$)/ lithium sulphate (Li_2SO_4) (LM),
 - (e)L-Lysine with and without Co-Doped Glycine Barium Chloride (GBC)/ $C_6H_{14}N_2O_2$ (Amino acid) (LGBA),
- 1.6.2 Characterization of the grown crystals to investigation their structural, optical, thermal, DFT, spectral and nonlinear optical properties.

1.7 Methodology

Crystal growth process and size of the grown crystal differ widely and are determined by the characteristics of the material (Buckley 1951; Mullin 1976). The principal methods of crystal growth can be classified as follows

- 1. Growth from melt
- 2. Growth from vapour
- 3. Growth from solution

There are number of growth methods in each category. Fig. 1.3 as the method of slow evaporation solution growth technique at room temperature occupies a prominent place owing to its versatility and simplicity.

Perforated closed Lid Crystallization Vessel Supersaturated Solution Seed Crystal

Fig. 1.3 show slow evaporation experimental process.

This solution growth procedure is based on the use of solvent due to its relatively high solubility of reactants. Analytical grade chemicals were used for initial synthesis process, then it is dissolved in solvents ethanol and stirred continuously for few hours to get the saturated solution depends on solubility range of the synthesized material. The saturated solution may contain impurities such as solid and dust particles and therefore it was filtered using Whatmann filter paper. Then the filtered solution was covered by polythene paper in which very few holes were made for controlled evaporation of ethanol. This solution was transferred to glass beaker and crystallization was allowed to take place by slow evaporation at room temperature. As a result of slow evaporation of solvent, the excess of solute which got deposited in the beaker resulted in the formation of crystals. After some period, colorless and transparent single crystals have been harvested. The grown crystals were characterized using various techniques such as Single crystal X-ray diffraction, Molecular geometry, UV-Vis-NIR spectrum, FT-IR, FT-Raman, thermal analysis, Theoretical DFT studies and NLO studies. A brief outline on various important techniques of crystal growth has been presented below

References

- [1] M. Mahadevan, M. Magesh, K. Ramachandran, P. Anandan, M. Arivanandhan, Y. Hayakawa, Synthesis, growth, crystal structure and characterization of a new organic NLO crystal: L-Lysine 4-nitrophenolate monohydrate (LLPNP), Spectrochimica Acta Part A: Molecular and Biomolecular Spectroscopy Volume 130, 15 September 2014, Pages 416-422.https://doi.org/10.1016/j.saa.2014.04.033.
- [2] B.Aneeba, S.V.AshvinSanthia, S.Vinu, R. Sheel, ChristyaDuni, A.A Farraj, NoorahA.Alkubaisi, Influence of most reactive inorganic cation in the optical and biological activities of L-Lysine monohydrochloride crystal. Saudi Journal of Biological Sciences Available online 18 July 2020.https://doi.org/10.1016/j.sjbs.2020.07.018.
- [3] J. Martin Sam Gnanaraj, M. IniyaPratheepa, M.Lawrence, L-Lysine doped Oxalic acid single crystals A potential phase matchable organic material for optical limiting applications. Optics & Laser Technology Volume 107, November 2018,

 Pages478-483.https://doi.org/10.1016/j.optlastec.2018.05.045
- [4] Imran Khan, Mohd Anis, Umar Bhati, Influence of l-lysine on optical and dielectric traits of cadmium thiourea acetate complex crystal. Optik Volume 170, October 2018, Pages 43-47. https://doi.org/10.1016/j.ijleo.2018.05.076.
- [5] K.Ramya, N.T.Saraswathi, C. Ramachandra Raja, Growth and characterization of L-Lysine adipate crystal. Optics & Laser Technology Volume 90, 1 May 2017, Pages 222-225. https://doi.org/10.1016/j.optlastec.2016.12.002
- [7] A.ShinyFebena, M.Victor Antony Raja, J.Madhavan, Systematic Investigation and Applications of an Efficient NLO Crystal: Glycine Lithium Sulphate. Materials Today: Proceedings Volume 8, Part 1, 2019, Pages 427-434. https://doi.org/10.1016/j.matpr.2019.02.132

- [8] A. Alexandar, P.Rameshkumar, Nucleation, growth, dielectric, polarizability, and Z-scan analysis of nicotinium tartrate & L-tartaric acid nicotinamide singlecrystals for third order NLO application: A comparative study Optik Volume 168, September 2018,Pages944-955.https://doi.org/10.1016/j.ijleo.2018.04.100
- [9] Jayaprakash Jeyaram. Krishna kumar Varadharajan, BoobasSingaram Ranjith Rajendhran, Growth and characterization of organic second order nonlinear optical (NLO) 4-chloroanilinium-l-tartrate monohydrate single crystals. Journal of Crystal Growth Volume 486, 15 March 2018, Pages 96-103. https://doi.org/10.1016/j.jcrysgro.2018.01.015
- [10] Z.H.Sun, G.H.Zhang, X.Q.Wang, X.F.Cheng, X.J.Liu, L.Y.Zhu, H.L.Fan, G.Yu, D.Xu, Growth and characterization of the nonlinear optical single crystal: 1-lysine acetate. Journal of Crystal Growth Volume 310, Issue 11, 15 May 2008, Pages 2842-2847. https://doi.org/10.1016/j.jcrysgro.2008.02.026
- [11] L.Wang, D.H.Wang, G.H.Zhang, D.Xu, W.X.Deng, Crystal structure, spectroscopic investigation and thermal properties of l-lysine p-toluenesulfonate. Journal of Molecular Structure Volume 1108, 15 March 2016, Pages 179-186. https://doi.org/10.1016/j.molstruc.2015.11.019
- [12] F.Helen, G.Kanchana, Growth and characterization of metal ions doped l-serine NLO single crystals for optoelectronic applications. Optik Volume 125, Issue 9, May 2014, Pages 2051-2056. https://doi.org/10.1016/j.ijleo.2013.09.084.

CHAPTER - 2

A NEW CLASS SINGLE CRYSTAL L-LYSINE HYDROGEN CHLORIDE (LLHC) FOR OPTOELECTRONIC APPLICATIONS

2.1 Introduction

These days, the applications in optoelectronics and photonics depend on nonlinear optical materials highly fundamental to substantially more than different materials [1]. The natural materials are deftly planned of sub-atomic dynamic that NLO crystals and stood out in light of the minimal expense required for applications utilizing reasonable contributor (donor) and acceptor. The gigantic optical nonlinearity is grown almost too unique properties of organic crystals, which is being used in low profile off frequencies in the UV locale. Along these lines, organic NLO crystals are needed for use in the use of optical gadgets. The feeble van der Waals are frequently planned as organic material. Hydrogen bonds subsequently have a severe level of delocalization. However, these organic crystals have specific limitations, such as poor mechanical and thermal stability. To overcome these problems, researching a combination of organic and inorganic hybrid compounds leads to finding a new class of materials for electronic industries, called semi-organic materials. The organic ligand is ionically bonded with an inorganic host; thus, the new semi-organic crystals have higher mechanical strength and chemical stability [2]. The amino acids are assuming a crucial part of nonlinear optical crystal development for a few specialists. The characteristic amino acids are separately showing nonlinear optical properties. They are a donor NH₂, acceptor COOH; likewise, intermolecular charge move is conceivable [3]. Particularly regular amino acids are aspartic, glutamic, just as arginine, lysine, 1-alanine [4]. The γ -glycine [5] was clearly showing NLO movement. It has resulted in the light of first in COOH group and NH₂ group an extra is developing of that materials. The dopant with amino acids materials [6-8] is improved by the material properties of nonlinear optical, ferroelectric properties also

applications. The semi-organic mixtures are organized with L-histidine tetrafluoroborate, L-arginine diphosphate single crystals. They are described for [9-10] with decently high mechanical and chemical solidness.

The capacity to utilize potential semi-organic materials has been developed the single crystals and the nonlinear optical properties of L-Lysine hydrogen chloride (LLHC - C₆H₁₅ClN₂O₂) with atomic weight of 182.65 and Parent Compound CID 5962 with creating strategy for slow evaporation solution growth method at environmental conditions. The crystallizes of LLHC in a monoclinic crystal structure in the space group of P2₁2₁2₁. The new crystals are affirmed that investigations of XRD and FT-IR analyzer are investigated in optical, thermal, and mechanical properties. The LLHC single-crystal outcomes are discussed and introduced in a component in the ensuing parts.

2.2 Experimental Techniques

2.2.1 Solubility test

The slow evaporation technique performs a fundamental function is observed relatively soluble with choice of a solvent, i.e., water, ethanol, methanol, and combined solvent. The deionized water with magnitude relation 1:1 is mixed solvents of ethanol usage of deionized water when obtaining that of solubility test and LLHC to be used for solubility find out about with growth to repeated recrystallization processes. The temperatures 30°C, 35°C, 45°C, and 55°C analysis of solubility scan is consistent temperature tub with accuracy ±0.01K as evidenced in Fig.2.1. The slow evaporation approach with the growth of the samples is administered with the utilization of deionized water and homogenized solvents with the assist of the solubility curve.

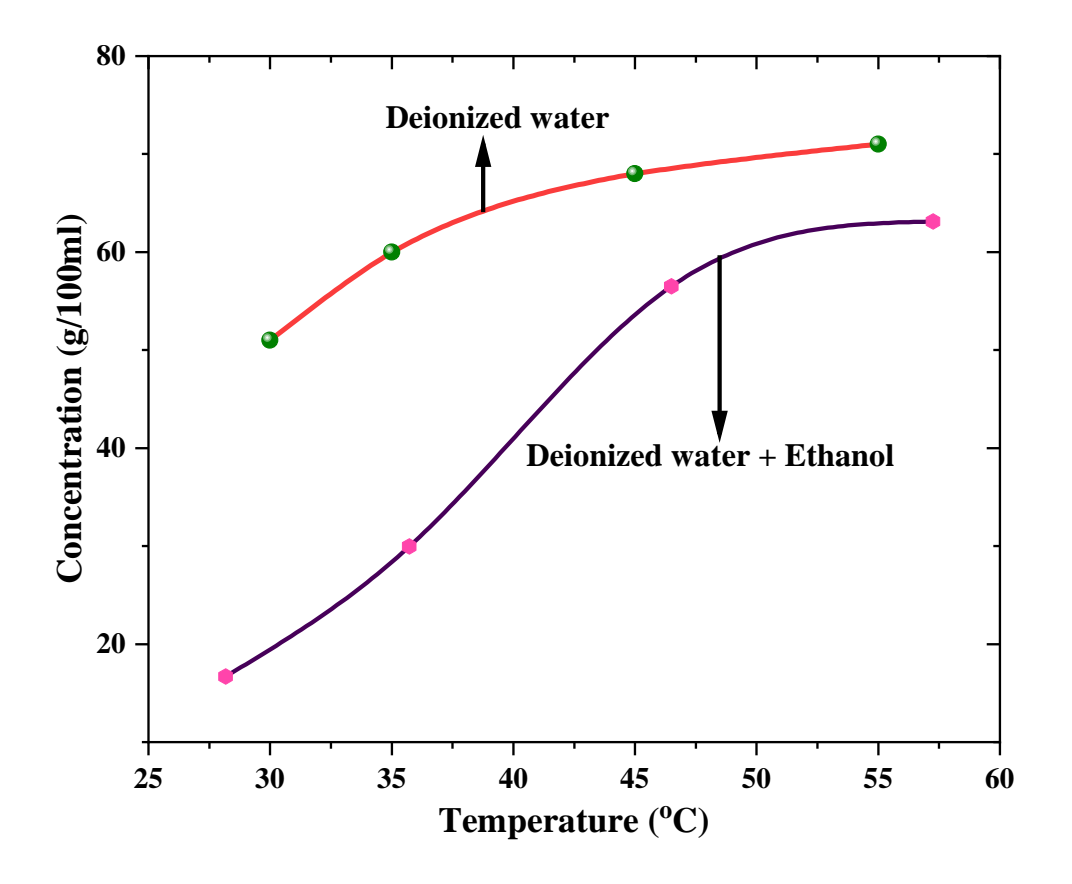
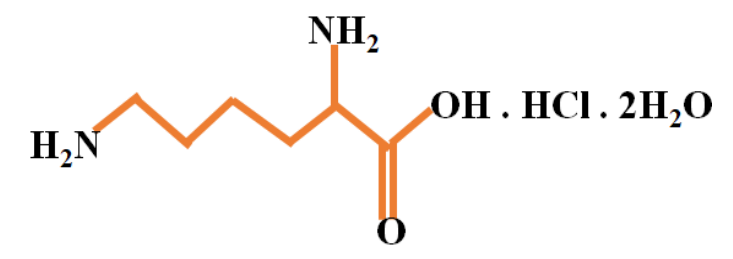


Fig. 2.1 Analysis of LLHC with solubility curve.

2.3 LLHCsingle crystals Growing process

The dissolved in an exceedingly 100ml of deionized water at 35°C have been recrystallized in LLHC. Then, the gaining to saturation from the choice's solution determined that micro filter paper utilizes a thickness of 10µm. The options of the resolution had been optimally closed with the employment of a perforated skinny polyethylene sheet. They positioned the solution in an exceedingly steady temperature bath within the seed growth method. The options solutions temperature bath has been gradually reduced considering at 35°C frequency 0.1K to 0.3K/day. Then, they have reached the room temperature at 31.6°C to accumulated for the appropriate seed crystals. The saturation solution equipped at 32°C has been targeted with seed crystal reserved in constant temperature, each of the solutions optimally connected precise evaporation. The solutions colorless single crystal with the magnitudes of 16 x 10 x 4 mm³ have been gathered consequently 34 days combined to

solvents of deionized water and ethanol of LLHC single crystals as proven in Fig. 2a and Fig. 2b. LLHC single crystals are received from combined solvent use decrease transparency related with the crystals growing the utilization of deionized water as a solvent for studies the chemical form of the crystals was agreed as shown in Fig. 2.2.



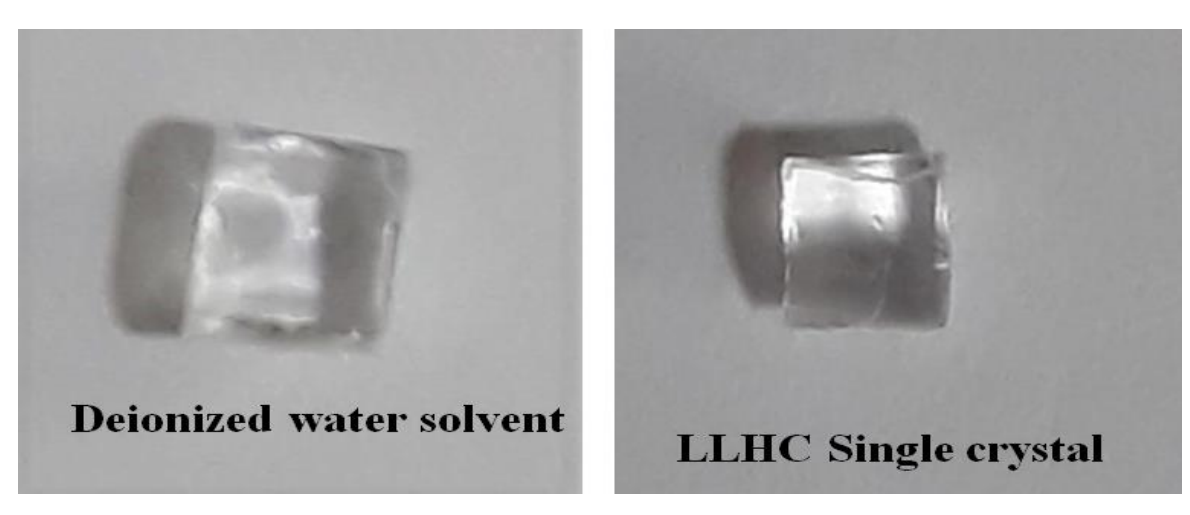


Fig.2. 2 shows an experimental growing process (a) deionized water solvent, (b)

Grown in LLHC Single crystal.

2.4 Result and Discussion

2.4.1 LLHC Characterization studies on X-ray powder diffraction evaluation

We are measured by using instruments of ENRAF NONIUS CAD4 X-ray diffractometer and analyzed the LLHC Single-crystal XRD facts to the cell's parameter values are a = 4.7531Å, b = 12.2467Å, c = 6.6134Å, then α = 90.12°, β = 96.54°, γ = 91.12°, and V = 614.376ų. The single crystal as LLHC powdered samples have been exposed with powder X-ray diffraction investigate in Rich Seifert X-ray diffractometer using CuK α radiation of wavelength 1.6329Å with a scan speed of

0.3°/sec. X-ray diffraction spectrum with top values has been analyzed by way of the usage in the Proszki software program package [11].

The single-crystal XRD statistics are won utilizing the powder XRD evaluation per the samples and powder X-ray diffraction sample of LLHC as shown in Fig.2.3.

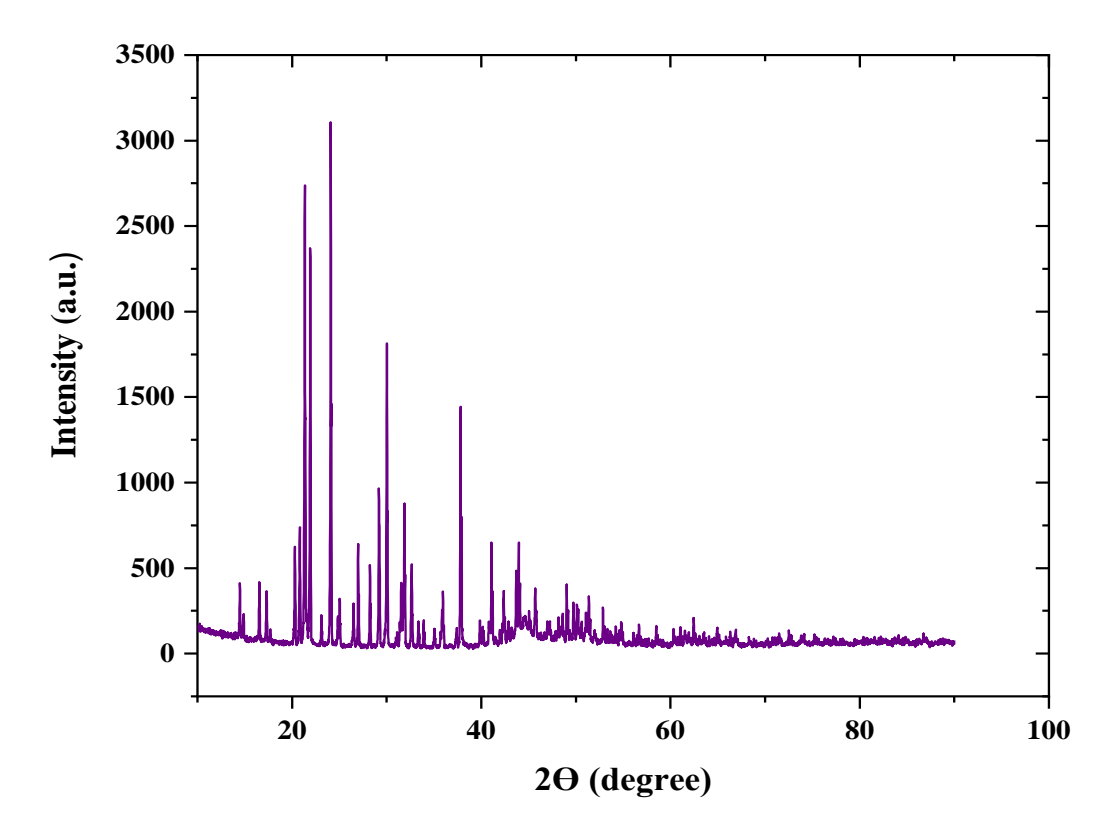


Fig.2. 3 shows in sample powder XRD pattern analysis of LLHC.

2.4.2 LLHC analysis of FTIR - FT-Raman spectra

Fig. 2.4 as the FTIR contemplates are perceived through the functional group's helpful assemblies utilizing BRUKER 66V FT-IR spectrometer with a 4000-400 cm⁻¹. FT-RAMAN examines used to be adjusted that new crystals for vibrational frequencies as demonstrated in Fig. 2.5. They have concerned via units of Bruker FRA 106 FT RAMAN Spectrometer with varying of 50-3500 cm⁻¹. The samples as NH₃ essentially dependent on the torsional mode band are found that wavenumbers from 563cm⁻¹ and 621 cm⁻¹ as Raman and FT-IR range, individually. A substance torsion shaped in a band has been found that wave number of 563 cm⁻¹ and related in torsion with C-C shape [12]. The pattern band vibrations of the

stressing with the guide of CO₂ mode are probably allocated at wave numbers 872 cm⁻¹ and 865 cm⁻¹ with a Raman - IR range, individually. The wave numbers are 931 cm⁻¹ with an IR of a band, and 919 cm⁻¹ in the Raman range is a wagging vibration of CO₂ - structure. The IR spectrum range with peak value is 811 cm⁻¹, and the Raman range wave range is 751 cm⁻¹. which is situated in the torsion of the C-O-H state of the composite. The Raman spectrum range of the intense band is 1114 cm⁻¹, and the IR spectrum range is 1001cm⁻¹. It identifies with stretching of C-C-N structure, which depends absolutely on the task of the equal state of one of the amino acids of L-Lysine [13]. The composite of C-C stretching vibrations was once perceived at groups with wave numbers of 1214 and 1248 cm⁻¹. The C-N-stretching vibrations have been stressed with a carbon shape. The nitrogen of the amino group has seemed that bands of wave number of 1806 cm⁻¹, which is discovered the band with wave amount of 1879 cm⁻¹ with IR spectrum range, it is C-C-N asymmetric stretching vibration as exhorted by Diem et al. [14]. The wave number top qualities are 1800 cm⁻¹ with an IR spectrum range has situated for the shaking of NH₃ shape, a similar wave assortment by [14]. The band of C-H group esteems discovered in LLHC with wave numbers of 1909, 2011, and 1291 cm⁻¹ in the IR range, and bend with vibrations of the CH₃ team is LLHC crystal with wave number 1417 cm-1. However, this height is absent in the IR spectrum. The disclosure with CO₂ on the LLHC gem wave number is 2214 cm⁻¹ [14]. The vibration worth of NH₃ with LLHC crystal [15] is resolved in wave numbers 1446 cm⁻¹ and 1452 cm⁻¹ in the IR and Raman spectra, separately. The Raman and IR spectra in stretching vibrations of NH₃ are excessive wave number areas of C-H structures, which is found at wave numbers of 2875 cm⁻¹ and 2939 cm⁻¹. The functional group assessment of FT-IR and FT-RAMAN with a composite LLHC crystal has been distinguished.

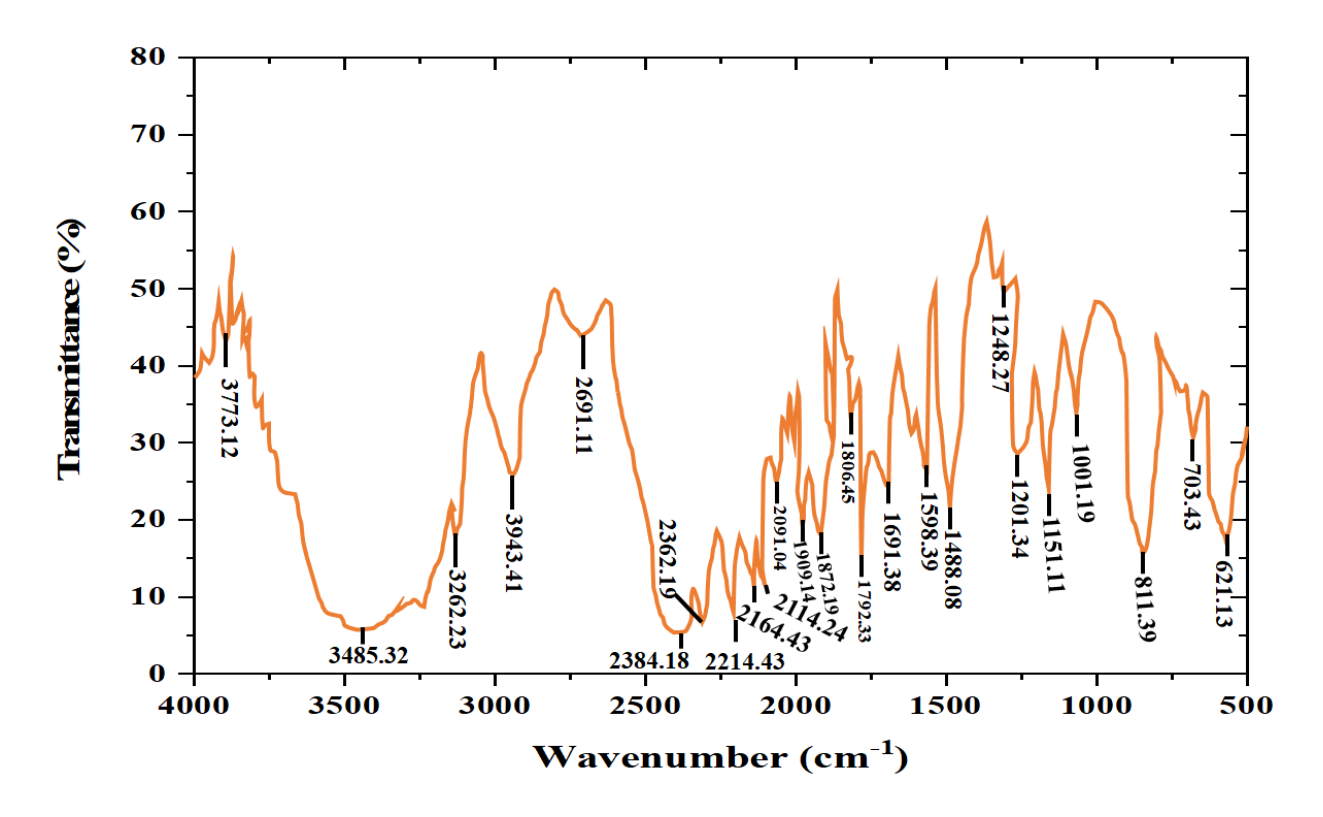


Fig. 2.4 shows in LLHC analysis of FT-IR spectrum.

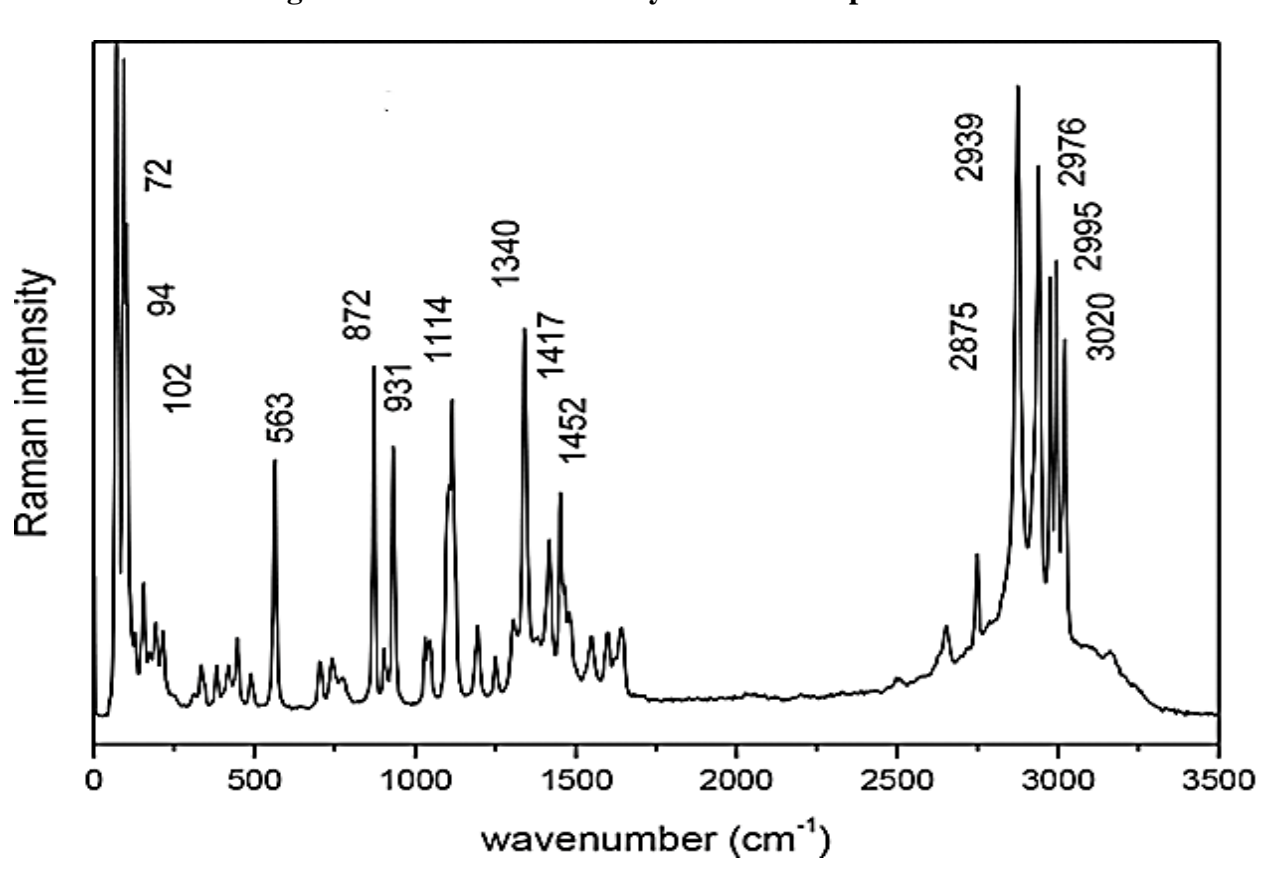


Fig. 2.5 shows in LLHC crystal analysis of FT-Raman spectrum.

2.4.3 LLHC crystal analysis of NMR process

The single crystals have been estimated that NMR spectra, which are utilized devices of JOEL GSX 400 NB FT NMR Spectrometer, 500 MHz, ¹H NMR range esteems are affirmed in Fig.2.6. An intense signal created 4.72ppm from the NH₂ and NH₃⁺ groups, and a 4.51ppm signal demonstrated in the methylene carbon outfitted to a carboxyl group, which is offered from a CH₂ signal of 4.10ppm. 3.38 ppm signal is affirmed in carbon conveying the terminal NH₂ group. The terminal carbon is at a 3.29ppm sign, and 2.24ppm is provided for the methylene carbon. Since it is not, at this point demonstrated the carboxyl proton signal from the range spectrum. It is stressed that the trait with signal to appears to be around 2.19 ppm. The new crystals are developed from the carbon intuitive of the NMR valuable is demonstrated the use of ¹³C NMR as shown in Fig. 2.7. The carboxylic carbon signal is 158.6ppm, consistent that substances and six signals are found with particular six kinds of carbons essentially affirm, which is virtue materials.

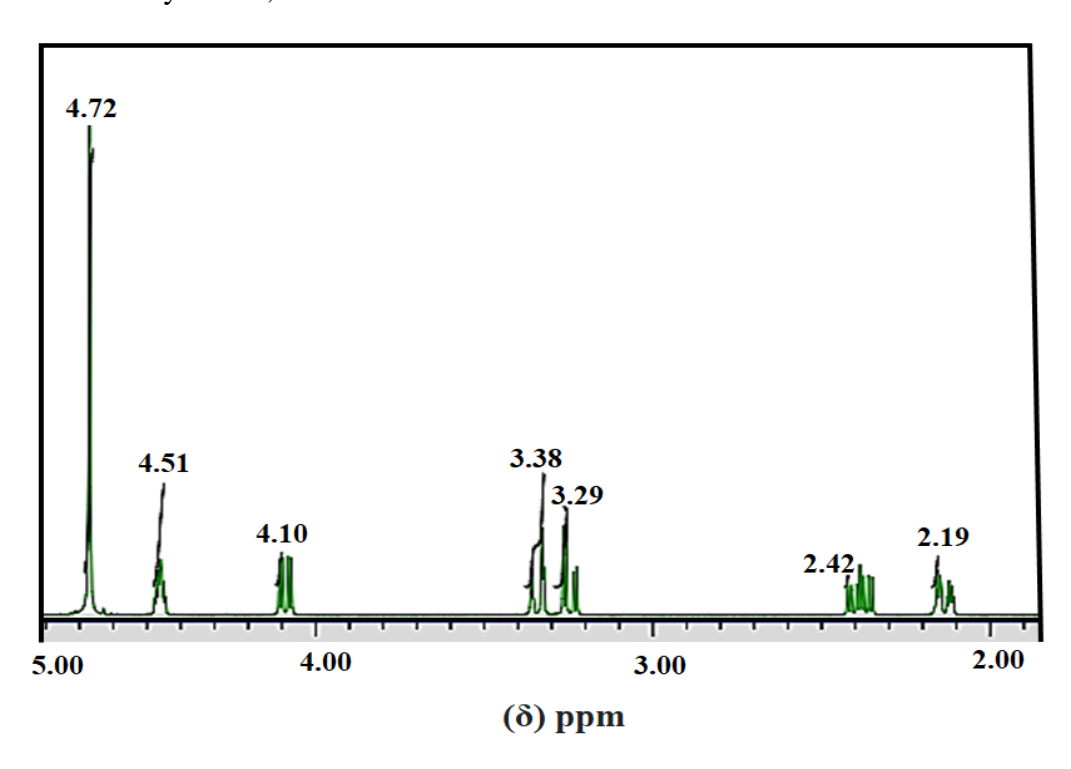


Fig. 2.6 shows LLHC crystal analysis of ¹H NMR spectra.

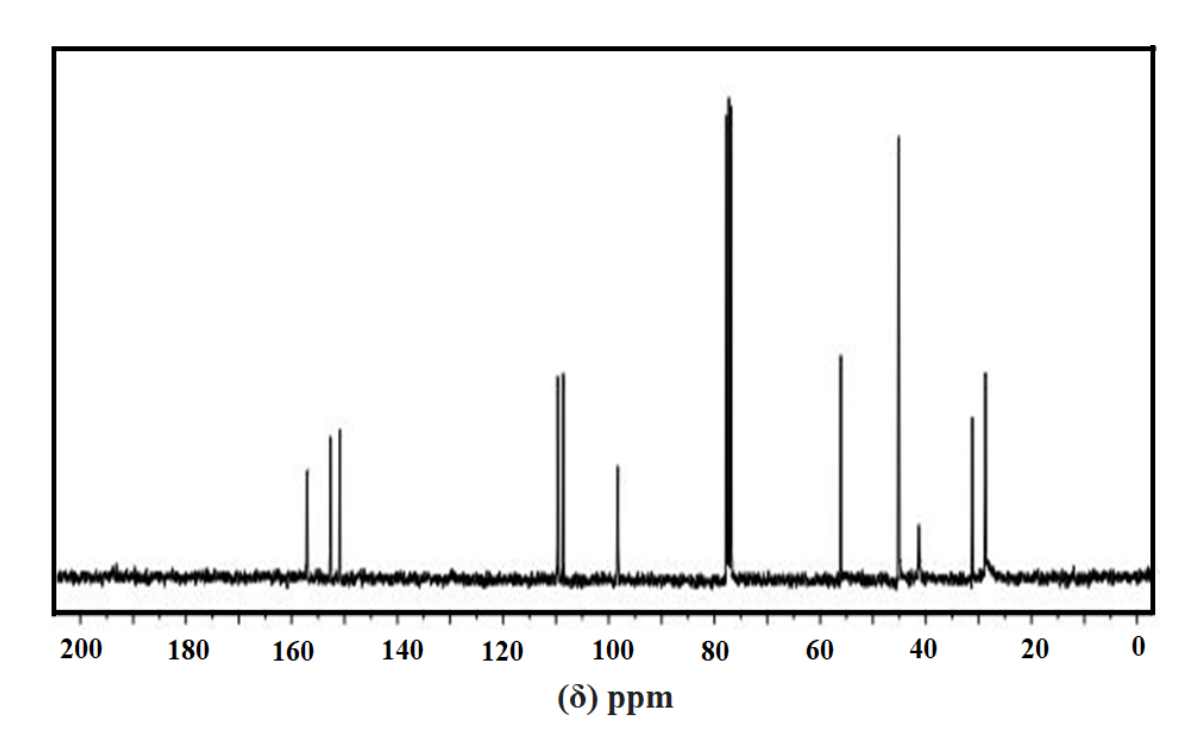


Fig. 2.7 shows LLHC crystal analysis of ¹³C NMR spectra.

2.4.4 LLHC crystal analysis of Thermal process

The new substances have been dissected of thermogravimetric (TG), Differential thermal (DT), which is estimated using the tools of NETSZCH STA 409C. LLHC crystal is estimated through thermogravimetric spectra in the middle differ of 40°C and 800°C. It is a heating charge of 12K/min with nitrogen air. 17.3% reduction 100°C because of water loss of a weight reduction thermogram and its differential shape (DTG) as demonstrated in Fig. 2.8. Weight reduction ascribed the failure of sharp grid water of the samples to the decomposition of models is a significant weight loss of about 51.13% in between 360°C and 250°C. They are one more weight loss the deterioration the somewhere in the range of 430°C and 540°C, and the significant weight reduction have corresponded to about 18.3%. The samples dependent on this examination are through the significant deterioration happens at 270°C, its misuse for application ought to be done underneath 60°C, the loses that lattice water over this temperature. The two water particles of LLHC crystal comprise through the deficiency of cross-section water, which is a genuine relationship with the crystal structure. Likewise, the

completed heating rate of 12K/minute in the N₂ air assessment of the differential thermogram fluctuates is 40°C and 800°C. Fig. 2.8 is ensuing of DTA suggestion an endotherm under 60°C that compares to the deficiency of cross-section water in the DTG curve. The arrangement of endothermic changes of LLHC crystals corresponds intimately with the deterioration exploratory in the DTG curve. It is reasoned that describes with a crystal decays even aside from dissolving.

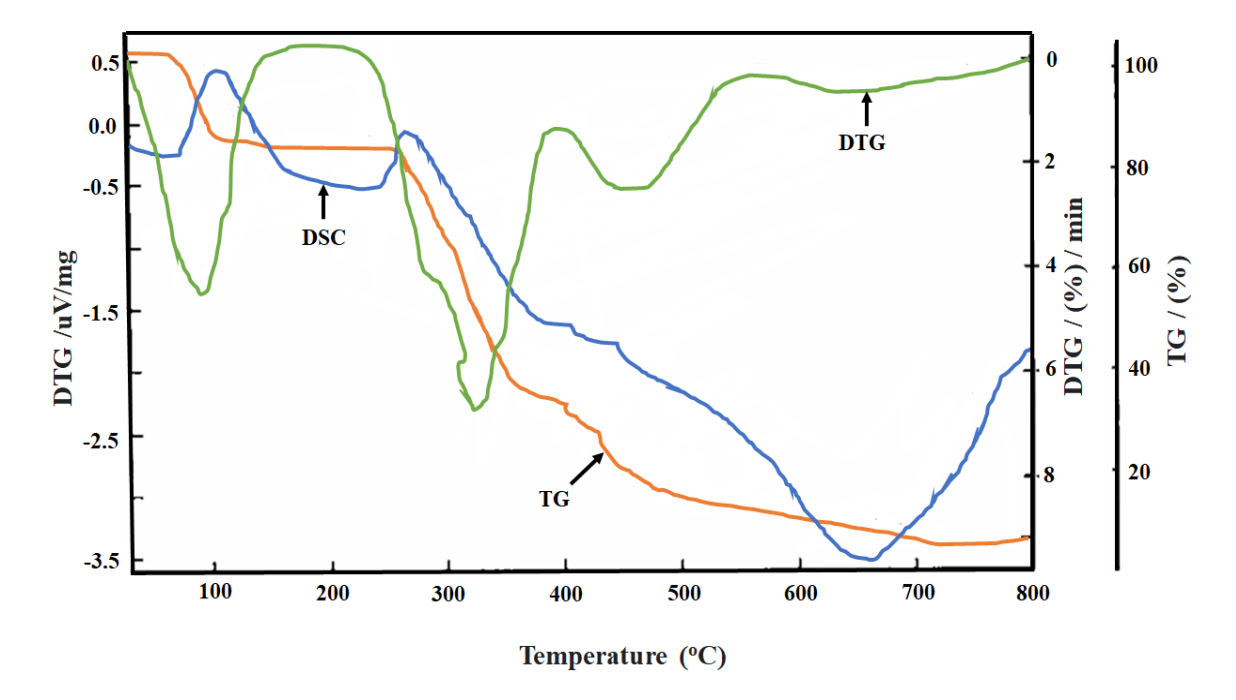


Fig. 2.8 shows LLHC crystal analysis of ¹³C TG-DTAspectra.

2.4.5LLHC crystal analysis of Vicker's microhardness

The organic crystals **evaluation** of Vicker's microhardness is required acceptable quality for gadget manufacture. The second harmonic generation analysis of a single crystal is constantly contrasted with bring down the inadequate areas from the more impressive areas. The optical exhibition of good quality crystals is required in mechanical conduct as [16-17]. The micro hardness is studies of crystals foster using in Vicker's micro hardness utilizing an optical microscope, i.e., an analyzer of Leitz Wetzler's hardness. The micro hardness studies are analyzed of the samples with various loads of 5, 10, 15, and 25g. The LLHC crystal is chosen

surface, which is cleaned utilizing a velvet cloth to get a smooth surface using the above loads of the hardness discovered. The LLHC crystal with Vicker's micro hardness has been estimated utilizing the H_v =1.8627 P/d^2 (kg/mm³) connection between solidity and load, as demonstrated in Fig. 2.9. The pack is expanded that LLHC crystal increments' hardness gradually diminishes with further raising of the shipment. The crystal breaks are shaped at 50g then it is relatively more complicated when contrasted with other organic crystals [18-19].

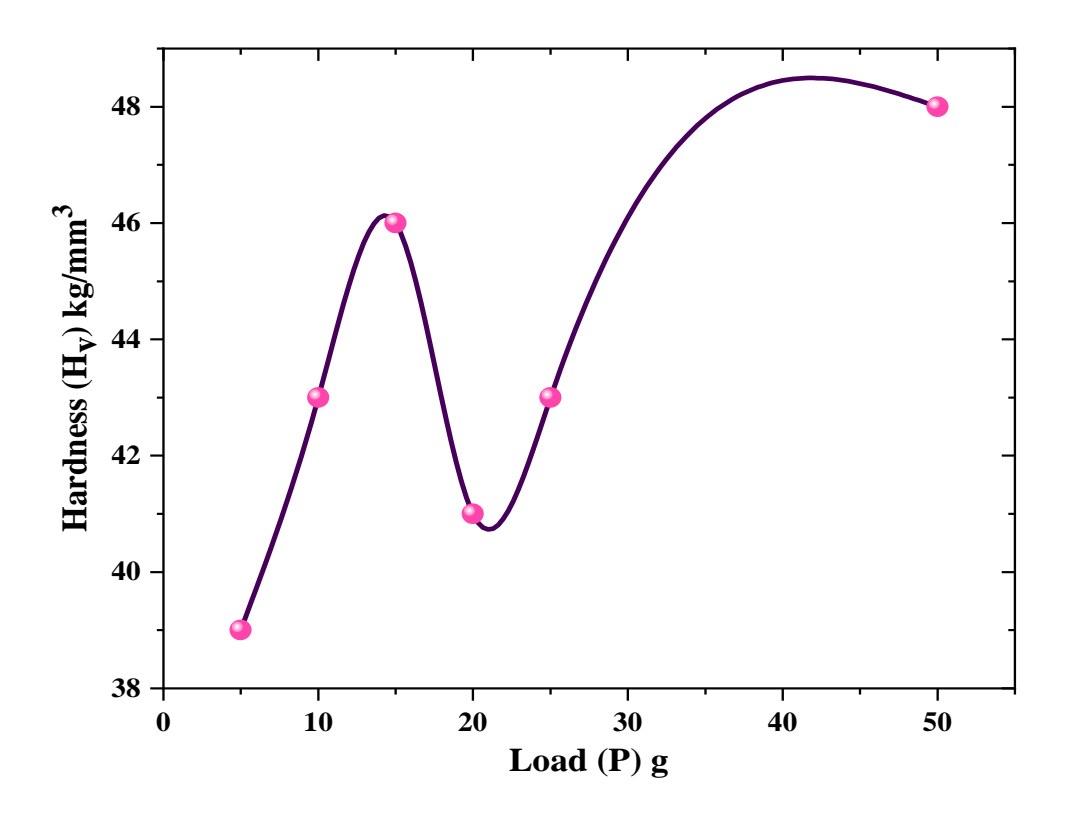


Fig. 2.9 shows LLHC crystal analysis of hardness vs. load.

2.4.6 LLHC crystal analysis of transmission spectra

This crystal is grown from deionized water, a blended dissolvable after recorded utilizing the UV-Visible spectrometer in the frequency range 200-800nm as demonstrated in Fig. 2.10 (i) and 10(ii). The LLHC crystal was once developed from deionized water and blended dissolvable from the cut-off frequencies range of 210nm and 240nm. The high

conveyance of 99% contrasted with blended dissolvable, it appears to be likewise developed crystal from deionized water, and frequency range is 210 nm to 800 nm. In these investigations, the new materials are precious for NLO applications.

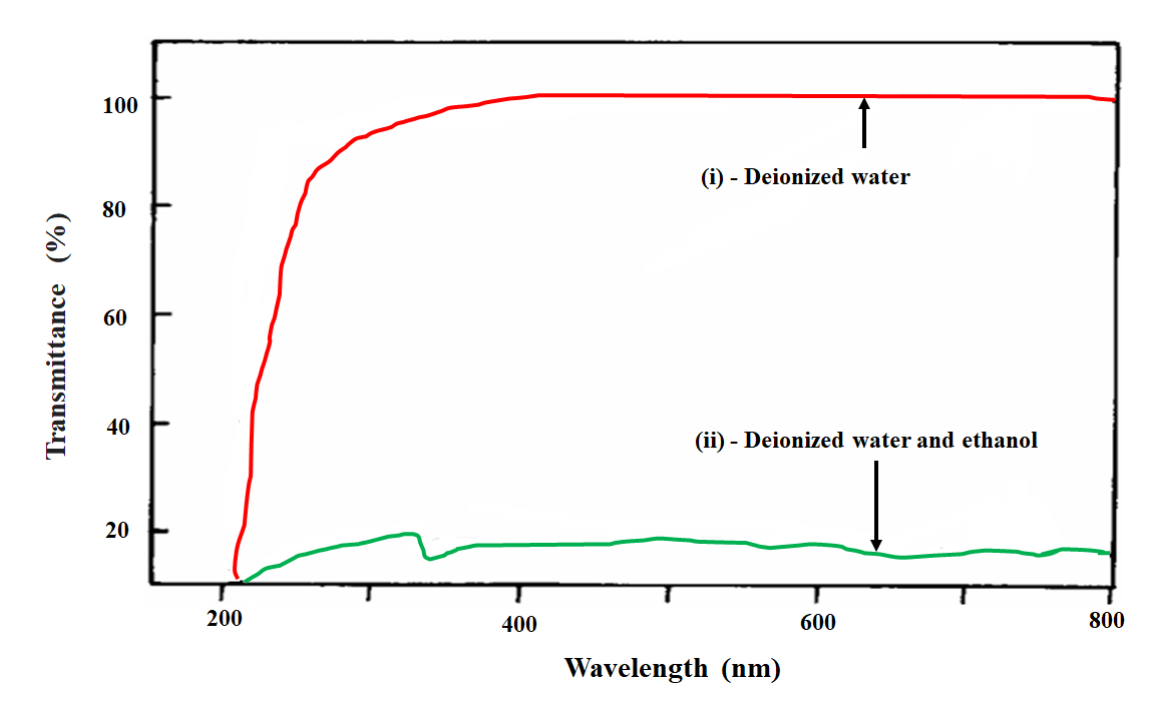


Fig. 2.10 (i) and (ii) shows transmittance spectra of LLHC crystal.

2.4.7 LLHC crystal analysis of NLO assessment:

The powder technique is estimated in an SHG analysis investigation of the LLHC powder tests. From the X-rayed about 1064nm through the Nd: YAG laser. It is seen that the green light frequency of 532nm. The information energy of 5.4mJ/pulse is achieved in a second harmonic signal of about 60.6mV

2.5 Conclusion

The LLHC crystals have been effectively filled in the environment utilizing the slow evaporation solution arrangement in the growth method. The deionized water and blended dissolvable ethanol at that point water have resolved the solubility of LLHC. The vibrational frequencies of LLHC are concentrated in FTIR and FT-RAMAN measures. It is located that it be NLO material having a short cut-off wavelength inside the UV locale.

Reference

- [1] D S Chemla and J Zyss Eds *Academic Press New York*496 (1987)
- [2] H S Nalwa and S Miyata CRC Press New York (1997)
- [3] P N Prasad and D J Williams Wiley New York (1991)
- [4] RW Boyd Academic Press San Diego 155 (1992)
- [5] B E Salch and M C Teich Wiley New York 113 (1991)
- [6] N Balamurugan, M Lenin and P Ramasamy *Mater. Lett.* 61 1896 (2007)
- [7] F Q Meng, M K Lu, Z H Yang and H Zeng *Mater. Lett.* 33 265 (1998)
- [8] R Rajasekaran, P M Ushasree, R Jayavel and P Ramasamy *J. Cryst. Growth* 229 563 (2001)
- [9] E Ilango, R Rajasekaran, K Shankar and V Chithambaram *Optical materials* 37 666 (2014)
- [10] A. Selvam, S Pandi, S Selvakumar and S Srinivasan J. Appl. Sci. Res. 4 2474 (2012)
- [11] M S Joshi and A V Antony J. Phys D: Appl. Phys. 10 2393 (1977)
- [12] P Geetha, S Krishnan, R K Natarajan and V Chithambaram *Current Applied Physics*15 201 (2015)
- [13] J M S Gnanaraj et al., Optics & Laser Technology 107 478 (2018)
- [14] R B Jarzebowska et al., Polyhedron 173 114 (2019)
- [15] S Kim *et al.*, Microchemical Journal 152 1043 (2020)
- [16] O.Castillo-Cruz et al., Materials Science and Engineering: C 102 887 (2019)
- [17] A S H Hameed, G Ravi, R Dhanasekaran and P Ramasamy *J. Cryst. Growth*212 227 (2000)
- [18] P. Saminathan *et al.*, Materials Today: Proceedings, 18 1256 (2019)
- [19] V Goma, C M Padma and C K Mahadevan Matt. Lett. 60 p 3701 (2006)
- [20] K Nakamoto Wiley New York (1978)

- [21] C P Smyth *MC Graw Hill New York* 132 (1965)
- [22] C Balarw and R.J Duhiew Solid State chemistry 55 1 (1984)
- [23] S K Kurtz and T T Perry J. Appl. phys. 39 3798 (1968)
- [24] M M Khandpekar and S P Pati Opt. Commun. 283 2700 (2010)
- [25] L Bellamy *Wiley New York*161 (1958)
- [26] H O Marcy et al., Applied Opts.3 5051 (1992)

CHAPTER - 3

GROWTH AND INVESTIGATION ON NOVEL SINGLE CRYSTAL OF B-CYCLODEXTRIN 2, 4-DINITROPHENYLHYDRAZINE FOR OPTICAL SENSORS APPLICATIONS

3.1 Introduction

Second order non-linear optical materials find different role of applications like optical communication, sensing, signal process- ing, data storages, optical logic gates, laser radiation protection and THz-wave generation [1–5]. In recent years the broad investi- gation is performed for the growth of nonlinear optical materials because it has wide applications in photonic and optoelectronic fields. Most of the organic materials have large nonlinear optical coefficient but poor mechanical and thermal properties. The growth of large size single crystal is very difficult for the device fabrication. Inorganic materials have excellent mechanical and thermal properties but less optical nonlinearity due to the lack of p-electron delocalization [6–10]. In the view of these problems interest has been made to grow the semi organic crystals because it has less delinquency, high damage threshold, exceptional mechanical and nonlinear optical property, low angular sensitivity, wide optical transparency range which make them comfortable for device fabrications [11–19]. Therefore, it is essential to grow novel semi organic crystals having consistent phantasy of both organic and inorganic materials.

In the present work the title compound was successfully synthesized by combining b-Cyclodextrin and 2, 4- dinitrophenyl hydrazine in equimolar ratio. The single crystals have been grown by solution growth slow evaporation technique using water as the solvent. A transparent good quality crystal was obtained within 4 weeks as shown in Fig. 3.1. The photograph was taken by using high megapixel camera. To have a

full understand- ing about the structure and its properties for the grown crystals Powder XRD, FTIR, Nonlinear Optical Property (Second Harmonic Generation) measurements were also been carried out.

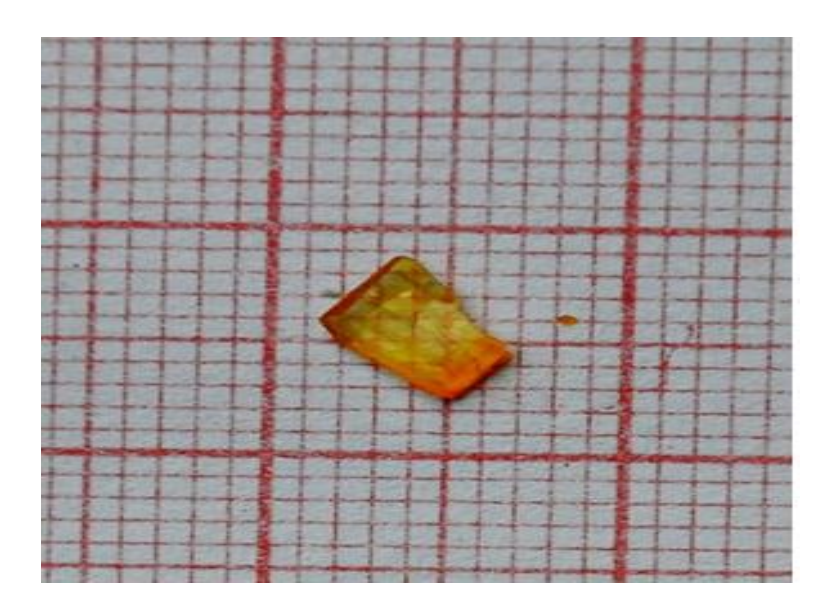


Fig. 3.1. Photograph of crystal formed by inclusion complex of DNPH:b-CD.

3.2 Results and Discussion

3.2.1 Single crystal x-raydiffraction

The good quality DNPH: b-CD grown crystal was subjected to single crystal X-ray diffraction analysis to collect the data using BRUKERKAPPAAPEXIICCD. The grown crystals have their triclinic non-centro symmetric space group P2. The cell parameters were measured to be a = 14.03 Å, b = 13.39 Å, C = 14.49 Å, a = 103° .b = 113° , c = 98° and V = 3651 Å³

3.2.2 Powder X-Ray diffraction Analysis

Powder X-Ray diffraction study was used for the identification of crystallinity of the grown crystal. The Ka radiations from a cop- per target were used. The sample was scanned in the range between 10 and 100°C. Fig.3.2(a), (b) and (c) represents the indexed powder diffractogram for the grown crystal of DNPH, b-CD and DNPH:b-CD.

The sharp intensity peaks found in spectra shows good crystalline nature and purity of the grown crystal.

3.3 Results and Discussion

3.3.1 Single crystal x-ray diffraction

The good quality DNPH: b-CD grown crystal was subjected to single crystal X-ray diffraction analysis to collect the data using BRUKER KAPPAAP EXIICCD. The grown crystals have their triclinic non-centro symmetric space group P2. The cell parameters were the infrared (FTIR) spectra of wave number from 4000 to 400 cm⁻¹ of DNPH, b-CD and the solid inclusion complex of DNPH with b-CD are registered by FTIR spectrometer and the complete band assignments can be found in Fig. 3.3. We can see that there are apparent differences between the FTIR spectra of b-CD (Fig. 3a), DNPH (Fig.3b) and DNPH: b-CD (Fig.3c) solid crystal which infers the formation of DNPH:b-CDcomplex.

The infrared (FTIR) spectra of wave number from 4000 to 400 cm⁻¹ of DNPH, b-CD and the crystal of DNPH with b-CD are registered by FTIR spectrometer and the complete band assignments can be found in Fig.3.3. We can see that there are apparent differences between the FTIR spectra of b-CD (Fig.3.3a), DNPH (Fig. 3.3b) and DNPH: b-CD (Fig.3.3c) solid crystal. The IR spectrum of DNPH (Fig. 3b) exhibits a strong peak at 3092 cm⁻¹ for stretch- ing vibration of C–H from aromatic ring. IR peak at 1135cm⁻¹ is noted for the bending vibration of C–H from aromatic ring.1637 and 1496 were noted for stretching vibration of C@C in benzene ring. However, in the IR spectrum of DNPH:b-CD crystal (Fig. 3c), absorption band due to the stretching (at 2926 cm⁻¹) and bending (at 1411 cm⁻¹) vibrations are shifted.

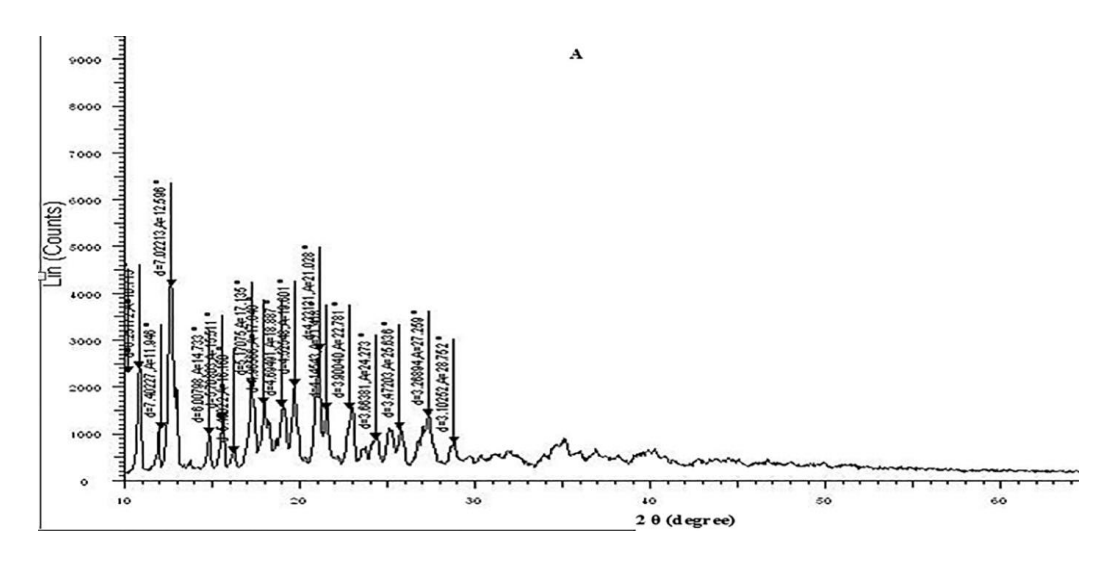
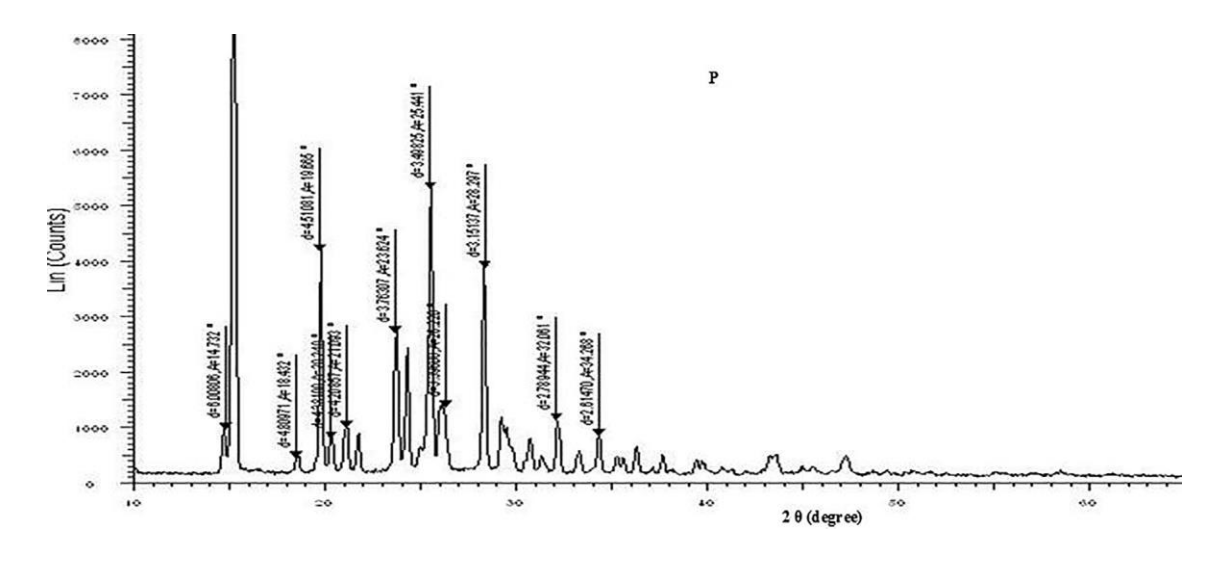
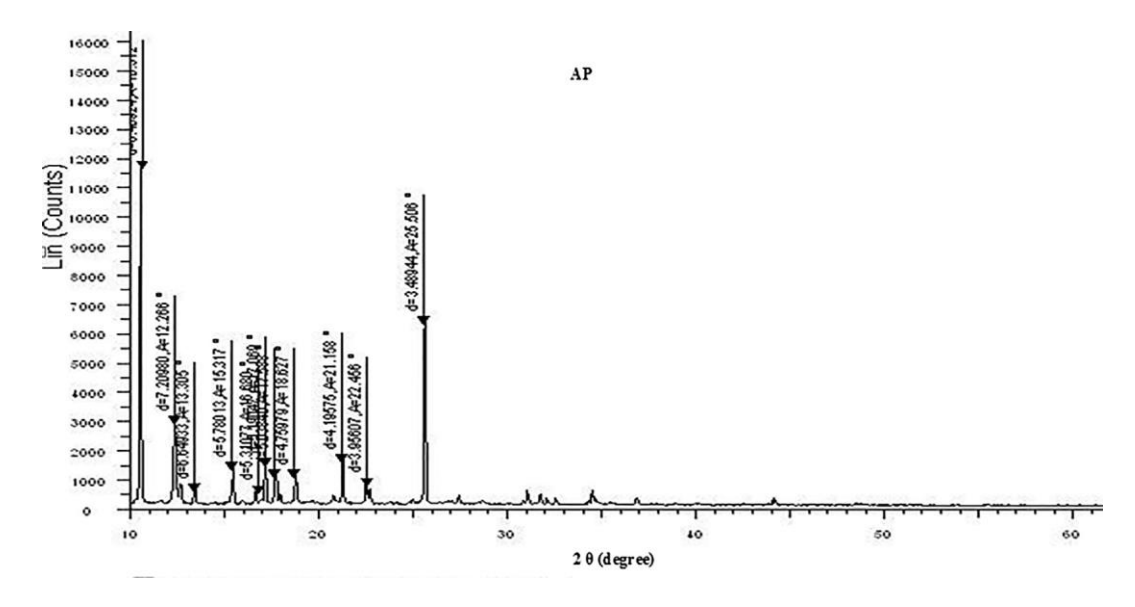
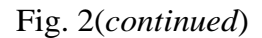


Fig. 3.2(a). The Powder XRD pattern of b-CD, DNPH and grown crystal by DNPH:







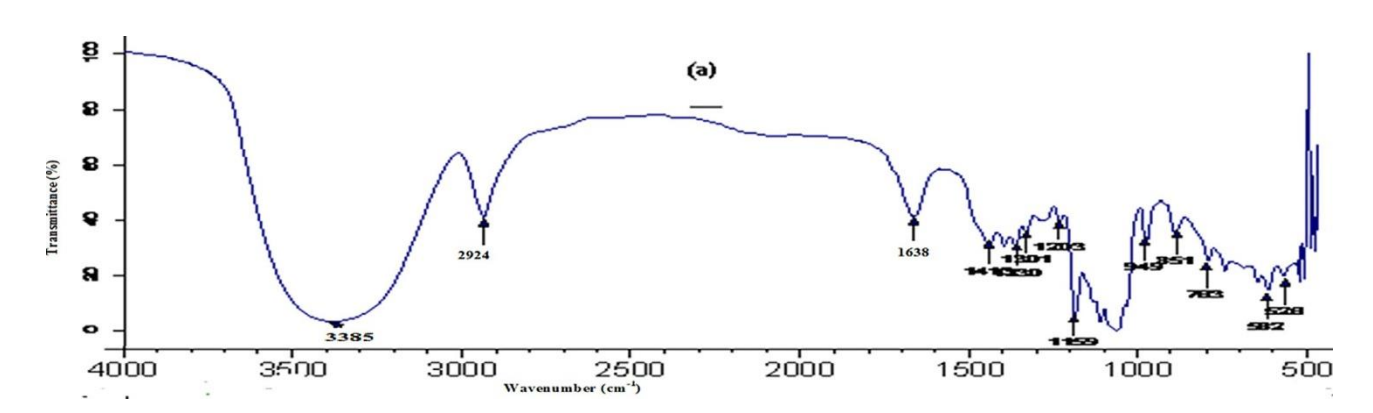


Fig. 3.3(a) FTIR Spectrum of (a) b-CD, (b) DNPH, (c) as grown crystal of DNPH:b-CD.

The stretching vibration of C@C (at 1643 and 1411 cm⁻¹) also shifted. In the IR spectrum of DNPH the intensity of N–H stretching is very high (3326 cm⁻¹) and there is slightly increased in the IRspectrum of DNPH: b-CD complex (3302 cm⁻¹). IR peak at 1219 cm⁻¹ is noted for the symmetric stretching vibration of N-O in DNPH and there is increased in IR spectrum of DNPH: b -CD complex (1151cm⁻¹).

Scanning electron Microscope studies

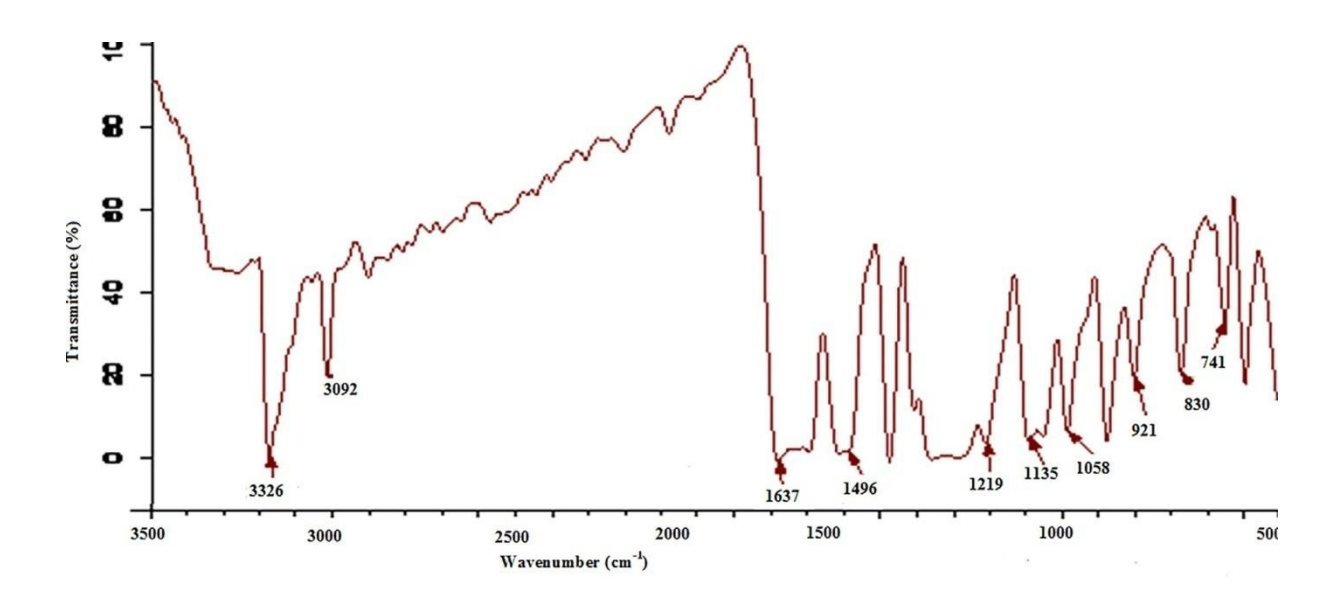


Fig. 3.3(b)(continued)

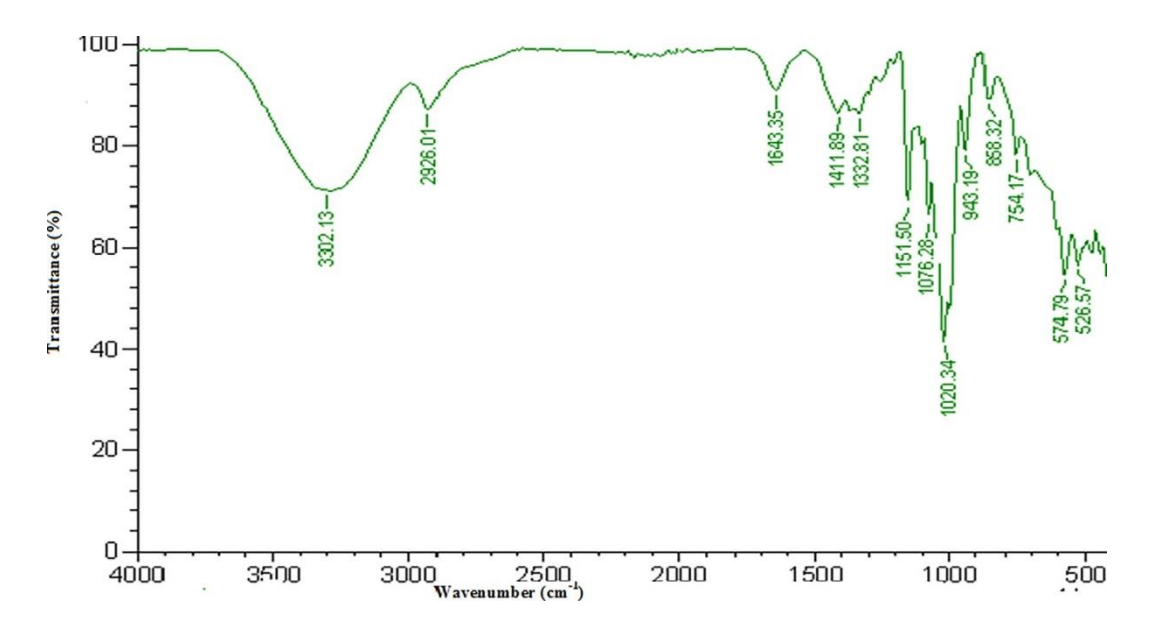


Fig. 3.3(c)(continued)

The Scanning electron microscopy (SEM) image of the grown crystal was recorded using FEI Quanta FEG 200 - High resolution Scanning Electron Microscope to study the surface mor-phology of DNPH: b-CD crystal. A two dimensional image was generated over a selected area of the sample. Since DNPH: b- CD is a single crystal, which is poor conducing in nature so the sample was subjected to gold/carbon

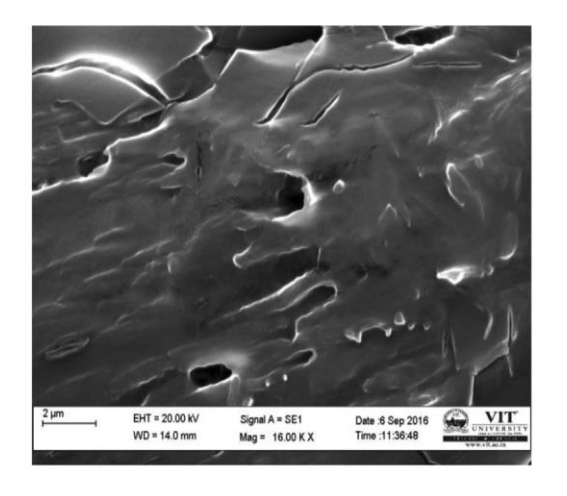
coating. THE SEM figures are recorded in different magnification. From the Fig. 3.4, it is clear that the surface of the grown crystal appears very smooth though it has pots and microcrystal on the surface. The grain boundaries are clearly seen which shows the perfect growth of the crystal.

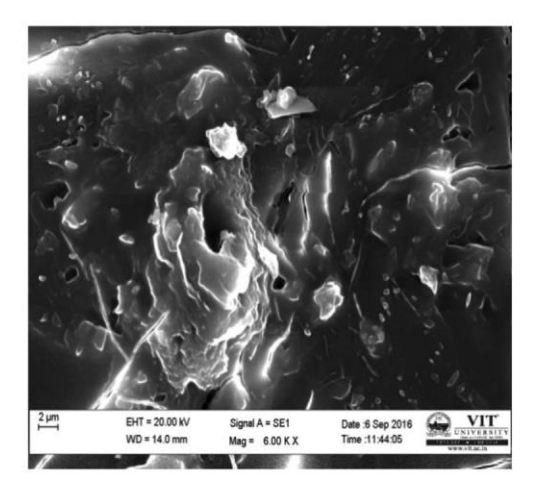
Energy dispersive X-ray analysis (EDAX) is a micro-analytical technique, used to obtain information about the chemical composition of the grown crystal. In this work, the grown crystal was subjected to EDAX analysis using the instrument FEI QUANTA 200F energy dispersive X-ray micro analyzer. The EDAX spectrum of the crystal is shown in Fig. 3.5. The weight percentage (wt %) of C,N and O as obtained from EDAX analysis is in concurrent with the theoretical values.

3.4 Nonlinear optical studies

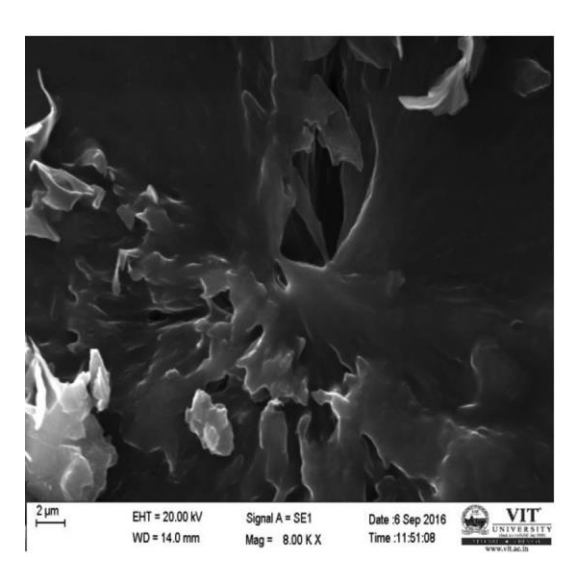
The second harmonic generation efficiency measurement was carried out to the grown crystal using the Kurtz–Perry powder technique. The crystal was well grinded into a homogenous powder and densely packed between two transparent glass plates. The powder sample with average particle size100–1151 wasilluminated using Q-switched Nd: YAG laser emitting a fundamental wavelength of 1064 nm with the pulse width of 8 ns. The value of SHG for the grown crystal is found to be 42.32 mV as in comparison with that of pure KDP crystal's value of 26.4 mV which asserts that the grown crystal has the efficiency of 0.62 times greater than that of KDP assuring itself to be a potential candidate for photonic applications.

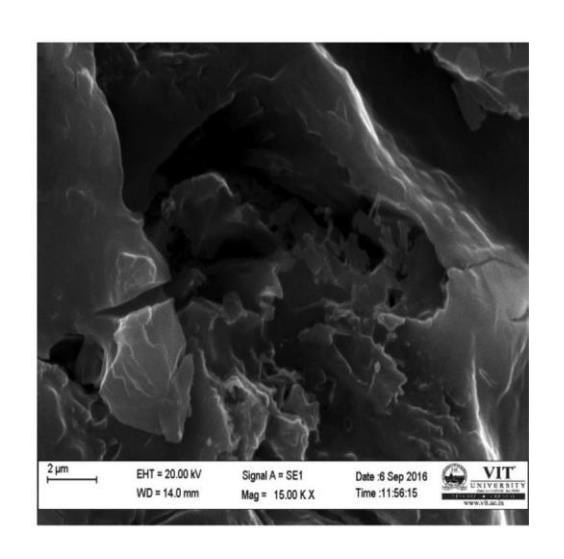
Fig. 4. SEM images of grown crystal of DNPH: b-CD. 4a 4b



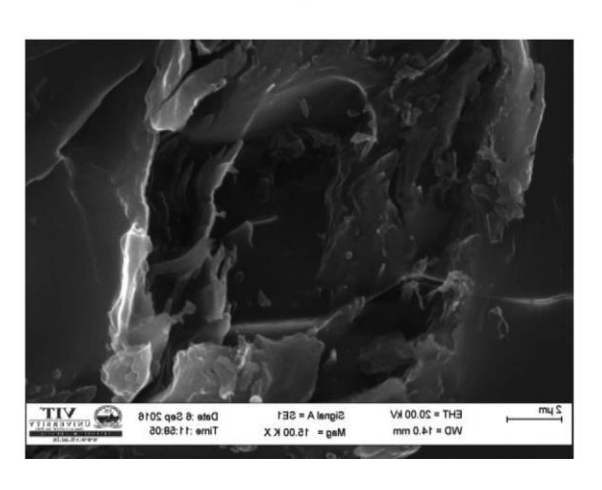


4c 4d





4e



method at ambient temperature. The characterization of Powder X – Ray diffraction peaks was confirmed the new crystalline system. Fourier transform infrared spectroscopic analysis(FTIR)was used to the identification of various functional groups present in the grown crystal. The range of optical transmittance exhibited by the grown CD-DNPH crystal was investigated by UV-Visible.

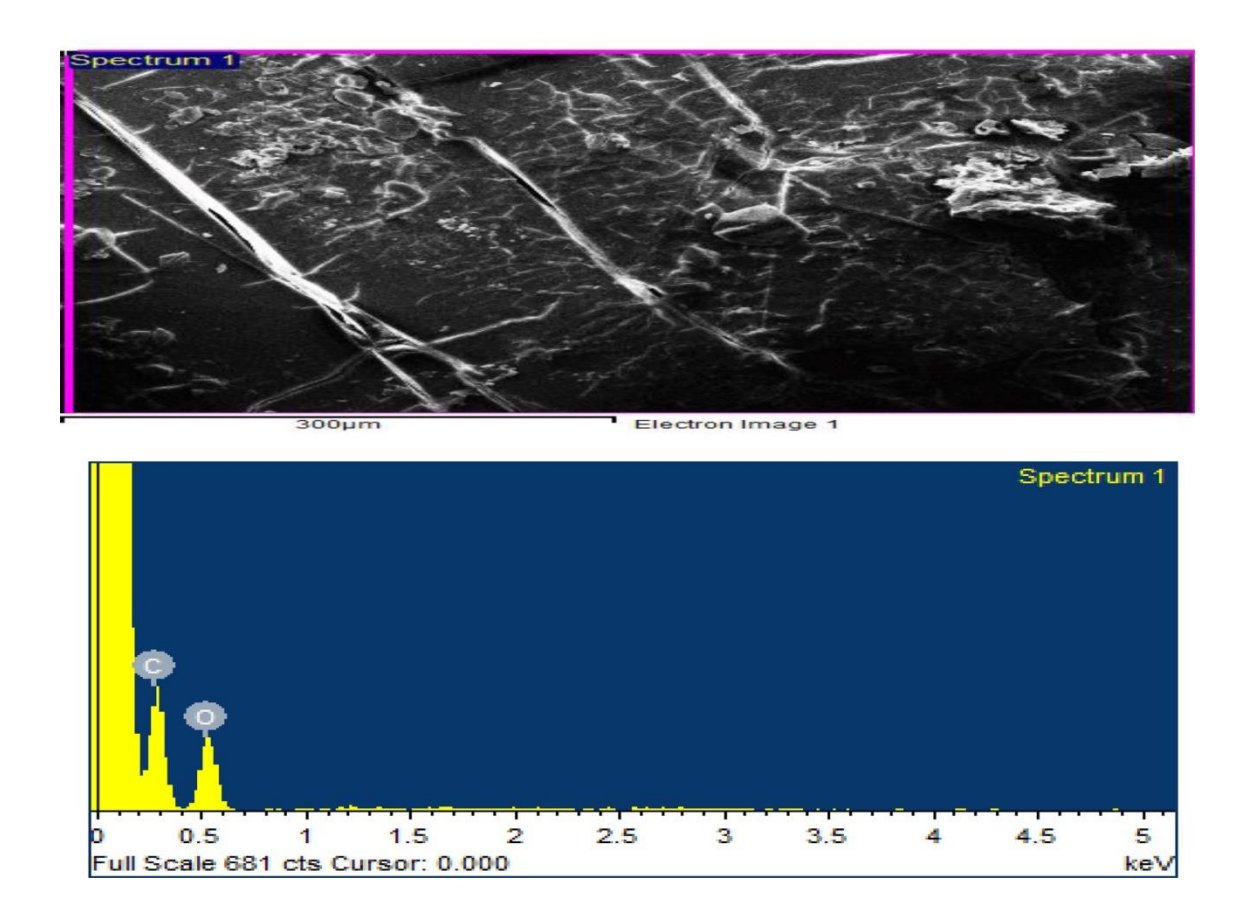


Fig. 3.5. EDAX spectrum of inclusion complex crystal of DNPH:b-CD.

3.5 Conclusion

Nonlinear optical (NLO) 2, 4-Dinitrophenylhydrazine (DNPH) single crystal was grown by slow evaporation solution growth. NIR spectral analysis. The lower cut off wavelength of the grown crystal is observed at 270 nm. The SEM figures are recorded in dif-ferent magnification. It is clear that the surface of the grown crystal appears very

smooth although it has pots and microcrystal on the surface. The grain boundaries are clearly seen which shows the perfect growth of the crystal. The weight percentage (wt %) of C, N and O as obtained from EDAX analysis is in concurrent with the theoretical values. The SHG efficiency of the grown crystal was determined. The grown crystal has the SHG efficiency was 0.62 times greater than that of KDP assuring itself to be a potential candidate for photonic applications.

References

- [1] Balamurugan N., Lenin M. and Ramasamy P., Growth of potassium acid phthalate crystals by Sankaranarayanan-Ramasamy (SR) method and its optical characterization, Mater. Lett., 61 (8-9), 1896-1898 (2007) https://doi.org/10.1016/j.matlet.2006.07.184.
- [2] Siva Rama Krishna Reddy K., Swapna K., Mahamuda Sk., Venkateswarlu M., Srinivas Prasad M.V.V.K., Rao A.S. and Vijaya Prakash G., Structural, optical absorption and photoluminescence spectral studies of Sm3b ions in Alkaline-Earth Boro Tellurite glasses, Optical Materials, 79, 21–32 (2018) https://doi.org/10.1016/j.optmat.2018.03.005.
- [3] Annapurna Devi Ch.B., Mahamuda Sk., Swapna K., Venkateswarlu M., Srinivasa Rao A. and Vijaya Prakash G., Compositional dependence of red luminescence from Eu³b ions doped single and mixed alkali fluoro tungsten tellurite glasses, Optical Materials, 73, 260-267 (2017) http://dx.doi.org/10.1016/j.optmat.2017.08.010.
- [4] Shaik Babu, Radhia Trabelsi, Tadikonda Srinivasa Krishna, Noureddine Ouerfelli & Adel Toumi, Reduced Redlich–Kister functions and interaction studies of Dehpa + Petrofin binary mixtures at 298.15K, Journal Physics and Chemistry of Liquids An International Journal, 57(4), 1-11 (2019) https://doi.org/10.1080/00319104.2018.1496437.
- [5] Nisha Deopa, Rao A.S., Mahamuda Sk., Mohini Gupta, Jayasimhadri M., Haranath D. and Vijaya Prakash G., Spectroscopic studies of Pr3b doped lithium lead alumino borate glasses for visible reddish orange luminescent device applications, Journal of Alloys and Compounds, 708, 911-921 (2017) http://dx.doi.org/10.1016/j.jallcom.2017.03.020.
- [6] Venkateswarlu M., Mahamuda Sk., Swapna K., Prasad M.V.V.K.S., Srinivasa Rao A., Suman Shakya, Mohan Babu A. and Vijaya Prakash G., Holmium doped Lead

- Tungsten Tellurite glasses for green luminescent applications, Journal of Luminescence, 163, 64–71 (2015) http://dx.doi.org/10.1016/j.jlumin.2015.02.052.
- [7] Nagababu P., Shaik Babu, Dheiver F., Santos and Gowrisankar M., Investigation of molecular interactions in binary mixtures of homologous series of aliphatic alcohols with 2-methoxyaniline at various temperatures, Physics and Chemistry of Liquids An International Journal, 57(5), 689-702 2018 https://doi.org/10.1080/00319104.2018.1511787.
- [8] Brahmanandam P. S., Uma G., Liu J. Y., Chu Y. H., Latha Devi N. S. M. P., Kakinami Y. and Global S., Index variations observed using FORMOSAT-3/COSMIC GPS RO technique during a solar minimum year, journal of geophysical research, 117, (2012) A09322, doi:10.1029/2012JA017966, 2012.
- [9] Ilango E., Rajasekaran R., Shankar K. and Chithambaram V., Synthesis, Growth and characterization of non-linear optical Bisthiourea Ammonium Chloride single crystals by slow evaporation technique, Optical materials, 37, 666-670 (2014) https://doi.org/10.1016/j.optmat.2014.08.011.
- [10] Parvez Ahmad, Venkateswara Rao A., Suresh Babu K. and Narsinga Rao G., Effect of hydrogen annealing on structure and dielectric properties of zinc oxide nanoparticles, Materials Chemistry and Physics, 224, 79–84 (2019) https://doi.org/10.1016/j.matchemphys.2019.122226.
- [11] Venkateswara Rao, Ranjith Kumar B. and Ramarao S.D., Structural, microstructural and electrochemical studies on LiMn₂-x(GdAl)xO₄ with spinel structure as cathode material for Li-ion batteries, Ceramics International, 44, 15116–15123 (2018) https://doi.org/10.1016/j.ceramint.2018.05.148.
- [12] Krishna Jyothi N., Venkata Ratnam K.K., Narayana Murthy P. and Vijaya Kumar K., Electrical Studies of Gel Polymer Electrolyte based on PAN for Electrochemical Cell

- Applications, Materials Today: Proceedings, 3, 21–30 (2016) doi: 10.1016/j.matpr.2016.01.112.
- [13] Shahenoor Basha S.k., Sunita Sundari G., Vijay Kumar K., Ramachandra Rao K. and Raod M.C., Preparation and characterization of ruthenium based organic composites for optoelectronic device application, Optik, 164, 596–605 (2018).https://doi.org/10.1016/j.ijleo.2018.03.071.
- [14] Hameed A S H, Ravi G Dhanasekaran R and Ramasamy P, Studies on organic indole-3-aldehyde single crystals, *J. Cryst. Growth*, **212** (1–2), 227-232 (2000) https://doi.org/10.1016/S0022-0248(99)00896-9
- [15] Saminathan P, SenthilKumar M, Shanmugan S and Chithambaram V, Growth and Characterization of L-Lysine Monohydrochloride Dihydrate (LMHCl) Single Crystals by Slow Evaporation Technique, *Materials Today: Proceedings*, **18** (3), 1256-1262 (2019) https://doi.org/10.1016/j.matpr.2019.06.587
- [16] Manivannan, S., Dhanuskodi, S., Synthesis, growth, structural, optical, and thermal properties of a new semi organic crystal: 4-dimethylamino pyridinium dihydrogen phosphate, Crystal growth and design, 4, 845-850 (2004). https://doi.org/10.1021/cg049950c
- [17] S. Manivannan, S. Dhanuskodi, S.K. Tiwari, Laser induced surface damage, thermal transport and microhardness studies on certain organic and semiorganic nonlinear optical crystals, J. Philip, J. Pure Appl. Phys. Vol. B 90, pp. 489–496, 2008.
- [18] H. Nagatani, W.R. Bosenberg, L.K. Cheng, C.L. Tang, Laser-induced damage in beta-barium metaborate, Appl. Phys. Lett. Vol. 53, pp. 2587–2589, 1988
- [19] N. Vijayan, G. Bhagavannarayana, K.R. Ramesh, R. Gopalakrisnan, K.K. Maurya, P. Ramasamy, Compositional dependence of cationic displacements in lithium niobate and lithium tantalate crystals, Cryst. Growth Res. Vol. 6, pp. 1542–1546, 2006.

- [20] S. Kurtz and T. Perry, "A powder technique for the evaluation of nonlinear optical materials," Journal of applied physics, vol. 39, pp. 3798-3813, 1968.https://doi.org/10.1063/1.1656857.
- [21] M. Senthilkumar and C. Ramachandraraja, "Growth, structural, spectral and optical studies on pure and l-alanine mixed bisthiourea cadmium bromide (LABTCB) crystals," Journal of Minerals and Materials Characterization and Engineering, vol. 11, p. 631, 2012.
- [22] S. Masilamani, A. M. Musthafa, and P. Krishnamurthi, Synthesis, growth and characterisation of a semiorganic nonlinear optical material: L-threonine cadmium chloride single crystals, Arabian Journal of Chemistry 10 (2017) S3962-S3966. https://doi.org/10.1016/j.arabjc.2014.06.003

CHAPTERS – IV

GROWING, CHARACTERISTICS ON L-LYSINE HYDROGEN CHLORIDE (LLHC) SINGLE CRYSTAL FOR OPTOELECTRONIC APPLICATIONS

4.1 Introduction

These days, the applications in optoelectronics and photonics depend on nonlinear optical materials highly fundamental to substantially more than different materials [1]. The natural materials are deftly planned of sub-atomic dynamic that NLO crystals and stood out in light of the minimal expense required for applications utilizing reasonable contributor (donor) and acceptor. The gigantic optical nonlinearity is grown almost too unique properties of organic crystals, which is being used in low profile off frequencies in the UV locale. Along these lines, organic NLO crystals are needed for use in the use of optical gadgets. The feeble van der Waals are frequently planned as organic material. Hydrogen bonds subsequently have a severe level of delocalization. However, these organic crystals have specific limitations, such as poor mechanical and thermal stability. To overcome these problems, researching a combination of organic and inorganic hybrid compounds leads to finding a new class of materials for electronic industries, called semi-organic materials. The organic ligand is ionically bonded with an inorganic host; thus, the new semi-organic crystals have higher mechanical strength and chemical stability [2]. The amino acids are assuming a crucial part of nonlinear optical crystal development for a few specialists. The characteristic amino acids are separately showing nonlinear optical properties. They are a donor NH₂, acceptor COOH; likewise, intermolecular charge move is conceivable [3]. Particularly regular amino acids are aspartic, glutamic, just as arginine, lysine, l-alanine [4]. The γ -glycine [5] was clearly showing NLO movement. It has resulted in the light of first in COOH group and NH2 group an extra is developing of that materials. The dopant with amino acids materials [6-8] is improved by the material properties of nonlinear optical, ferroelectric properties also applications. The semi-organic mixtures are organized with L-histidine tetrafluoroborate, L-arginine diphosphate single crystals. They are described for [9-10] with decently high mechanical and chemical solidness.

The capacity to utilize potential semi-organic materials has been developed the single crystals and the nonlinear optical properties of L-Lysine hydrogen chloride (LLHC - C₆H₁₅ClN₂O₂) with atomic weight of 182.65 and Parent Compound CID 5962 with creating strategy for slow evaporation solution growth method at environmental conditions. The crystallizes of LLHC in a monoclinic crystal structure in the space group of P2₁2₁2₁. The new

crystals are affirmed that investigations of XRD and FT-IR analyzer are investigated in optical, thermal, and mechanical properties. The LLHC single-crystal outcomes are discussed and introduced in a component in the ensuing parts.

4. 2. Experimental Techniques

4.2.1 Solubility test

The slow evaporation technique performs a fundamental function is observed relatively soluble with choice of a solvent, i.e., water, ethanol, methanol, and combined solvent. The deionized water with magnitude relation 1:1 is mixed solvents of ethanol usage of deionized water when obtaining that of solubility test and LLHC to be used for solubility find out about with growth to repeated recrystallization processes. The temperatures 30°C, 35°C, 45°C, and 55°C analysis of solubility scan is consistent temperature tub with accuracy ± 0.01 K as evidenced in Fig.4.1. The slow evaporation approach with the growth of the samples is administered with the utilization of deionized water and homogenized solvents with the assist of the solubility curve.

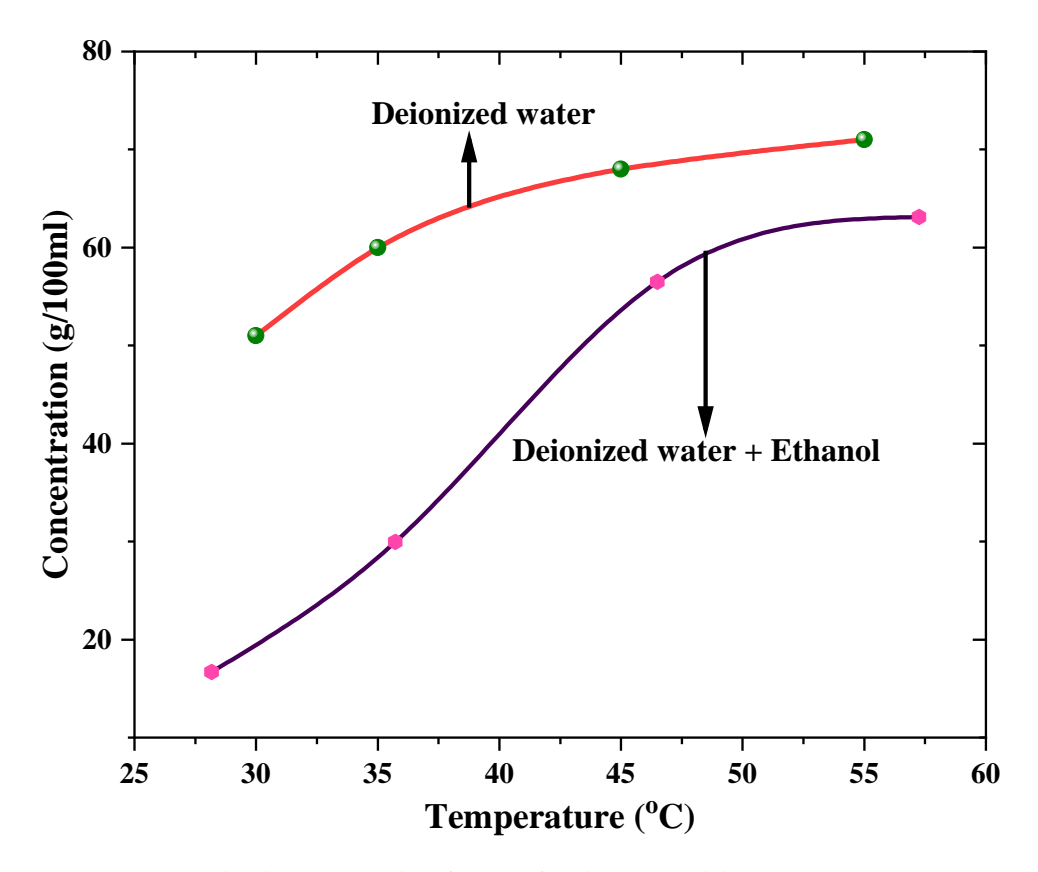


Fig.4. 1 analysis of LLHC with solubility curve.

4.2.2 LLHCsingle crystals Growing process

The dissolved in an exceedingly 100ml of deionized water at 35°C have been recrystallized in LLHC. Then, the gaining to saturation from the choice's solution determined that micro filter paper utilizes a thickness of 10µm. The options of the resolution had been optimally closed with the employment of a perforated skinny polyethylene sheet. They positioned the solution in an exceedingly steady temperature bath within the seed growth method. The options solutions temperature bath has been gradually reduced considering at 35°C frequency 0.1K to 0.3K/day. Then, they have reached the room temperature at 31.6°C to accumulated for the appropriate seed crystals. The saturation solution equipped at 32°C has been targeted with seed crystal reserved in constant temperature, each of the solutions optimally connected precise evaporation. The solutions colorless single crystal with the magnitudes of 16 x 10 x 4 mm³ have been gathered consequently 34 days combined to solvents of deionized water and ethanol of LLHC single crystals as proven in Fig. 2a and Fig. 2b. LLHC single crystals are received from combined solvent use decrease transparency related with the crystals growing the utilization of deionized water as a solvent for studies the chemical form of the crystals was agreed as shown in Fig. 4.2.

$$H_2N$$
 OH . HCl . $2H_2O$

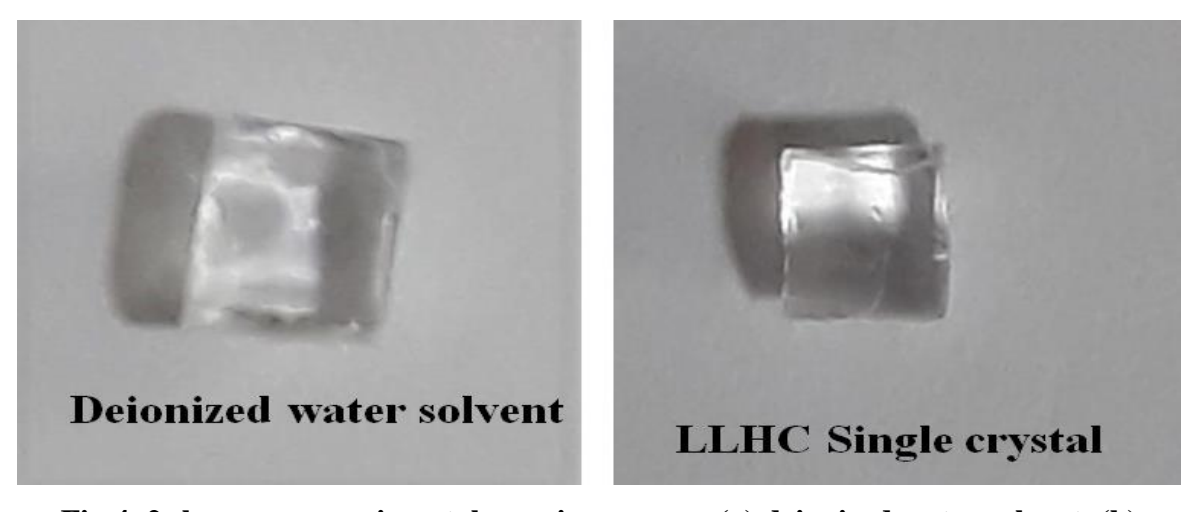


Fig.4. 2 shows an experimental growing process (a) deionized water solvent, (b)

Grown in LLHC Single crystal.

4.3. Result and Discussion

4. 3.1 LLHC Characterization studies on X-ray powder diffraction evaluation

We are measured by using instruments of ENRAF NONIUS CAD4 X-ray diffractometer and analyzed the LLHC Single-crystal XRD **facts** to the cell's parameter values are a = 4.7531\AA , b = 12.2467\AA , c = 6.6134\AA , then α = 90.12° , β = 96.54° , γ = 91.12° , and V = 614.376\AA^3 . The single crystal as LLHC powdered samples have **been** exposed with powder X-ray diffraction investigate in Rich Seifert X-ray diffractometer using CuK α radiation of wavelength 1.6329\AA with a scan speed of 0.3° /sec. X-ray diffraction spectrum with top values has been analyzed by way of the usage in the Proszki software program package [11]. The single-crystal XRD statistics are won utilizing the powder XRD evaluation per the samples and powder X-ray diffraction sample of LLHC as shown in Fig. 4.3.

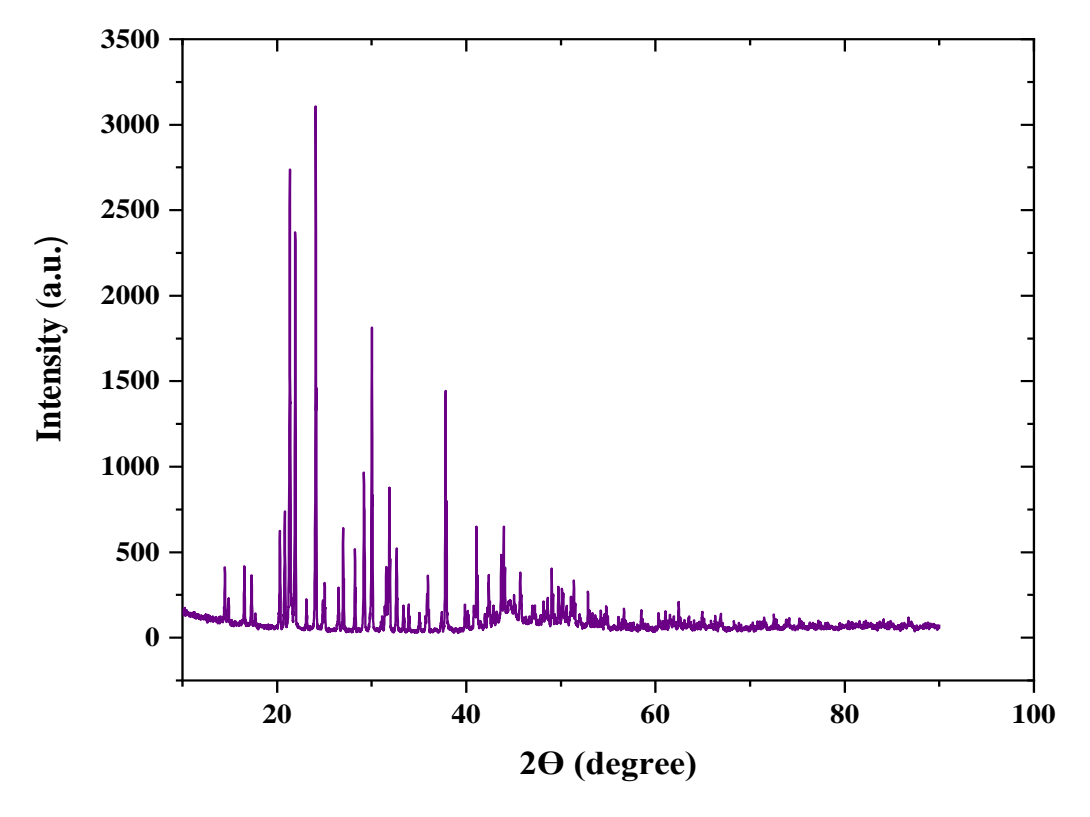


Fig.4.3 shows in sample powder XRD pattern analysis of LLHC.

4.3.2 LLHC analysis of FTIR - FT-Raman spectra

Fig. 4.4 as the FTIR contemplates are perceived through the functional group's helpful assemblies utilizing BRUKER 66V FT-IR spectrometer with a 4000-400 cm⁻¹. FT-RAMAN examines used to be adjusted that new crystals for vibrational frequencies as demonstrated in Fig. 4.5. They have concerned via units of Bruker FRA 106 FT RAMAN Spectrometer with

varying of 50-3500 cm⁻¹. The samples as NH₃ essentially dependent on the torsional mode band are found that wave numbers from 563cm⁻¹ and 621 cm⁻¹ as Raman and FT-IR range, individually. A substance torsion shaped in a band has been found that wave number of 563 cm⁻¹ and related in torsion with C-C shape [12]. The pattern band vibrations of the stressing with the guide of CO₂ mode are probably allocated at wave numbers 872 cm⁻¹ and 865 cm⁻¹ with a Raman - IR range, individually. The wave numbers are 931 cm⁻¹ with an IR of a band, and 919 cm⁻¹ in the Raman range is a wagging vibration of CO₂ - structure. The IR spectrum range with peak value is 811 cm⁻¹, and the Raman range wave range is 751 cm⁻¹, which is situated in the torsion of the C-O-H state of the composite. The Raman spectrum range of the intense band is 1114 cm⁻¹, and the IR spectrum range is 1001cm⁻¹. It identifies with stretching of C-C-N structure, which depends absolutely on the task of the equal state of one of the amino acids of L-Lysine [13]. The composite of C-C stretching vibrations was once perceived at groups with wave numbers of 1214 and 1248 cm⁻¹. The C-N-stretching vibrations have been stressed with a carbon shape. The nitrogen of the amino group has seemed that bands of wave number of 1806 cm⁻¹, which is discovered the band with wave amount of 1879 cm⁻¹ with IR spectrum range, it is C-C-N asymmetric stretching vibration as exhorted by Diem et al. [14]. The wave number top qualities are 1800 cm⁻¹ with an IR spectrum range has situated for the shaking of NH₃ shape, a similar wave assortment by [14]. The band of C-H group esteems discovered in LLHC with wave numbers of 1909, 2011, and 1291 cm⁻¹ in the IR range, and bend with vibrations of the CH₃ team is LLHC crystal with wave number 1417 cm⁻¹. However, this height is absent in the IR spectrum. The disclosure with CO₂ on the LLHC gem wave number is 2214 cm⁻¹ [14]. The vibration worth of NH₃ with LLHC crystal [15] is resolved in wave numbers 1446 cm⁻¹ and 1452 cm⁻¹ in the IR and Raman spectra, separately. The Raman and IR spectra in stretching vibrations of NH₃ are excessive wave number areas of C-H structures, which is found at wave numbers of 2875 cm⁻¹ and 2939 cm⁻¹. The functional group assessment of FT-IR and FT-RAMAN with a composite LLHC crystal has been distinguished.

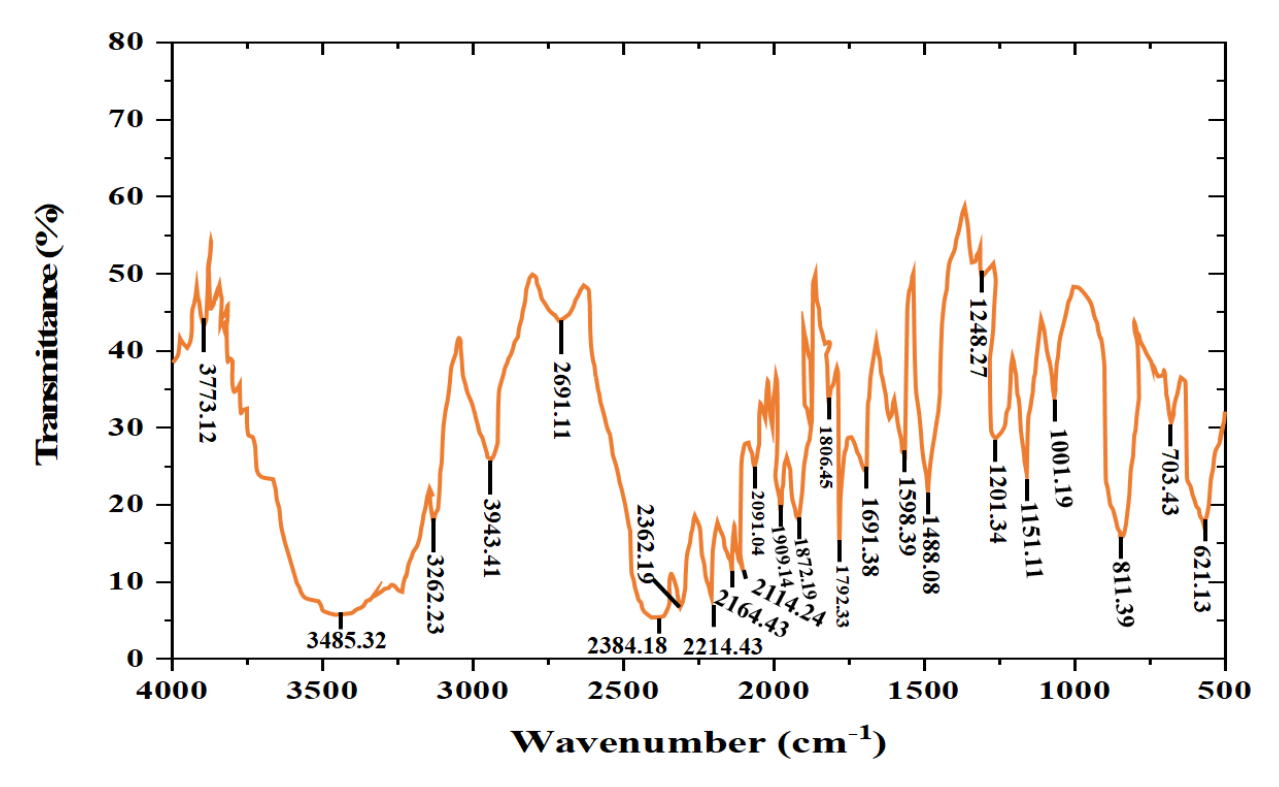


Fig.4. 4 shows in LLHC analysis of FT-IR spectrum.

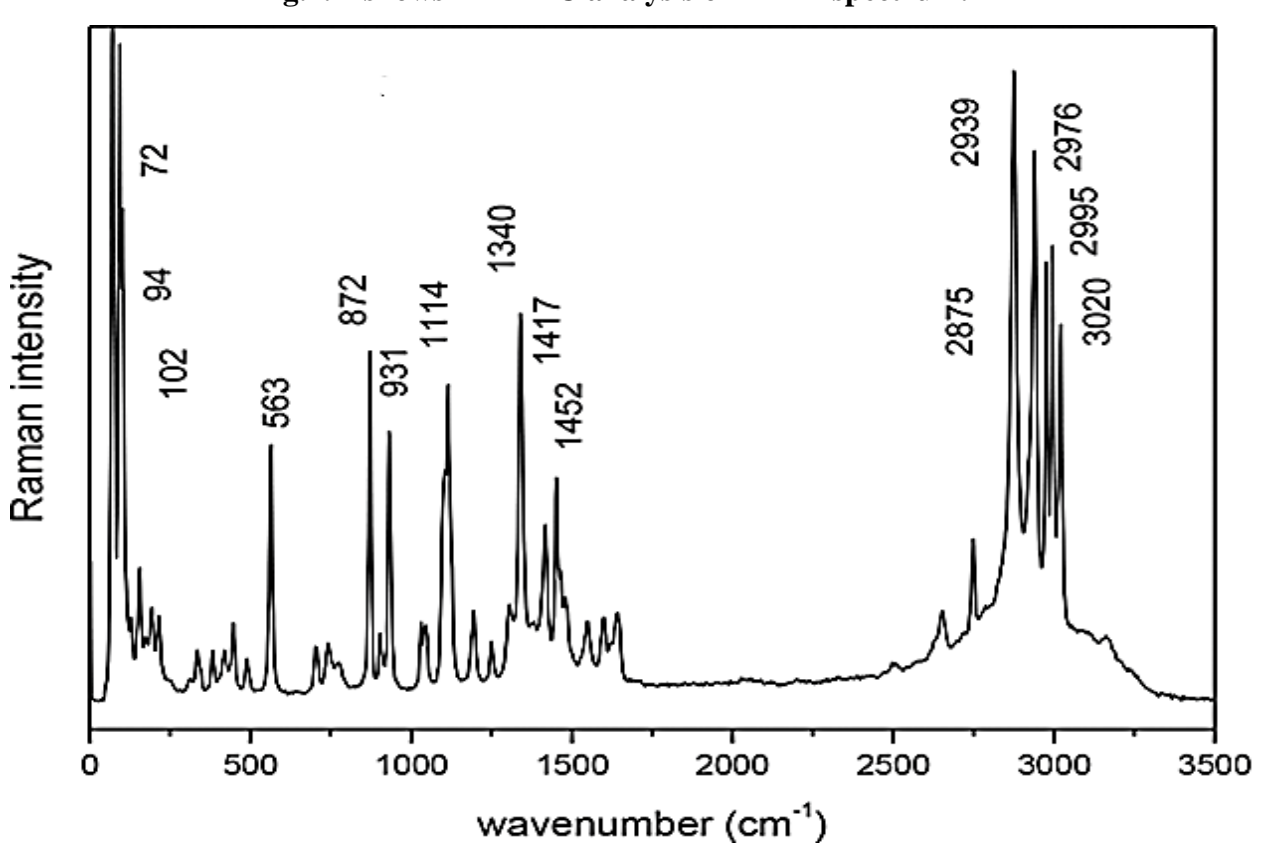


Fig.4. 5 shows in LLHC crystal analysis of FT-Raman spectrum.

4.3.3 LLHC crystal analysis of NMR process

The single crystals have been estimated that NMR spectra, which are utilized devices of JOEL GSX 400 NB FT NMR Spectrometer, 500 MHz, ¹H NMR range esteems are affirmed in Fig. 6. An intense signal created 4.72ppm from the NH₂ and NH₃⁺ groups, and a 4.51ppm signal demonstrated in the methylene carbon outfitted to a carboxyl group, which is offered from a CH₂ signal of 4.10ppm. 3.38 ppm signal is affirmed in carbon conveying the terminal NH₂ group. The terminal carbon is at a 3.29 ppm sign, and 2.24 ppm is provided for the methylene carbon. Since it is not, at this point demonstrated the carboxyl proton signal from the range spectrum. It is stressed that the trait with signal to appears to be around 2.19 ppm. The new crystals are developed from the carbon intuitive of the NMR valuable is demonstrated the use of ¹³C NMR as shown in Fig. 4.7. The carboxylic carbon signal is 158.6ppm, consistent that substances and six signals are found with particular six kinds of carbons essentially affirm, which is virtue materials.

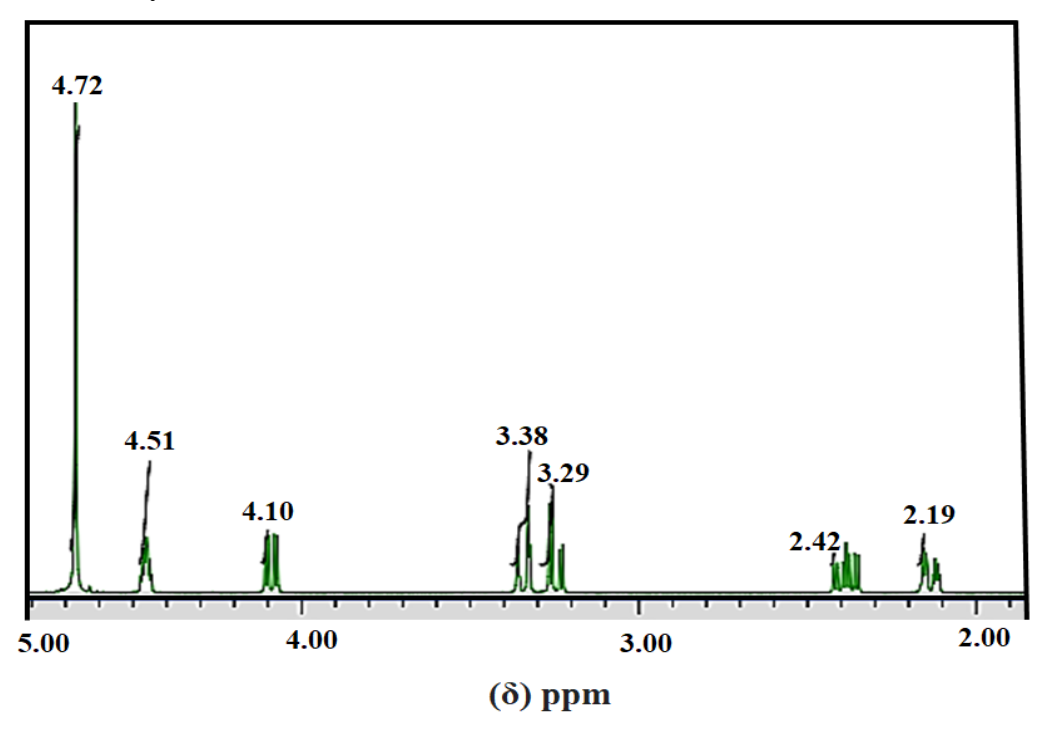


Fig.4.6 shows LLHC crystal analysis of ¹H NMR spectra.

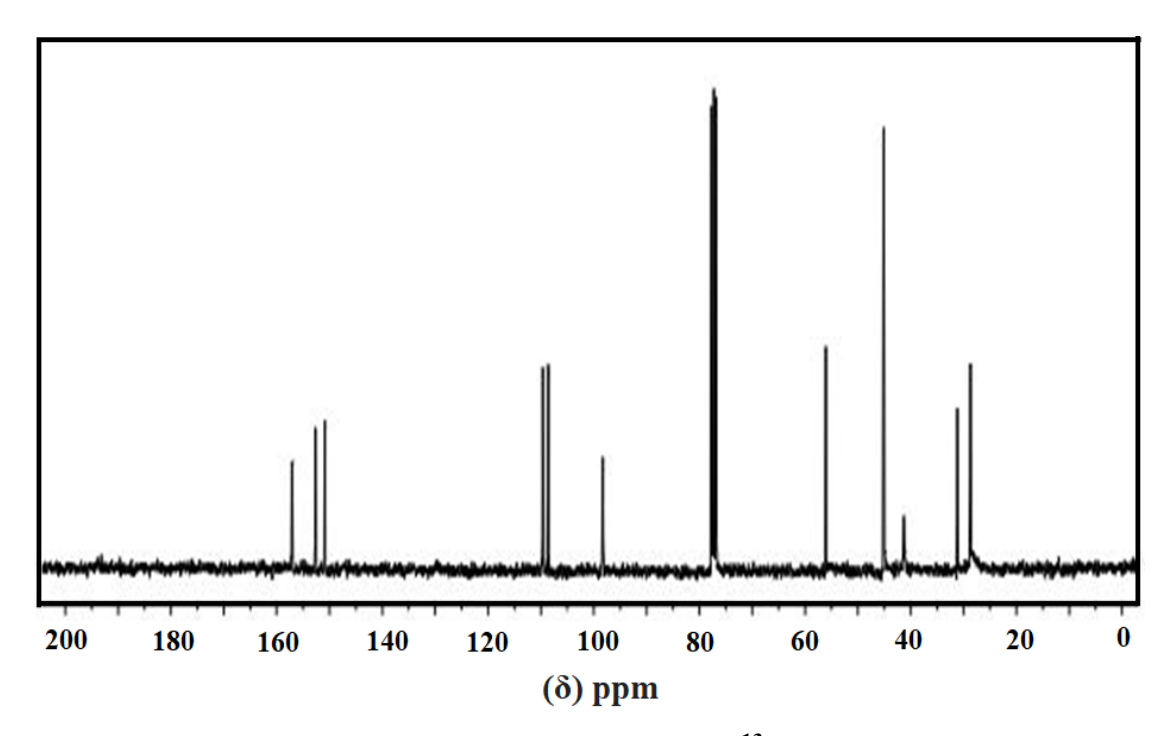


Fig.4. 7 shows LLHC crystal analysis of ¹³C NMR spectra.

4.3.4 LLHC crystal analysis of Thermal process:

The new substances have been dissected of thermogravimetric (TG), Differential thermal (DT), which is estimated using the tools of NETSZCH STA 409C. LLHC crystal is estimated through thermogravimetric spectra in the middle differ of 40°C and 800°C. It is a heating charge of 12K/min with nitrogen air. 17.3% reduction 100°C because of water loss of a weight reduction thermogram and its differential shape (DTG) as demonstrated in Fig. 8. Weight reduction ascribed the failure of sharp grid water of the samples to the decomposition of models is a significant weight loss of about 51.13% in between 360°C and 250°C. They are one more weight loss the deterioration the somewhere in the range of 430°C and 540°C, and the significant weight reduction have corresponded to about 18.3%. The samples dependent on this examination are through the significant deterioration happens at 270°C, its misuse for application ought to be done underneath 60°C, the loses that lattice water over this temperature. The two water particles of LLHC crystal comprise through the deficiency of cross-section water, which is a genuine relationship with the crystal structure. Likewise, the completed heating rate of 12K/minute in the N₂ air assessment of the differential thermogram fluctuates is 40°C and 800°C. Fig.4.8 is ensuing of DTA suggestion an endotherm under 60°C that compares to the deficiency of cross-section water in the DTG curve. The arrangement of endothermic changes of LLHC crystals corresponds intimately with the

deterioration exploratory in the DTG curve. It is reasoned that describes with a crystal decays even aside from dissolving.

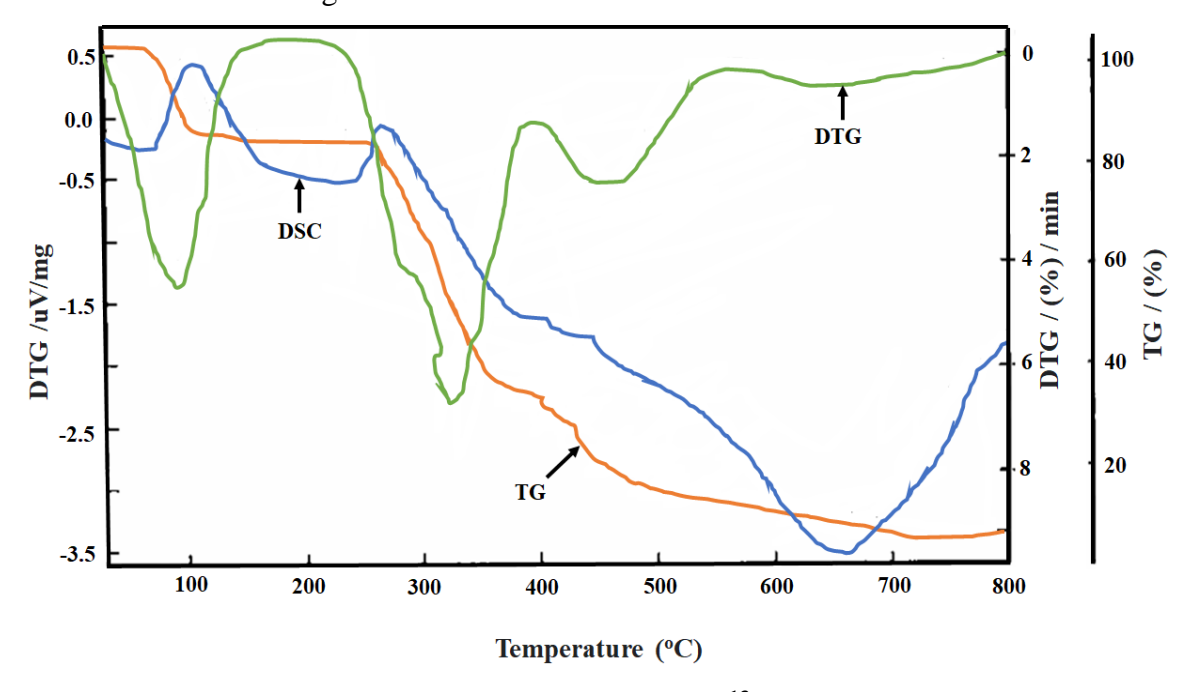


Fig. 4.8 shows LLHC crystal analysis of ¹³C TG-DTAspectra.

4.3.5 LLHC crystal analysis of Vicker's micro hardness

The organic crystals evaluation of Vicker's micro hardness is required acceptable quality for gadget manufacture. The second harmonic generation analysis of a single crystal is constantly contrasted with bring down the inadequate areas from the more impressive areas. The optical exhibition of good quality crystals is required in mechanical conduct as [16-17]. The micro hardness is studies of crystals foster using in Vicker's micro hardness utilizing an optical microscope, i.e., an analyzer of Leitz Wetzler's hardness. The micro hardness studies are analyzed of the samples with various loads of 5, 10, 15, and 25g. The LLHC crystal is chosen surface, which is cleaned utilizing a velvet cloth to get a smooth surface using the above loads of the hardness discovered. The LLHC crystal with Vicker's micro hardness has been estimated utilizing the H_v=1.8627 P/d² (kg/mm³) connection between solidity and load, as demonstrated in Fig. 4.9. The pack is expanded that LLHC crystal increments' hardness gradually diminishes with further raising of the shipment. The crystal breaks are shaped at 50g then it is relatively more complicated when contrasted with other organic crystals [18-19].

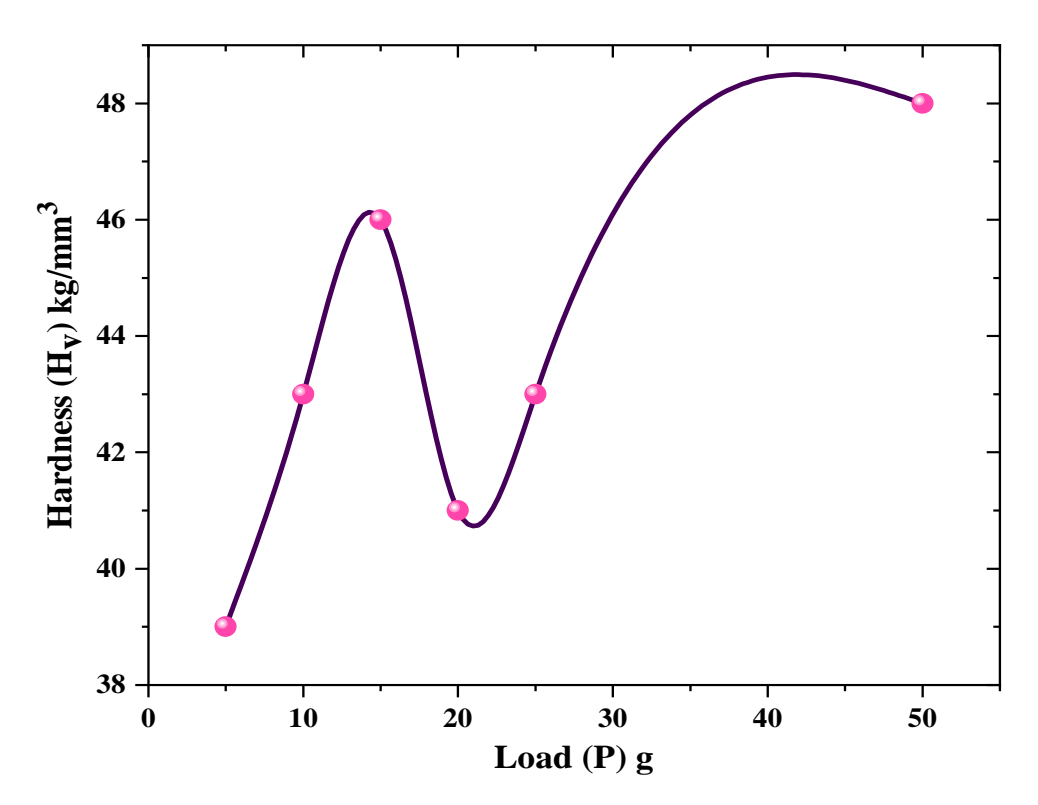


Fig. 4.9 shows LLHC crystal analysis of hardness vs. load.

4.3.6 LLHC crystal analysis of transmission spectra

This crystal is grown from deionized water, a blended dissolvable after recorded utilizing the UV-Visible spectrometer in the frequency range 200-800nm as demonstrated in Fig. 10 (i) and 10(ii). The LLHC crystal was once developed from deionized water and blended dissolvable from the cut-off frequencies range of 210nm and 240nm. The high conveyance of 99% contrasted with blended dissolvable, it appears to be likewise developed crystal from deionized water, and frequency range is 210 nm to 800 nm. In these investigations, the new materials are precious for NLO applications.

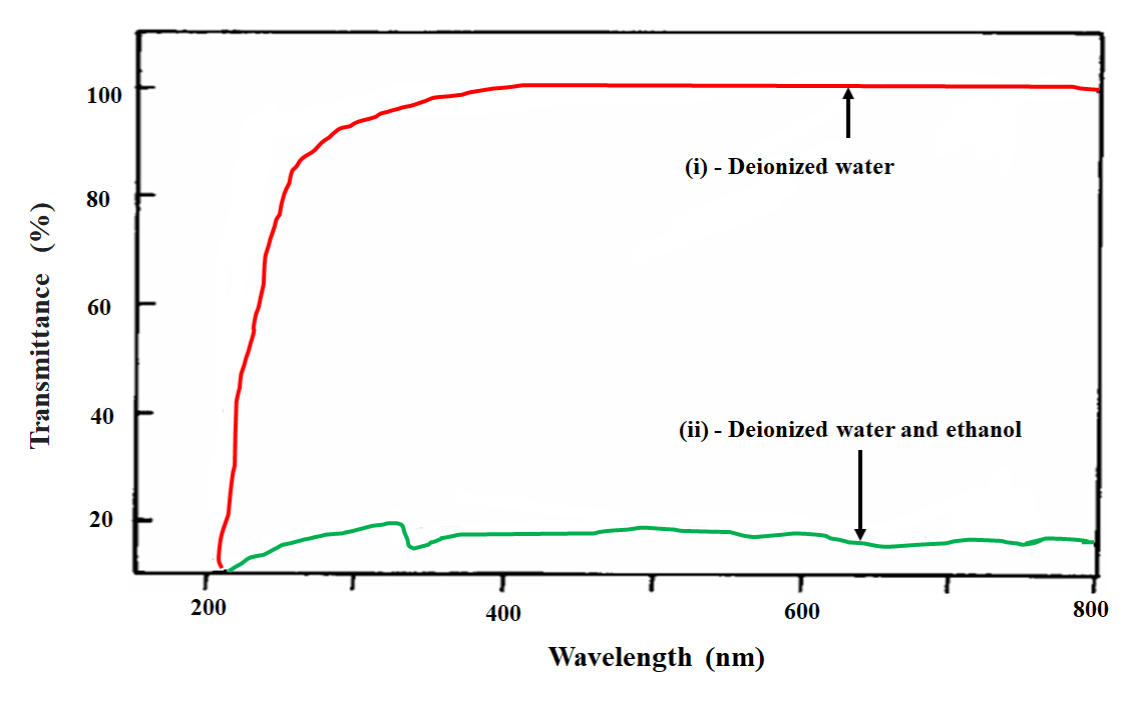


Fig.4. 10 (i) and (ii) shows transmittance spectra of LLHC crystal.

4.3.7 LLHC crystal analysis of NLO assessment

The powder technique is estimated in an SHG analysis investigation of the LLHC powder tests. From the X-rayed about 1064nm through the Nd: YAG laser. It is seen that the green light frequency of 532nm. The information energy of 5.4mJ/pulse is achieved in a second harmonic signal of about 60.6mV

4.4 Conclusion

The LLHC crystals have been effectively filled in the environment utilizing the slow evaporation solution arrangement in the growth method. The deionized water and blended dissolvable ethanol at that point water have resolved the solubility of LLHC. The vibrational frequencies of LLHC are concentrated in FTIR and FT-RAMAN measures. It is located that it be NLO material having a short cut-off wavelength inside the UV locale.

References

- [1] BalamuruganN, LeninM and RamasamyP, Growth of TGS crystals using uniaxially solution-crystallization method of Sankaranarayanan-Ramasamy, *Crystal Research & Technology*, **42** (2),151-156 (2007)https://doi.org/10.1002/crat.200610788
- [2] Krishna ReddyKSR, SwapnaK, Mahamuda Sk, VenkateswarluM, Srinivas PrasadMVVK, RaoAS and Vijaya Prakash G, Structural, optical absorption and photoluminescence spectral studies of Sm3+ ions in Alkaline-Earth Boro Tellurite glasses,

 Optical Materials, 79, 21-32(2018)

 https://doi.org/10.1016/j.optmat.2018.03.005
- [3] Annapurna DeviCh B, MahamudaSk, SwapnaK, Venkateswarlu M, Srinivasa RaoA and Vijaya PrakashG, Compositional dependence of red luminescence from Eu 3+ ions doped single and mixed alkali fluoro tungsten tellurite glasses, *Optical Materials*, 73, 260-267 (2017) DOI: 10.1016/j.optmat.2017.08.010
- [4] Shaik Babu, Radhia Trabelsi,and Tadikonda Srinivasa Krishna,Reduced Redlich–Kister functions and interaction studies of Dehpa + Petrofin binary mixtures at 298.15 K, *Journal Physics and Chemistry of Liquids An International Journal*, **57** (4),536-546 (2019) https://doi.org/10.1080/00319104.2018.1496437
- [5] Nisha Deopa, RaoAS, MahamudaSk, Mohini Gupta, JayasimhadriM, HaranathD and Vijaya PrakashG, Spectroscopic studies of Pr3+ doped lithium lead alumino borateglasses for visible reddish orange luminescent device applications, *Journal of Alloys and Compounds*, 708, 911-921 (2017) https://doi.org/10.1016/j.jallcom.2017.03.020
- [6] Shweta, MalodeJyothi J, AbbarSharanappa C and NandibewoorT, Mechanistic aspects of uncatalyzed and ruthenium(III) catalyzed oxidation of dl-ornithine monohydrochloride by silver(III) periodate complex in aqueous alkaline medium,

- Inorganica Chimica Acta, **363**(11), 2430-2442 (2010) https://doi.org/10.1016/j.ica.2010.03.081
- [7] NagababuP, Shaik Babu, Dheiver, SantosF and GowrisankarM, Investigation of molecular interactions in binary mixtures of homologous series of aliphatic alcohols with 2-methoxyaniline at various temperatures, *Physics and Chemistry of Liquids an Int. J.*, **57**(5), 689-702 (2019)https://doi.org/10.1080/00319104.2018.1511787
- [8] Viswanath Valikalaa, Induja and Santhakumar Kannappana, Synthesis and effect of pegylation on citric acid dendritic nano architectures anchored with cefotaxime sodium,

 J. of Photochemistry & Photobiology B: Biology, 201, 111683 (2019)

 https://doi.org/10.1016/j.jphotobiol.2019.111683
- [9] IlangoE, RajasekaranR, ShankarK and Chithambaram V, Synthesis, growth and characterization of nonlinear optical Bisthiourea ammonium chloride single crystals by slow evaporation technique, *Optical materials*, **37**, 666-670 (2014) https://doi.org/10.1016/j.optmat.2014.08.011
- [10] ParvezAhmad, VenkateswaraRaoA, SureshBabuK, NarsingaRaoG, Particle size effect on the dielectric properties of ZnO nanoparticles, *Materials Chemistry and Physics*, **224**, 79-84 (2019) https://doi.org/10.1016/j.matchemphys.2018.12.002
- [11] Venkateswara Rao, Ranjith KumarB and RamaraoSD,Structural, microstructural and electrochemical studies on LiMn2-x(GdAl)xO4 with spinel structure as cathode material for Li-ion batteries, *Ceramics Int.*,44(13), 15116-15123 (2018) https://doi.org/10.1016/j.ceramint.2018.05.148
- [12] Krishna JyothiN, Venkata RatnamK, Narayana MurthyP and Vijaya Kumar K, Electrical Studies of Gel Polymer Electrolyte based on PAN for Electrochemical Cell Applications, *Materials Today: Proceedings*, **3**(1), 21-30 (2016) https://doi.org/10.1016/j.matpr.2016.01.112

- [13] Shahenoor BashaSk, Sunita SundariG, Vijay KumarK and Ramachandra RaoK M C,

 Preparation and dielectric properties of PVP-based polymer electrolyte films for solidstate battery application, *Optik*, **164**596-605 (2018)

 https://doi.org/10.1016/j.ijleo.2018.03.071
- [14] SureshC and ShanmuganS, Effect of water flow in a solar still using novel materials, *J. of Thermal Analysis and Calorimetry*, (2019)https://doi.org/10.1007/s10973-019-08449-5
- [16] Shahenoor BashaS K, Vijay KumarK, Sunita Sundari G and RaoM C, Structural and Electrical Properties of Graphene Oxide-Doped PVA/PVP Blend Nanocomposite Polymer Films, *Advances in Materials Science and Engineering*,1-11 (2018) https://doi.org/10.1155/2018/4372365
- [15] KhandpekarMM and PatiSP,Growth and characterisation of new nonlinear optical material α-glycine sulpho-nitrate (GLSN) with stable dielectric and light dependent properties, *Opt. Commun.*,**283**(13), 2700-2704 (2010) DOI: 10.1016/j.optcom.2010.03.01
- [17] HameedASH, RaviG Dhanasekaran R and RamasamyP, Studies on organic indole-3-aldehyde single crystals, *J. Cryst. Growth*, **212** (1–2), 227-232 (2000)https://doi.org/10.1016/S0022-0248(99)00896-9
- [18] SaminathanP, SenthilKumarM, Shanmugan S and Chithambaram V,Growth and Characterization of L-Lysine Monohydrochloride Dihydrate (LMHCl) Single Crystals by Slow Evaporation Technique, *Materials Today: Proceedings*, **18**(3),1256-1262 (2019) https://doi.org/10.1016/j.matpr.2019.06.587
- [19] Dinakaran S., Sunil Verma, Das, S.J. *et al.*, Determination of crystalline perfection, optical indicatrix, birefringence and refractive-index homogeneity of ZTS crystals, Appl. Phys. B,**103**, 345–349 (2011) https://doi.org/10.1007/s00340-010-4256-7

- [20] Suresh C, ShanmuganS, Bharath MV, Naveen B and Chithambaram V, Experimental analysis of Energy and Environment redeemable in solar Nano-basin still to improve Sullage Water Natural Treatment of Fuzzy Application, *Materials Today:*Proceedings, 18(3), 1263-1271 (2019) https://doi.org/10.1016/j.matpr.2019.06.588
- [21] PalanikumarG, ShanmuganS, JanarthananB, SangaviR and GeethanjaliP, Energy and Environment control to Box type Solar Cooker and Nanoparticles mixed bar plate coating with Effect of Thermal Image cooking pot, *Materials Today:**Proceedings, 18(3),1243-1255 (2019) https://doi.org/10.1016/j.matpr.2019.06.586
- [22] BhavaniS, ShanmuganS, SelvarajuP, MonishaC and SuganyaV, Fuzzy Interference Treatment applied to Energy Control with effect of Box type Affordable Solar Cooker,

 *Materials** Today: Proceedings, 18(3), 1280-1290

 (2019) https://doi.org/10.1016/j.matpr.2019.06.590
- [23] Peter Muller, Practical suggestions for better crystal structures, Crystallography Reviews, **15** (1), 57-83 (2009)https://doi.org/10.1080/08893110802547240
- [24] Ben SalahA M, NailiH, MhiriT and BatailleT, Synthesis and crystal structure of a chiral aromatic amine chloride salt (C₈H₁₂N)Cl, *Crystallography Reports* **60**(7),1053–1057(2015) https://doi.org/10.1134/S1063774515070032
- [25] Synder A W, Coupled-Mode Theory for Optical Fibers, Journal of the Optical Society of America, 62 (11), 1267-1277 (1972) https://doi.org/10.1364/JOSA.62.001267
- [26] Valsecchi G B, Milani A, Gronchi G F, Chesley S R, Resonant returns to close approaches: Analytical theory, Astronomy & Astrophysics (A&A), 408 (3), 1179-1196 (2003) https://doi.org/10.1051/0004-6361:20031039

CHAPTER - 5

GROWTH AND CHARACTERIZATION OF L-LYSINE DOPING WITH EFFECT
OF HYDROCHLORIDE CITRIC ACID - GLYCINE BARIUM CHLORIDE
(LHCAGBC) ON THE GROWN SINGLE CRYSTALS FOR OPTICAL SENSOR
APPLICATIONS

5.1 Introduction

Nowadays, modern life has improved the society and commercial, industrial day by day developing for scientific researchers have done in consume approximately 60% of the world's optical sensors device. It is almost impossible to offer a universal characterization of crystalline resources for energy transfer because the feeling of a single crystal is affected by changing favourites and specific characters of the civilization of humans living in different fabrications of NLO zones. An insufficient study was showing on NLO satisfaction of energy transfer before to date; The main goal of the current study is to attract a contrast between the NLO parameters for evaluation of energy transfer of fabrication occupant of the effect materials.

Optical data storage (ODA), optical switches (OS), optical frequency conversion (OFC) and optical communication (OC) devices have extended for applications of optoelectronic by use of novelty in NLO techniques as reviewed by [1 -6]. The organic large NLO coefficients of optical materials were associated with inorganic material, then which have approached to their deprived thermal, mechanical properties, the damage of threshold in low laser performed as [7]. NLO material of novel kinds of the hybrid system to solving the problems are were traveled since organic elements and developments inorganic by [8]. In a study for change metal dopant Co²⁺ have supplementary to the molar (%) for soaked LMHCl explanation for progress NLO possessions of LMHCl crystals reported by [9]. Neelam Rani *et al.*, [10] were developed in L-Lysine mono hydrochloride monohydrate single crystal. The

systematic of the studies were grown the crystal and characterized with improve the strength of the sample to checked and its appropriateness for device manufactures. Saminathan *et al.*, [11] was developed in single crystals of L-Lysine Mono hydrochloride Dihydrate (LMHCl) by used method of slow evaporation. It was studied of the single crystal like XRD, FTIR, optical, thermal properties, UV–Vis and optical absorption visible is found to be at 250 nm. Martin *et al.*, [12] studied in fixed LLOA samples. Optical Constants are estimated from UV analysis, point competition clever, its exhibition of nature defocused behavior. We are used in the Z-scan technique through the third-order nonlinear optical susceptibility was tested in order of 10^{-6} esu. The visual preventive act for a crystal is 532 nm and are verified by means of continuities wave laser rays.

This article intelligence a systematics (synthesis, growth, characterization) are an organic sample, L-Lysine doped Malic acid (C₄H₆O₅) /Oxalic acid (C₂H₂O₄)/ lithium sulphate (Li₂SO₄) (LMOL), which is developed through the conventional slow evaporation solution growth method. The development of the crystal has been considered consuming in the crystal of XRD, Powder XRD, FTIR investigation, UV-vis. Spectroscopy, Thermo gravimetric Analysis (TGA), Differential Thermal Analysis (DTA) and Z-scan process. The entitle also highpoints the nonlinear optical properties of the growth solid which can be used in a nonlinear optical application.

5.2 Materials and Experimental Methodology

The L-lysine single crystals are developed by dissolving AR score to the quantity of L-Lysine Mono hydrochloride Dihydrate in 100ml purified water as tracked of $134.087~g\cdot mol^{-1}$ to 3mol% of Malic acid $(C_4H_6O_5)$ / $126.07~g\cdot mol^{-1}$ to 2mol% of Oxalic acid $(C_2H_2O_4)$ / $109.94~g\cdot mol^{-1}$ 4mol% of lithium sulphate (Li₂SO₄) is supplementary the above translucent solution lower magnetic stirring - pH=2. The soaking solution is sieved through the permitted to dissolve at ambient temperature. Subsequently, seed crystals are increasing

historical to the colors of the solution that have been transformed the solution. The moral excellence of crystals was garnered to a duration of around 42days. The slow evaporation method form of the crystal is determined sizes of $10x12x6mm^3$ and advanced for the novelty crystal is exposed in Fig. 5.1. The enhanced growing state of pure and doped L-Lysine single crystal as follows in Table 5.1.

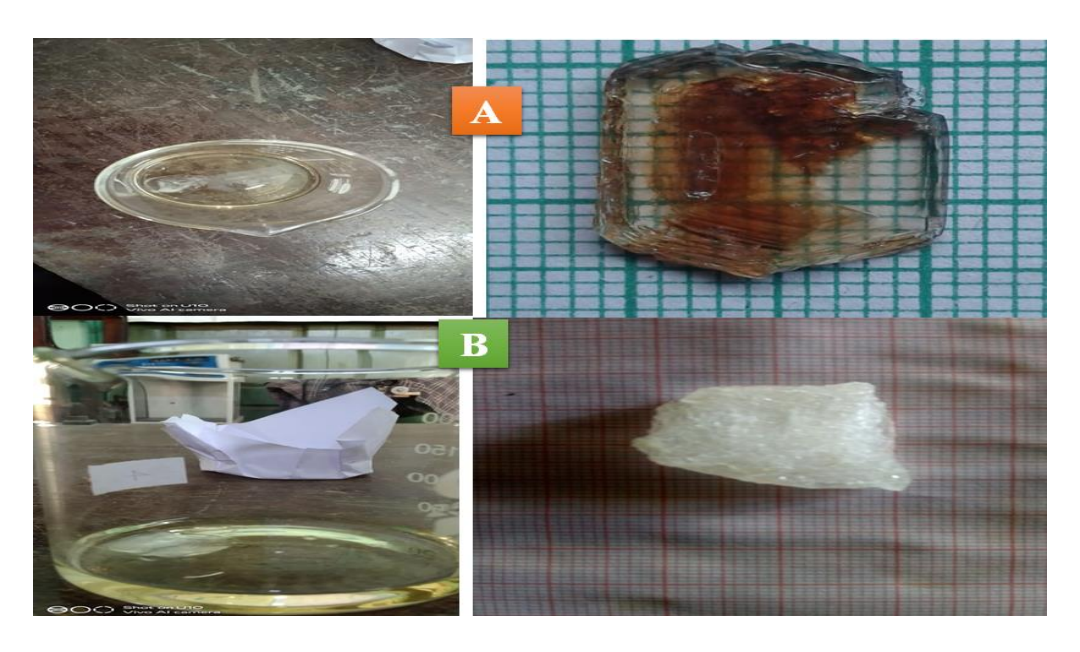


Fig. 5.1 shows effect of pure L-lysine (A) and doped L-Lysine (B - LMOL) grown of single crystals.

Table 5.1. The enhanced growing state of pure and doped L-Lysine single crystal.

S. No	Order of way	Pure L-Lysine	Doped L-Lysine	
1	Technique	Slow evaporation	Slow evaporation	
		solution	solution	
2	Solvent mixer	Pure water	Pure water	
3	Molar relation	L-lysine + Malic	L-lysine+ Malic acid +	
		acid	Oxalic acid + lithium	
			sulphate	
4	Temperature	Room Temperature	Room Temperature	
5	During growth	30 days	42 days	
6	Measurement	$11\times15\times5$ mm ³	10x12x6mm ³	
	of the crystal			
7	Stability	Energy transfer	Energy transfer Strong	
		Week NLO	NLO properties	
		properties		

5.2.1 Characterization of L-Lysine single crystal

The novel single-crystal to XRD analysis of L-Lysine single crystal have been chronicled consuming Enraf Nonius CAD4F & CAD4MV31 involuntary X-ray diffractometer. Developed the crystal is imperiled to FTIR analysis through the sample organized through the palletized method for KBr. FTIR spectra the L-Lysine single crystal is chronicled in the province of 4000-400cm⁻¹ using in Bruker IFS 66W Spectrometer. The novel investigation crystal to an arrangement of characterizing the metal elements is exposed to ICP (Inductively-coupled plasma) investigation to approve an occurrence of L-Lysine in established crystal by ICP-OES-Perkin Elmer Optima 5300DV. Optical properties of the L-Lysine crystal are evaluated by consuming UV-visible to absorption spectra consuming the Varian Cary 5E spectrophotometer in the range of 200–2000nm.

5.3 Results and Discussion

The L-Lysine (LMOL) crystal is absorbed into the light intensity measure the spectrometer and implemented of single crystals by using in NLO applications. An environments control through the LMOL samples has arranged the crystalline advantages of good performance of the structure, compact, convenient to an investigation of results following in crystal XRD, FTIR, UV-vis-NIR, TGA, DTA, and Z-scan process.

5.3.1 The analysis of X-ray diffraction

L-Lysine pure single crystal XRD exposed which the cell parameters are a = 4.88 Å, b = 12.28Å, c = 8.57Å, $\alpha = 90^{\circ}$, $\beta = 98.79^{\circ}$, $\gamma = 90^{\circ}$, Volume = 570Å³. The arrangement of the crystal structure is monoclinic through the space group P2₁. The considered lattice parameters for the doped LMOL was found to be Solubility, g/100 mL a=4.78 Å, b = 12.23Å, c = 8.61Å, and Volume = 583.45Å³ approved with reported value [13, 14]. Therefore, Powder XRD outcomes approve to the combination of metal ions in the crystal lattice of

L-Lysine then do not alteration the crystal system however there is an alteration in the lattice parameters as follow in Fig. 5.2. As formerly, described [9,13] values were associated with the novel crystal investigations are recorded in Table 5.2.

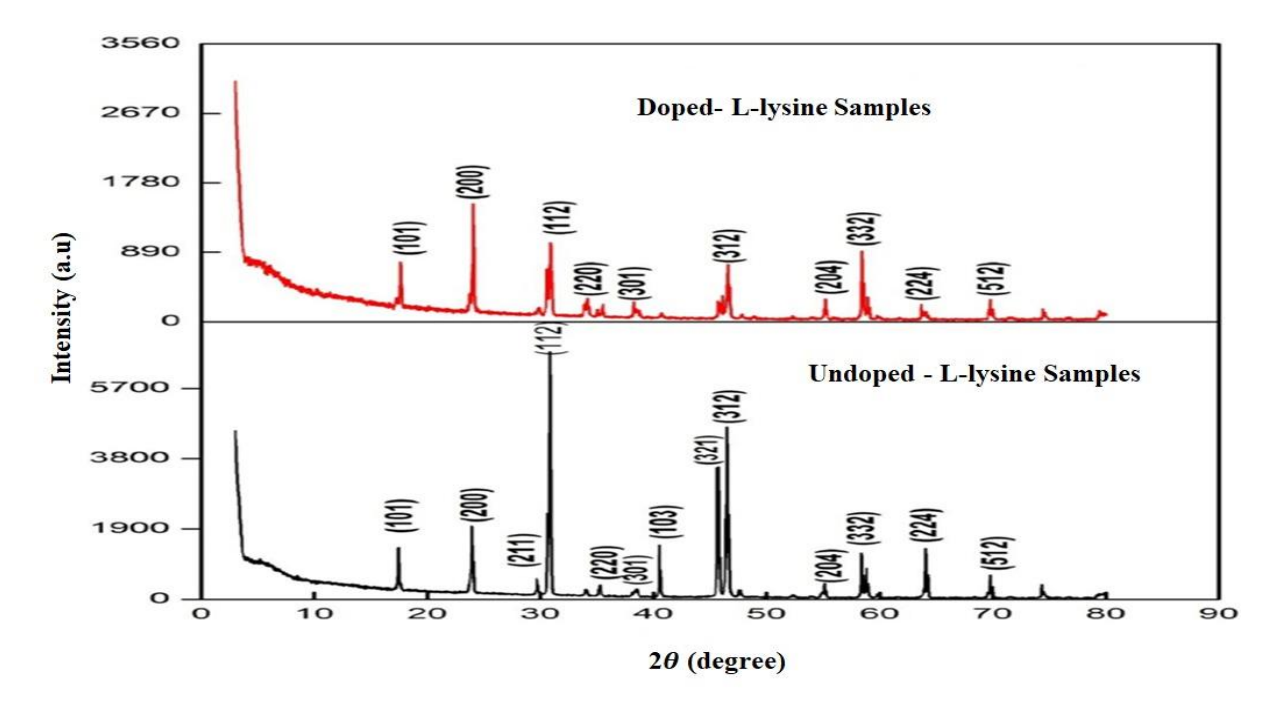


Fig. 5.2 shows doped and undoped LMOL samples on Powder XRD patterns.

Table 5.2. Cell parameters of pure and doped L-lysine single crystals.

Samples	a (Å)	b (Å)	c (Å)	Volume (Å ³)
Pure L-lysine	4.88	12. 28	8.67	570
Doped- L-lysine	4.78	12. 23	8.61	583.45

5.3.2 Solubility test of doped LMOL single crystals

The solubility studies are developed in recrystallized for the process. The solubility of doped LMOL materials in water was determined by dissolving the solute for the water is used in a sealed container upheld at a constant temperature with incessant stirring. Then reaching saturation, the equilibrium absorption of the solute was investigated gravimetrically. The solubility of the manufactured by the doped LMOL crystal as an occupation of temperature for five changed temperatures range of 30°C to 50°C in water is strong minded and designed

as exposed in Fig. 5.3. It is strong minded that the doped LMOL material keeps an optimistic gradient of solubility with a moral solubility.

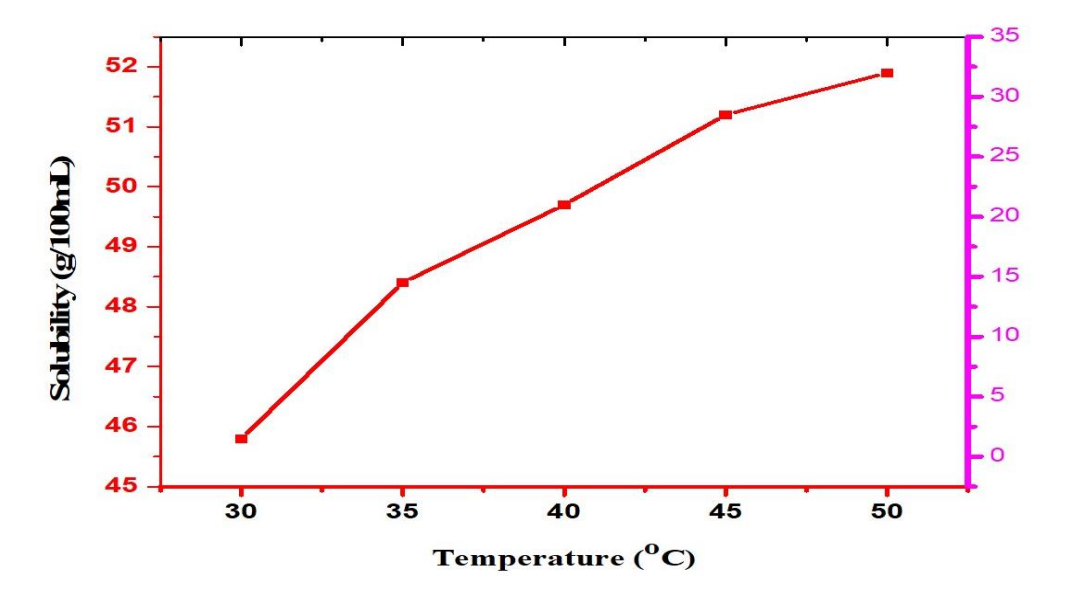


Fig. 5.3 The solubility curve of doped LMOL crystal.

5.3.3 FTIR analysis of LMOL single crystals

The doped LMOL crystals form of infrared spectral analysis is chemical bonding to information productively to use of atomic structure the exposed compound materials. The pure and doped LMOL have been pelletized consuming in KBr. A spectrum is verified by means of the Thermo Scientific Nicolet iS50 FTIR Spectrometer in the series 4000 - 400 cm⁻¹ wave number province. A powder analysis of FTIR spectrum pure and doped LMOL are exposed in Fig. 5.4. The point of peaks about 3438 cm⁻¹ have qualified near NH irregular extending while in doped LMOL sample, its method is originated of 3442cm⁻¹. A point with wave number of a doped LMOL sample is owing towards a contribution for Lysine collections trendy a hydrogen attachment establishment. A point of higher (peak) gained of 3093, 3064 then 2987 cm⁻¹ for doped and undoped LMOL samples, individually are allocated towards CH extending. A higher values (peak) are IR spectra about 2584, 2589 cm⁻¹ used for doped then undoped LMOL sample qualified vibration is experimental as a sharp peak at 1574 cm⁻¹. It is strong observed of 1484 cm⁻¹ by L-lysine doped crystal and deformation for

pure L-lysine however this peak is shifted to 1478 cm⁻¹. A doped then undoped LMOL sample, a highest about 1333 and 1338 cm⁻¹ were owing toward C-N-H symmetric winding. A highest about 1119 cm⁻¹, 899 then 670 cm⁻¹ qualified towards CH₂ shocking then the higher about 1035 then 1040 cm⁻¹ aimed at C-C-N-C symmetric widening aimed at doped then undoped LMOL individually.

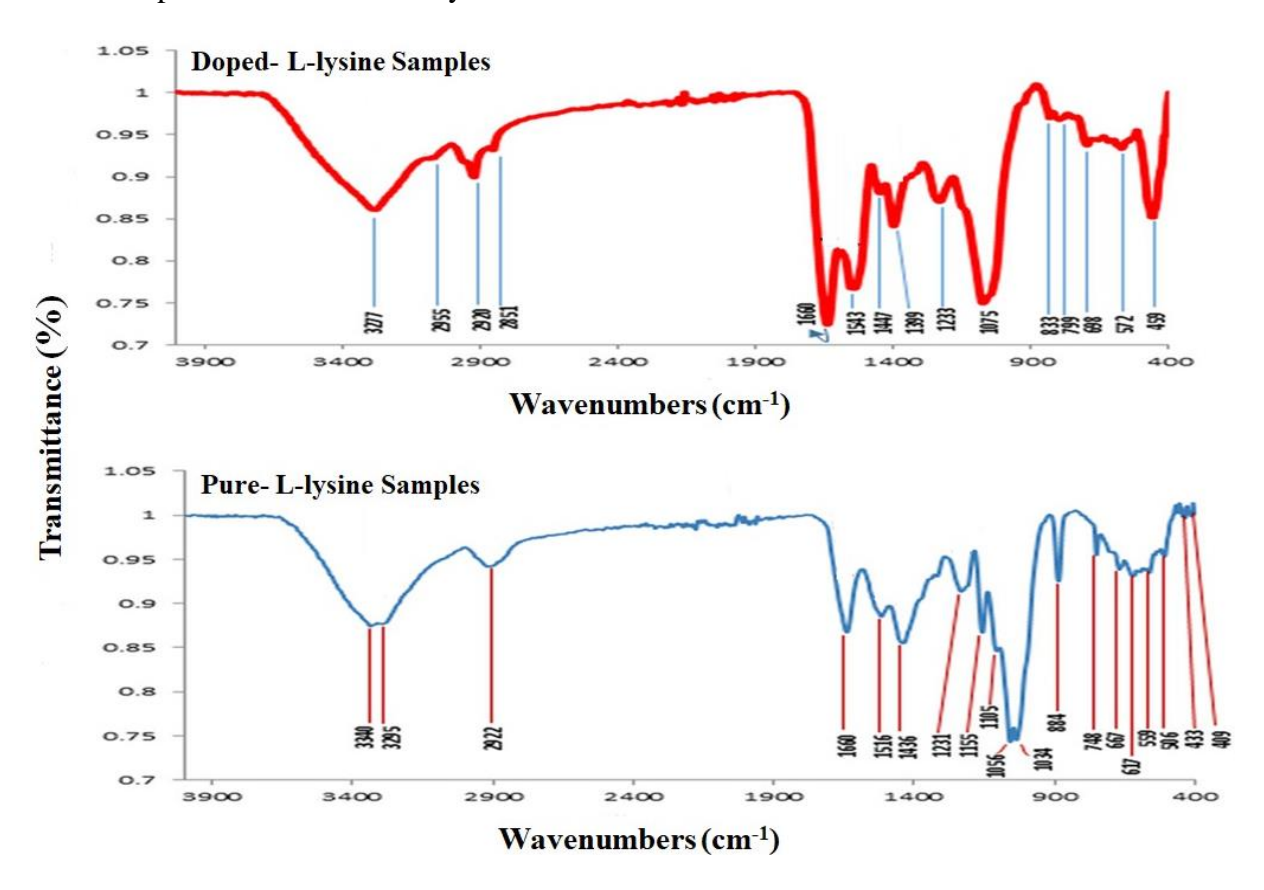


Fig. 5.4. The FTIR spectrum of pure and doped LMOL crystals.

5.3.4 LMOL Crystals analysis of Optical Transmission

A dish of doped and undoped LMOL crystals by the thinness about 1mm is censored. It is refined deprived of slightly covering aimed at optical magnitudes. Optical spread ranges are verified aimed at a grownup sample with a wavelength of 200 to 1200nm. We are used in dual ray UV vis. spectrum in doped then undoped LMOL samples are exposed in Fig. 5.5. A spread range have considered too that doped then undoped LMOL sample is higher transmission trendy a whole vis. NIR section of the spectra property qualifies a crystal resources aimed at a nonlinear optical property. The UV cut off wavelength for pure and

doped LMOL is experimental at 238nm and 261nm with respectively. It is an increased individual for the construction of optoelectronic devices by [15].

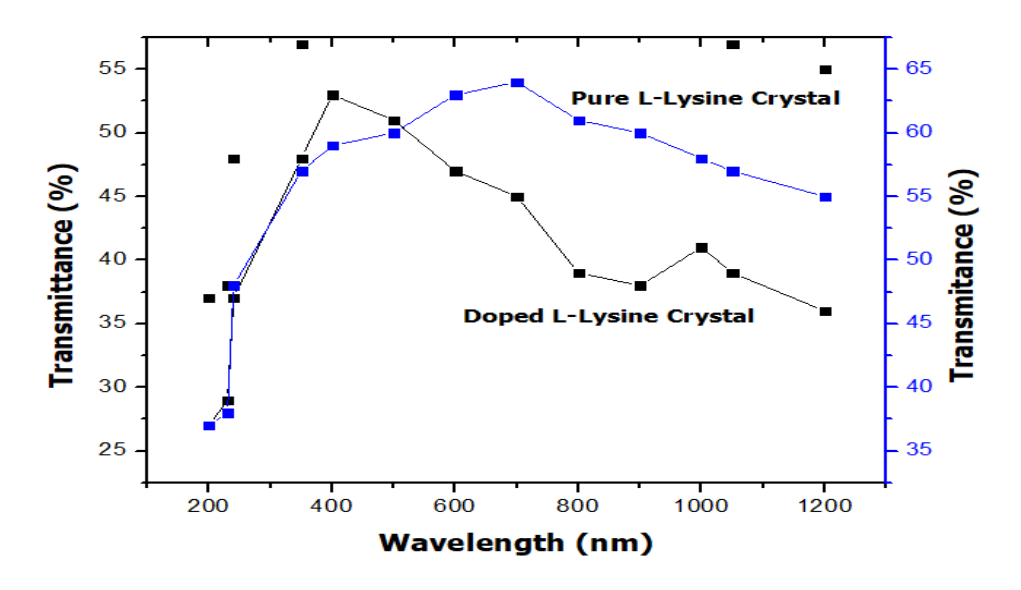


Fig.5. 5 Optical transmission of pure and doped LMOL Crystals.

5.3.5 Assessment of optical Energy:

The samples are studied in the absorption coefficient, transmittance value as following relation of Tauc's plot as shown in Fig. 5.6. L-Lysine samples are used in doped and undoped LMOL with acts from the optical bandgap that were valued at about 5.78eV and 6.10eV. Doped L-Lysine materials have been confirmed to revelations good transmittance in the visible section. Subsequently, the bandgap is 5.5eV by the lower cut off about 300nm and a suitable sample should be used in optoelectronic devices.

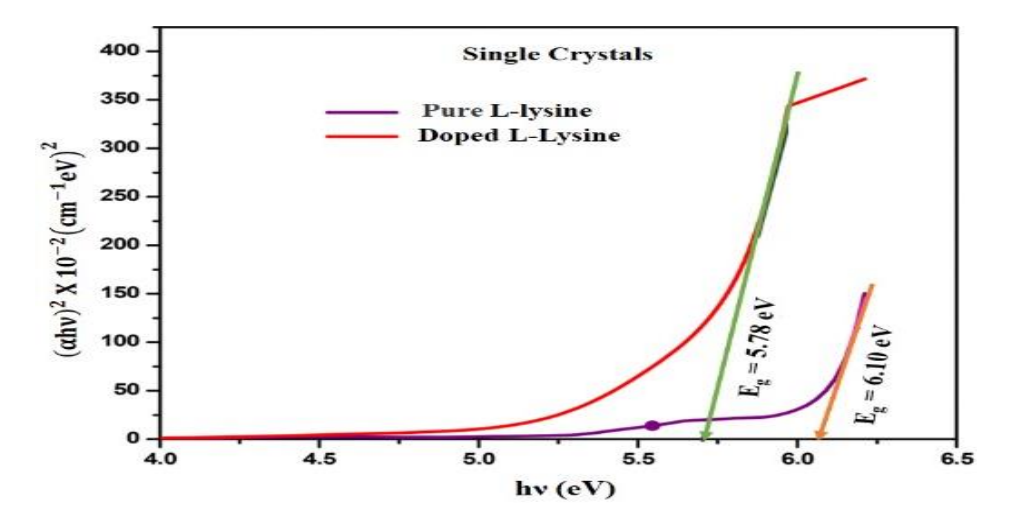


Fig. 5.6. Tauc's scheme of doped and undoped LMOL samples.

5.3.6 LMOL crystal analysis of Vicker's microhardness

The crystal is studied in micro hardness and is used in the capacity to attack depression. The hardness of the samples was the quantity its confrontation the local twist and was associated by further mechanical properties [16]. Then, Good polished by the samples are fixed to the stand of Vickers micro hardness analysis of different load by the magnitude functionals are fixed intermission of time.

The depression time is earmarked with 15s aimed at a loads and hardness number (h_v) have been considered utilizing the relative

$$h_v = \frac{1.8544 \times M}{L^2} \qquad \text{kg / mm}^2$$

where M is applied load, L is the diagonal length of the indentation impression in micrometer. Fig. 5.7 isplanned between applied different loads (M) and hardness numbers (h_v). The mutually of the L-Lysine samples are doped and undoped the linear difference of hardness number with load is observed of the materials and developed absorption of the impurity the combined with hardness grows saturated. The relative involving the M and L of the indenter is assumed by Meyer's law,

$$M = sL^2$$

where a is a constant for an assumed sample and n is hardening coefficient the thought on several resources. It is sharp obtainable n lies amid 1 then 1.6 aimed at hard resources then was greater than 1.6 aimed at soft resources. An effort inurement quantity n Undoped LMOL is 3.8 and doped LMOL is 4.2. Fig. 5.7 (a, b) islog M vs log d for doped and undoped LMOL crystal.

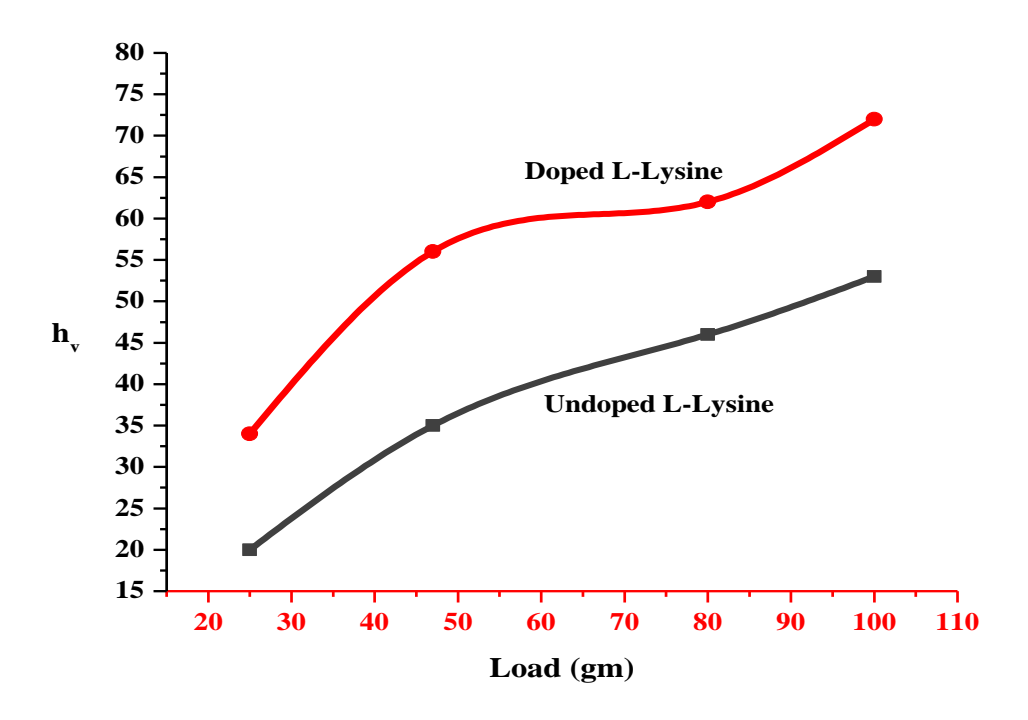


Fig. 5.7 doped and undoped LMOL crystal of Log M vs Log L scheme relation.

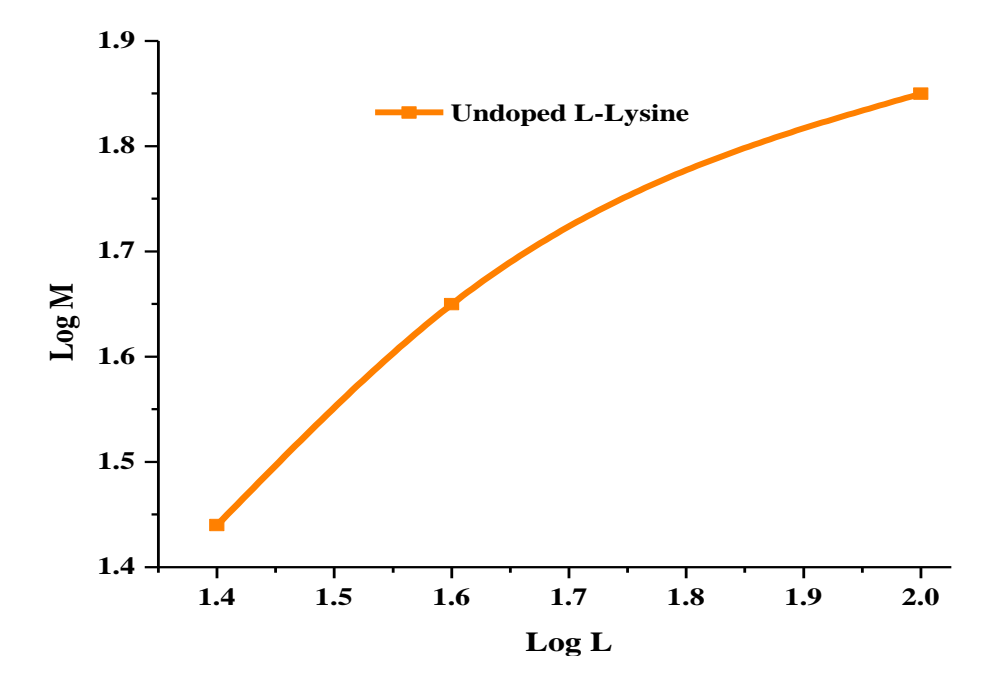


Fig. 5.7a Meyer's law Log M vs Log L scheme of undoped LMOL crystal.

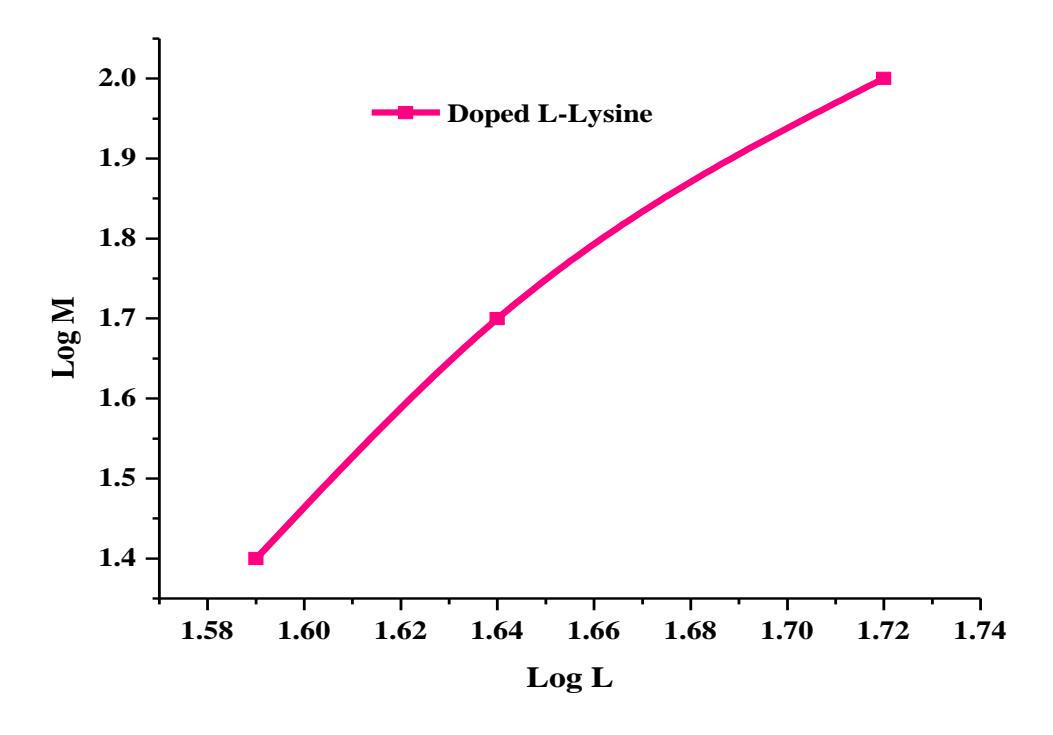


Fig. 5.7b Meyer's law Log M vs Log L scheme of doped LMOL crystal.

5.3.7 Z-scan Studies

Fig. 5.8 is an analysis of an investigational arrangement for the only one ray Z-scan process. The Z-scan technique have developed in two modes like (i) close aperture (ii) open aperture. A quantity trendy exposed opening method stretches our data around the nonlinear absorption quantity then a locked opening mode benefits the estimate the III-order nonlinear refractive index. It is the critical instrument established to consider the magnitude and is studied in nature of nonlinear refraction good the nonlinear absorption by [17].

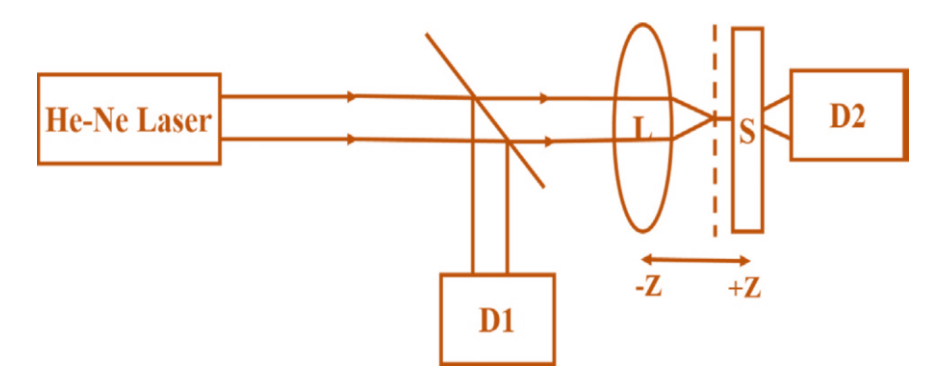


Fig. 5.8 analysis of single beam Z-scan technique.

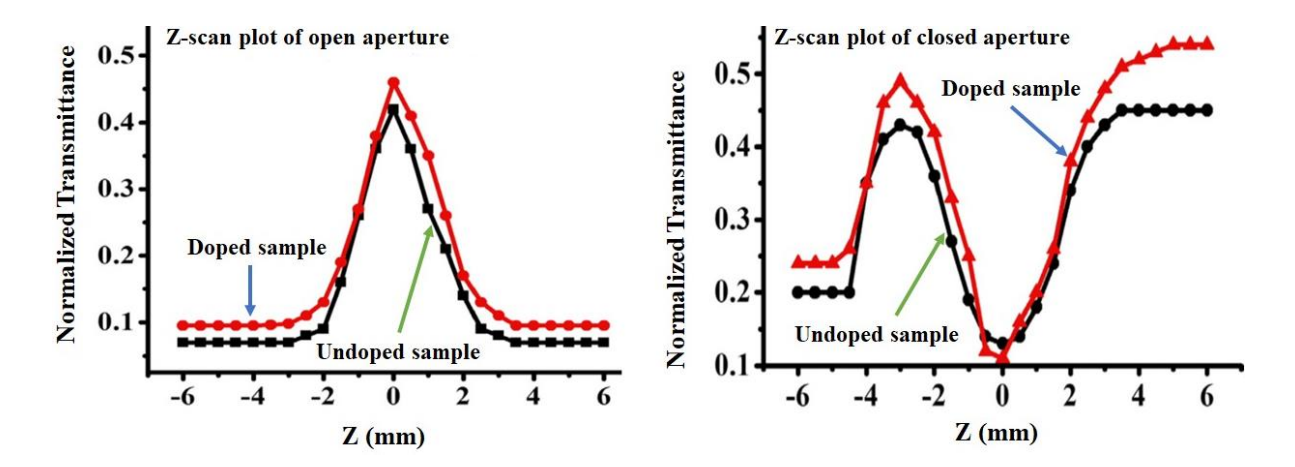


Fig. 5.9 Z-scan plots of closed and open aperture by doped and undoped LMOL crystal.

The sample is closed and open space Z-scan analysis the very high repetitive Gaussian beam of He-Ne laser and doped LMOL cover the lens and is decoded back, ray's irradiated path focus on Z=0. Figs. 5.9 are exposed the exposed then locked aperture Z scan plots of transmittance in fixed and undoped LMOL sample respectively. The LMOL materials are stimulated crosswise the important section from -z to +z lengthways the axial way, it is the direction of propagation of the laser beam transmitted through the crystal has been composed by a photodetector over an aperture. The intensity is slow by a numerical control pulse involved in an indicator. Nonlinear refractive index is followed a peak design experimental an adverse sign and estimation a nonlinear refractive index (n_2) for a sample is considered utilizing the average relatives as.

$$n_2 = \frac{\Delta \emptyset_0}{k I_b L_s}$$

where k is the wavenumber $(\mathbf{k} = \frac{2\pi}{\lambda})$, I_b is the strength of laser ray, L_s is the thickness of the sample at focus Z = 0. Then, the nonlinear absorption coefficient (β) is considered by the relative as

$$\beta = \frac{2\sqrt{2}\Delta T}{I_h L_s}$$

where ΔT is a single highest rate, an exposed opening Z-scan plots. Thus, a III-order nonlinear optical susceptibility is written as,

$$\chi^{III} = \sqrt{(Re(\chi^{III})^2 + Im(\chi^{III})^2)}$$

The nonlinear optical all parameters are n_2 , β then NLO susceptibility (χ^{III}) was estimated and organized in Table 5. 3.

Table 5.3. L-Lysine doped and undoped crystal of III order nonlinear optical parameters by [19].

Nonlinear optical	L-Lysine Undoped sample	L-Lysine doped sample
Parameters		
Nonlinear refractive index	- 6.18	- 5.11
$(n_2) \times 10^{-8} \text{ cm}^2/\text{W}$		
Nonlinear absorption	- 7.23	- 6.73
coefficient (β) × 10 ⁻³ cm /W		
Real part of the III-order	3.71	3.25
non-linear optical		
susceptibility [Re χ^{III}] × 10 ⁻⁶		
esu		
Imaginary part of the III-	2.41	2.13
order non-linear optical		
susceptibility $[\text{Im} \boldsymbol{\chi}^{III}] \times 10^{-6}$		
esu		
III-order nonlinear optical	3.85	3.45
susceptibility $[\chi^{III}] \times 10^{-6}$		
esu		

5.3.8 Optical limiting studies

An optical limiting is studied to procedure an experimental as exposed in Fig. 5.10 (a, b). The doped and undoped LMOL relation can be used to reply time of optical limiting achievement of the crystal.

$$\tau = \frac{r^2}{\alpha_{td}}$$

where r is the radius of a laser beam, which worth was specified through r = 14.98mm. A thermal diffusivity (α_{td}) for a crystal is valued through enhanced to investigation for the photo pyroelectric instruments. Fig. 5.11 is exposed to an optical limiting from doped and

undoped LMOL crystal. The distinguished reduction has detected in transmitted influence at incident powers around 20mW, substantiating the crystals are the perfect applicant for optical limiting at 389nm constant wave lasers.

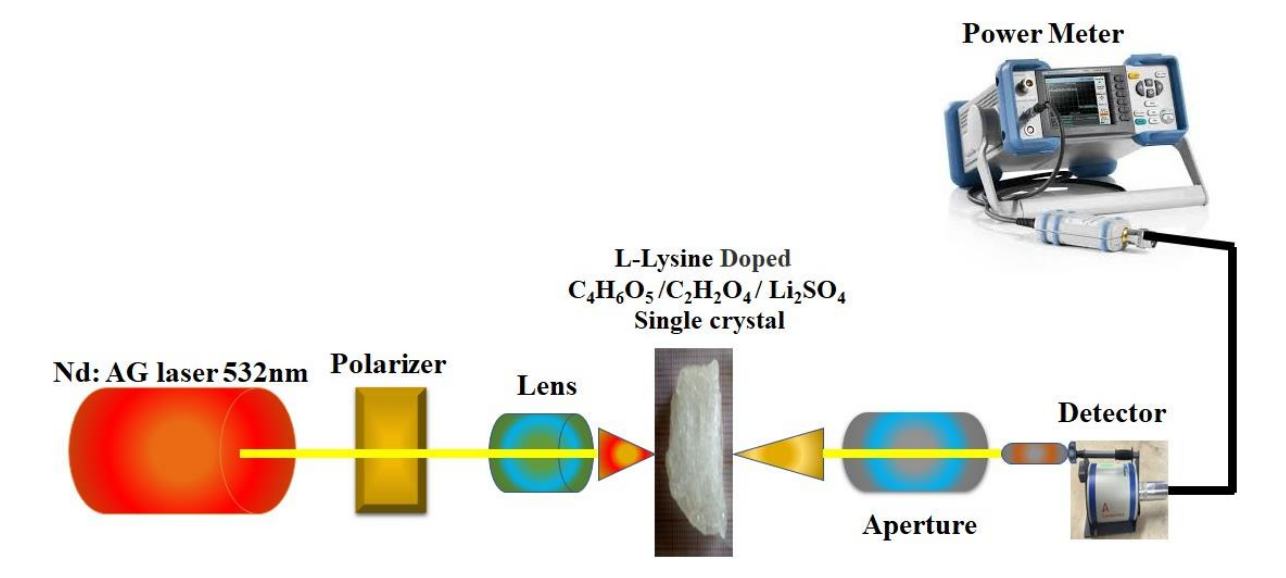


Fig. 5.10a schematic experimental arrangement for optical limiting analysis.



Fig. 5.10b Experimental setup for optical source by KLEF-LAB.

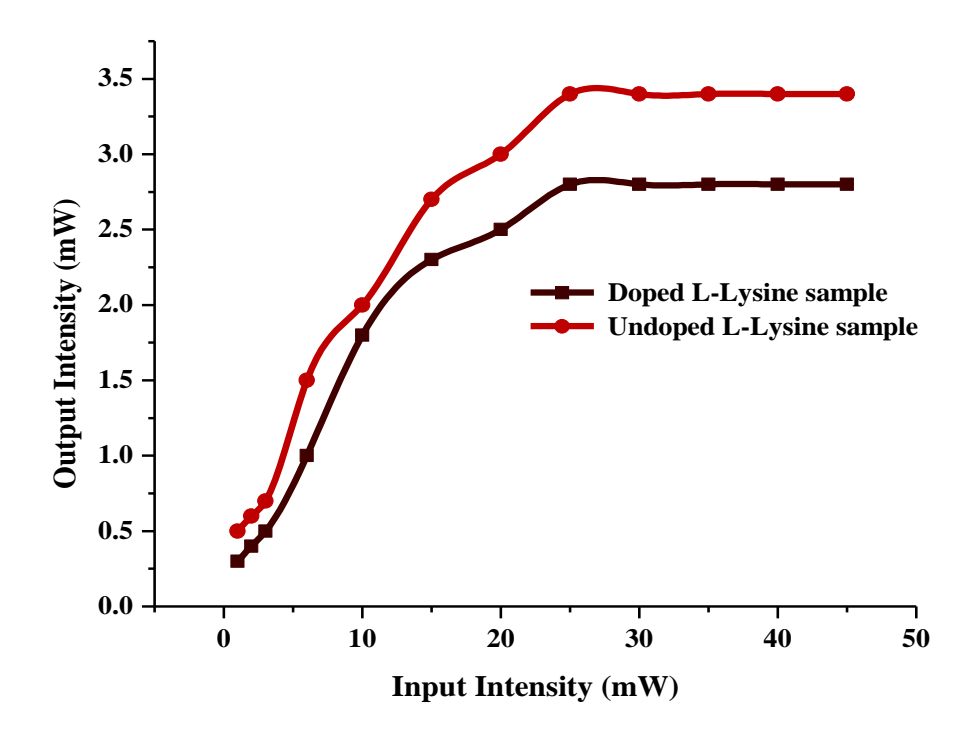


Fig. 5.11 exposed doped and undoped LMOL crystals optical limiting behaviour.

5.3.9 LMOL Crystals analysis of Nonlinear optical

Kurtz and Perry [18] have done for use in the technique of measurements with SHG conversion efficacy. The Nd: YAG laser ray for a wavelength of 1066nm by an effort ray source about 1.4 mJ/pulse then its beat size 15ns through the recurrence frequency about 10Hz is followed by the materials. The developed of the novel samples for doped then undoped LMOL sample have been ground by even size of particles. It was strongly crammed in a microcapillary of even bore and is visible to the laser radiation. The light source ($\lambda = 533$ nm) emission is detected which shows a simple hormonic generator performance with developed materials. Simple hormonic generator is qualified for the efficiency of the pure LMOL around 11.76 mJ and doped LMOL of 16.81mJ have approximately 1.41 and 1.66 times that of KDP around 8.64mJ with respectively.

5.3.10 LMOL Crystals analysis of TG - DTA

The LMOL crystals have been studied of thermal properties for TGA and DTA measure equipment's of STA 490C at with in between range of temperature of 50 to 1000°C. It is used the atmosphere range of the heating rate of 20°C. Fig. 5.12 and Fig. 5.13 explain a

TG and DTA arc with doped and undoped LMOL samples individually. Nonappearance for a water molecule in doped then undoped LMOL sample is detected through nonappearance for heaviness damage around 100°C. The pure LMOL crystal for endothermic peak of DTA arc is exposed in peak of 168.7°C and doped LMOL materials are reached in melting point of the crystals around of 175.6°C. The LMOL crystal is used in thermal stability of pure and doped LMOL are 168.7 °C and 175.6 °C and is augmented around of 5 °C. The L-Lysine single crystal with performance of TG arc is taken by the temperature around 168.7°C and is originate to be 43%. Since the overhead investigation to a melt opinion ford undoped then doped LMOL is 168.7°C and 175.6°C. It is used in the crystal compare to higher than the other semi organic materials such as tetra glycine barium chloride (160°C), α-glycine sulphonitrate (143°C), bisglycine hydrogen chloride (146.8 °C) by [19-20].

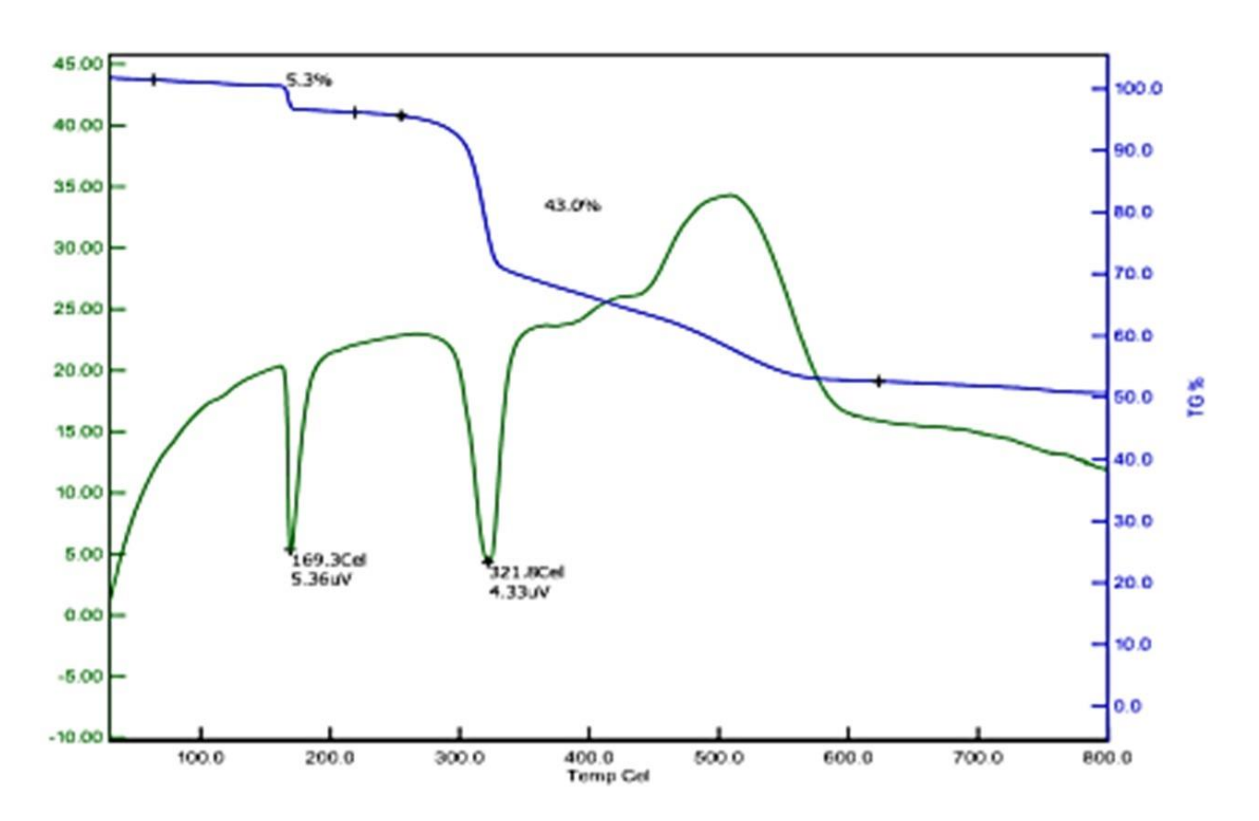


Fig. 5.12 Shows in pure LMOL crystal in TG and DTA arc.

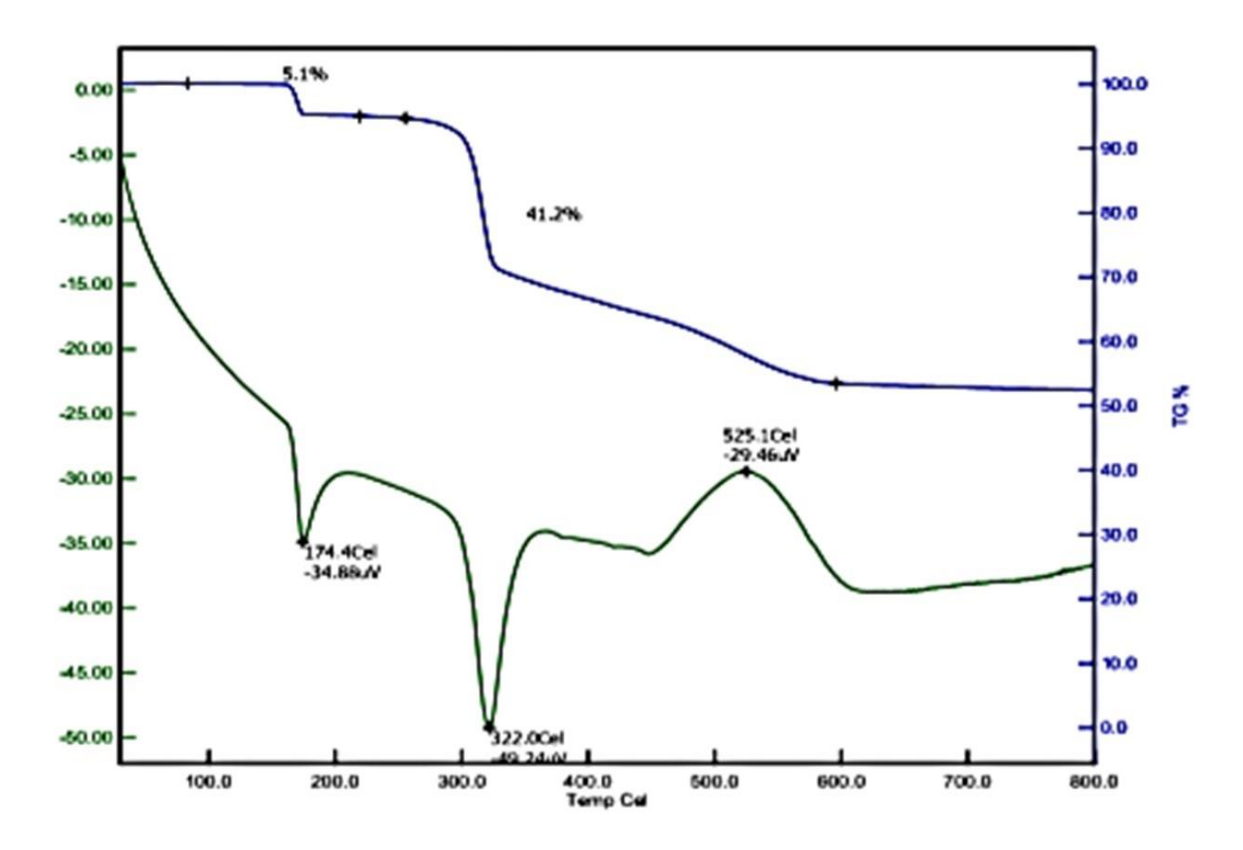


Fig. 5.13 Shows in doped LMOL crystal TG and DTA arc.

5.4 Conclusion

L-Lysine doped and undoped (pure) LMOL single crystals are grown through the conservative slow evaporation resolution growing technique. Parameters used the unit cell could be valued through the sample XRD, FTIR spectral, UV-Vis.-NIR spectra properties also investigation through the optical energy is valued since Tauc's scheme. Mechanical stability to the LMOL samples was investigated through the Vicker's micro hardness valuation. It is observed of the work hardening coefficient of greater than 1.6. Compare to analysis of doped and undoped LMOL crystals are grouped by soft material. The SHG performance of pure and doped LMOL crystals are achieved around 1.41 and 1.66 times that of KDP and SHG efficiency is an increase. The thermo optic source showed through the doped LMOL about 389nm. The optical limiting nature source is verified by low power laser and calculated through the Z-scan method and it showed that a good NLO refractive index. TGA and DTA of the LMOL crystals are studied in the melting point from the values of

168.7°C and 175.6°C. The presence of the LMOL crystals could be used in crystalline resources for energy transfer fabrication its good response of NLO devices and tools can be developed for industrial applications. The optical activities with transmission spectrum and SHG were explored in good stability NLO properties. These materials will be developed NLO application for the benefit of society.

References

- [1] J. Martin Sam Gnanaraj, M. Iniya Pratheepa, M. Lawrence, Optics and Laser Technology 107 (2018) 478–483. https://doi.org/10.1016/j.optlastec.2018.05.045.
- [2] S.R. Thilagavathy, P. Rajesh b, P. Ramasamy b, K. Ambujam, Molecular and Biomolecular Spectroscopy 127 (2014) 248–255. http://dx.doi.org/10.1016/j.saa.2014.01.137.
- [3] Yuting Wang, et al., Int. J. Electrochem. Sci., 13 (2018) 147 158, Doi: 10.20964/2018.01.20.
- [4] Zhang-Gui Hu, et al., Journal of Applied Physics 41(2) (2002) 10B 654. DOI https://doi.org/10.1143/JJAP.41.L1131
- [5] S. Dhanuskodi, K. Vasantha, Spectrochim Acta A Mol Biomol Spectrosc 61(8)(2005) 1777-82. DOI: 10.1016/j.saa.2004.07.008.
- [6] W.J. Liu, C. Ferrari, M. Zha, L. Zanotti, S.S. Jiang, Crystal Research and Technology banner 35 (10) (2000) 1215-1219. <a href="https://doi.org/10.1002/1521-4079(200010)35:10<1215::AID-CRAT1215>3.0.CO;2-4">https://doi.org/10.1002/1521-4079(200010)35:10<1215::AID-CRAT1215>3.0.CO;2-4
- [7] Min-hua Jiang Qi Fang, Advanced Materials banner 11(13) (1999) 1147-1151.
 <a href="https://doi.org/10.1002/(SICI)1521-4095(199909)11:13<1147::AID-ADMA1147>3.0.CO;2-H">https://doi.org/10.1002/(SICI)1521-4095(199909)11:13<1147::AID-ADMA1147>3.0.CO;2-H
- [8] S. Ariponnammal, S. Radhika, R. Selva Vennila, N. Victor Jeya, Crystal Research and Technology 40(8) (2005) 786-788. https://doi.org/10.1002/crat.200410432.
- [9] R. Robert, C. Justin Raj, S. Jerome Das, Current Applied Physics 10(2) (2010) 670-675. https://doi.org/10.1016/j.cap.2009.08.019.
- [10] Neelam Rani, N.Vijayan, M.A.Wahab, G.Bhagavannarayan, B.Riscob, K.K.Maury, Optik 124(13) (2013) 1550-1554. https://doi.org/10.1016/j.ijleo.2012.04.030.

- [11] P. Saminathan, M. SenthilKumar, S. Shanmugan, V. Chithambaram, Materials

 Today: Proceedings 18(3), (2019) 1256-1262

 https://doi.org/10.1016/j.matpr.2019.06.587.
- [12] J. Martin SamGnanaraj, M. IniyaPratheep, M.Lawrenc, Optics & Laser Technology 107 (2018) 478-483. https://doi.org/10.1016/j.optlastec.2018.05.045.
- [13] P.V.Dhanaraj, G.Bhagavannarayana, N.P.Rajesh, Materials Chemistry and Physics 112(2) (2008) 490-495. https://doi.org/10.1016/j.matchemphys.2008.06.003.
- [14] R. Ramesh Babua, K. Sethuramana, R. Gopalakrishnana, P. Ramasamy, Journal of Crystal Growth 297 (2) (2006) 356-360. https://doi.org/10.1016/j.jcrysgro.2006.09.050.
- [15] S. K. Kurtz, T. T. Perry, Journal of Applied Physics 39 (1968) 3798 <u>https://doi.org/10.1063/1.1656857</u>.
- [16] M. Lawrence, J. Felicita Vimala, Int. J. Engg. Sci. Innov. Tech. 4 (2015) 208.
- [17] M.S. Bahae, A.A. Said, Tai-Hue Wei, D.J. Hagan, E.W. Van Stryland IEEE J Quant Electron, 26 (1990), pp. 760-769.
- [18] C. Sekar, R. Parimaladevi Journal of Optoelectronics and Biomedical Materials 1(2) (2009) 215 – 225.
- [19] K. Kirubavathi, K. Selvaraju, R. Valluvan, N. Vijayan, S. Kumararaman, Materials Letters 62(1) (2008) 7-10. https://doi.org/10.1016/j.matlet.2007.04.059.
- [20] S. Chennakrishnan, S. M. Ravikumar, D. Sivavishnu, M. Packiya Raj, S. Varalakshmi, Materials Science & Engineering Journal, Magnolithe (2017) 8. DOI: 10.2412/mmse.05.501.447.

CHAPTER - 6

SYNTHESIS AND CHARACTERIZATION OF L-LYSINE - LITHIUM SULFATE - CITRIC ACID (LLCA) GROWN ON SINGLE CRYSTAL FOR NLO MATERIALS: AN EXPERIMENTAL FOR SLOW EVAPORATION TECHNIQUES

6.1 Introduction

The currently great performance of the NLO materials was developed in capable in SHM form of organic, inorganic and semi-organic received due to their commercial positions of the research area like as frequency conversion, high-speed information processing, optical communications, and optical data storage [1, 2 & 3]. The crystals have implementations of NLO techniques of amino acids performance an energetic part. It is display natural chiral properties and non-centrosymmetric space groups of crystallization. The accumulation of the crystal to include of amino acids have specific structures of nature molecules like as weak Van der Waals and wide transparency hydrogen bonds of visible area. Conventionally, crystals of organic materials were grown from the dissolve [4,5], solution [6,7] and vapour [8 & 9]. The slow evaporation solution of the techniques has the use of very high purity solvent, solute and low viscosity to control in suitable growth system. The p-electron structure is a symmetrized through the electron donor of the organic molecules and highly polarizable is objected of acceptor groups for NLO methods. Azhar et al., [10] was studied in TTPBS synthesized and formation of spectroscopic analysis and is used in slow solvent evaporation method. TTPBS crystal was seemed within 200-900 nm to observe the optical transparency. The magnitude of TONLO refractive index (n₂), absorption coefficient (β) and susceptibility (χ3) of title crystal was showed using the Z-scan data. The Nd: YAG laser shortened surface damage threshold of TTPBS crystal is determined and it is found to be in MW/cm² range. Sivasankari1 and P. Selvarajan [11] have developed in Single crystals of

pure and ammonium chloride-doped urea L-malic acid (ULMA) have grown by slow evaporation technique. It is different studied as follows in morphology, optical, and hardness properties are studied. The functional groups are appraised by FTIR analysis. The lattice parameters of XRD, Powder X-ray diffraction studies are established the diffraction planes of the grown crystals. The UV-visible spectrum displays the cut off wavelength at 220 nm. The NLO property of the grownup crystals was established by SHG studies. Saminathan *et al.*, [12] was developed in single crystals of L-Lysine Monohydrochloride Dihydrate (LMHCl) by used method of slow evaporation. It was studied of the single crystal like XRD, FTIR, optical, thermal properties, UV–Vis and optical absorption visible is found to be at 250 nm.

At present form of values, the synthesis and description of Crystalline perfection unique as organic pure L-Lysine and Co-Doped Glycine Barium Chloride / C₆H₁₄N₂O₂: Novel Crystal for NLO materials, which have developed through the conservative slow evaporation method. A method of crystals has been characterized through the powder X-ray diffraction, HRXRD studies, FTIR spectral analysis, SHG test, refractive index and birefringence measurements, micro hardness and dielectric studies, likewise highpoints the nonlinear and linear optical studies, it can be using in nonlinear optical applications.

6.2. Materials and Experimental Methodology

6.2.1 Synthesized of the L-Lysine doped crystal growth

Pure L-Lysine (undoped) Lithium sulfate - Citric Acid (LLCA)single crystals have been grown through the mol (%) of one (Grade- AR) melting Glycine Barium Chloride (98% -Merck) in distilled water. The element is motivated consuming in magnetic stirrer by ambient temperature for M.R. College, at Department of Physics LAB. The attained salt of GBC has been recrystallized different periods with direction toward acquire crystal by moral photograph. Developed of the materials are collected in 42 days. The equivalent organization

have been implemented for increasing L-Lysine Co-doped Lithium sulfate - Citric Acid (LLCA)crystals. A new crystal was developed through melting one mol (%) (Grade- AR) GBC/C₆H₁₄N₂O₂ (Amino-acid) (98% - Merck) and mol% 0.5 / 0.3 mol% (Grade - AR) L-Lysine (97%) with distilled water. They are nervous energetically consuming magnetic stirrer on ambient temperature at 5hours. L-Lysine Co-doping GBC/C₆H₁₄N₂O₂ have been gotten which is recrystallized different periods with direction toward get samples by moral photograph. New samples are collected at 75days, grown L-Lysine Co-doped GBC/C₆H₁₄N₂O₂crystal is exposed in Fig.6. 1.

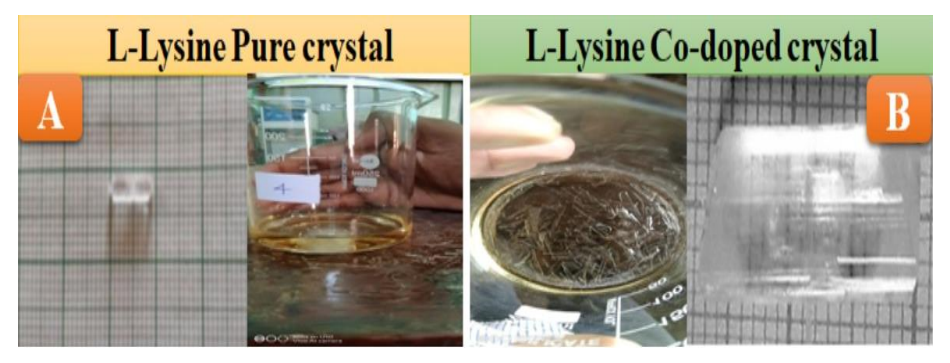


Fig. 6.1 illustration as grown single crystals of pure (A) and (B) co-doped L-LGBCAC.
6.2.2 Characterization analysis of pure L-Lysine and Co-Doped with effect of single crystals

The new developed of the crystals have been imperiled to numerous description study with direction toward estimate the properties of structural, optical and mechanical. A crystal sizes of the unit cell is studied through the ENRAF NONIOUS CAD4 X-Ray diffractometer prepared by MoKa radioactivity. An efficient collection has been recognized use PERKIN ELMER FTIR inside the wave number series from 400 – 4000cm⁻¹. A crystals implementation proof of the optical properties has been inspected use LAMBDA 35 UV–Vis NIR spectrophotometer. Productivity of NLO material is established Kurtz and Perry investigational method consuming Nd: YAG laser by way of the foundation. The grown of the crystal conform to mechanical properties have been considered consuming Leitz Wetzler

Vickers micro hardness sample formfitting by the shape indenter through flexible load from 40g - 100g.

6.3 Results and Discussion

6.3.1 Pure L-Lysine and Co-Doped Single Crystal Powder XRD analysis

Fig. 6.2 illustrations the powder XRD pattern of L-lysine Co-Doping GBC/C₆H₁₄N₂O₂ materials. It is detected that the sample grows with monoclinic equilibrium by the interplanetary collection of P_{21}/n . It is 2θ morals from countless diffraction planes and the equivalent strengths have been composed of the crystal. The valued cell parameters for undoped GBC/C₆H₁₄N₂O₂ was a = 4.894 Å; b = 21.554Å, c = 19.596Å, with V= 2121.27Å³.

Circumstance of L-Lysine Co-doping GBC/C₆H₁₄N₂O₂, small modifications are saved to the cell limitations with combination through the materials. Novel single crystal is calculated to the lattice cell parameters morals, a =4·885Å, b =21·548 Å, c =19·590Å and V = 2241·57Å³. It is also possessing of the no centrosymmetric P₂₁/n through the monoclinic symmetry. We are reliable through the consequences described by means of the single crystal to the X-ray diffraction with the reported literature [13]. The compare to the lattice parameters has been considered too with good described morals in diffraction of the crystalline quality. Fig. 6.3 illustrations the High-Resolution X – rays Diffraction Curve (HRXRD) verified for a characteristic solution grown L-Lysine Co-doped new crystal consuming (012) diffracting planes in equal Bragg geometry through using the multicrystal XRD by MoK α_1 radiation. The DC covers a single peak and designates that the sample is allowed from structural grain limits. All at half width of the curve is 39 arcs as reviewed by [14]. It is closed to that probable for an initial perfect actual L-Lysine Co-doped crystal.

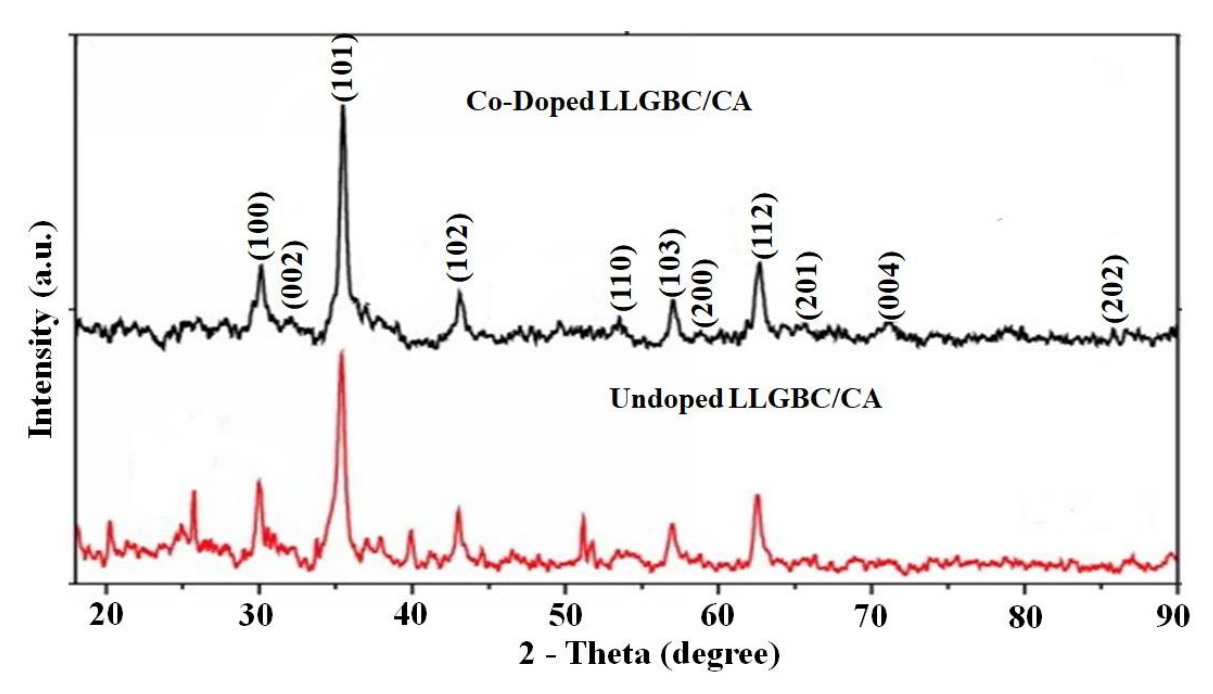


Fig. 6.2. Exposed XRD pattern of pure and Co-doping L-LGBCAC.

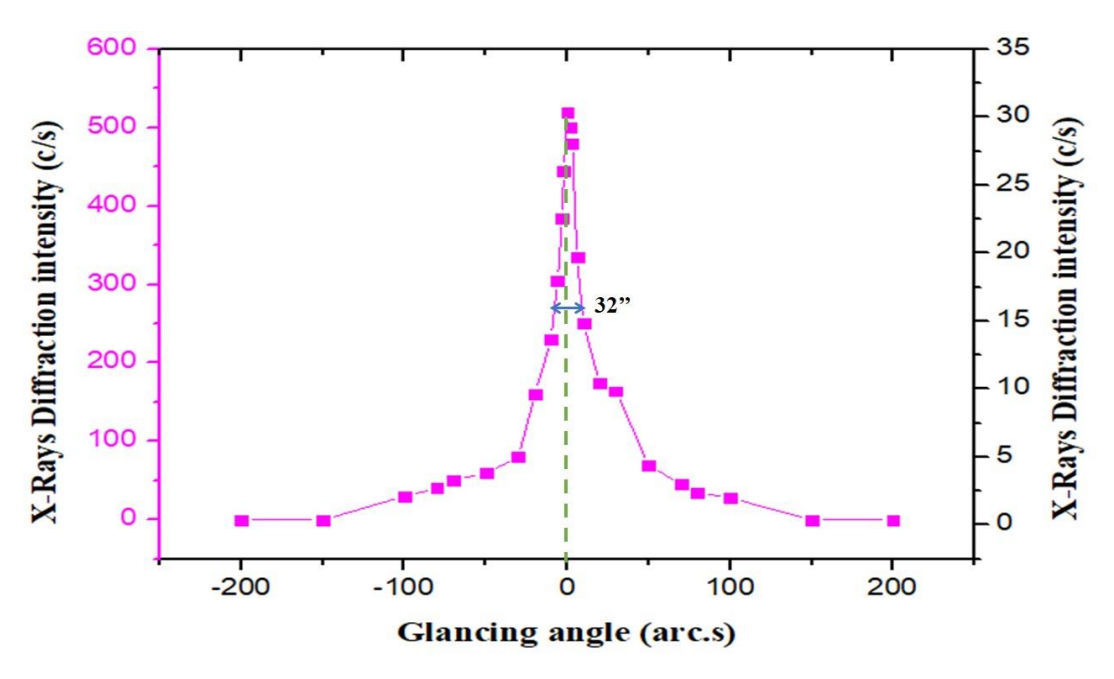


Fig. 6.3 exposed HRXRD of L-LGBCAC.

6.3.2. Pure L-Lysine and doped samples analysis of FTIR studies

The Fig.6.4 as follow in FT-IR spectra of mutually in undoped and L-Lysine Co-doped $GBC/C_6H_{14}N_2O_2$ verified at Thathanur (M.R. College) Department of Physics LAB room temperature in between to 400 and $4000cm^{-1}$ have been exposed in Fig. 4.4. The extending method rates of L-Lysine undoped $GBC/C_6H_{14}N_2O_2$ spectrum expressions two

absorption bands about 441.2 and 564.5cm^{-1} . The extending method rates of L-Lysine doped samples in band everywhere 867.5 cm^{-1} is outstanding to the establishment of tetrahedral corresponding in $C_6H_14N_2O_2$. The samples all connected to the group of symmetric and asymmetric extending vibrations in band of $1577.2 \text{ and } 1412.5 \text{cm}^{-1}$. The peaks of $3428.1 \text{ and } 2364.3 \text{cm}^{-1}$ have been credited to GBC stretching of Lysine by [15, 16].Moreover, indications detected from the GBC of 0.5 mol% / 0.3 mol% of $C_6H_14N_2O_2$ doped Lysine spectrum about 714, 1050, 1080 and 3609 cm⁻¹ have been allocated to vibration group methods [17] respectively. The extensive absorption band about 451.1cm^{-1} in doped L-Lysine mighty be assigned to GBC/ $C_6H_14N_2O_2$ extending method settling that are presented in the L-Lysine samples.

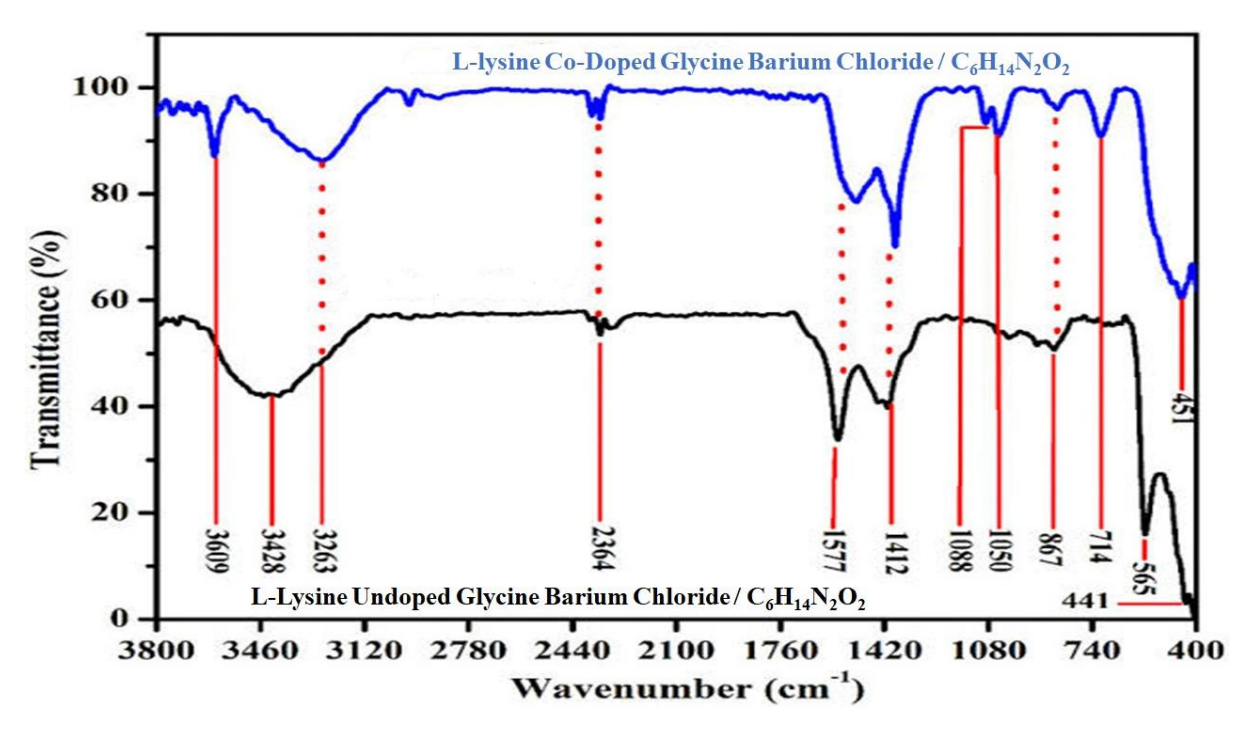


Fig.6. 4. Exposed FTIR spectrum of pure and Co-doping L-LGBCAC.

6.3.3. Pure L-Lysine and doped samples analysis of Optical Transmission studies

Absorption coefficient (α) and transmittance value (T) of the L-LGBCAC single crystals have been considered from the succeeding relative [18]:

$$\alpha = \frac{2.3026 \log \left(\frac{1}{T}\right)}{t}$$

where T & t is transmittance & thickness of the L-LGBCAC crystal and the optical band gap energy (E_g) should be considered from the relative

$$h\alpha\nu = S(h\nu - E_g)^{1/2}$$

where S, Eg, h, ν were the constant, optical band gap, Planck's constant, frequency of incident photons. The optical band gap is valued through intrigue $(h\alpha\nu)^2$ vs $h\nu(eV)$ as exposed in Tauc's plot, Fig. 6.5. Since the graph, the optical band gap of undoped L-LGBCAC and doped L-LGBCAC is valued to be 3.74eV and 3.94eV. The L-LGBCAC crystal is approved that shows respectable transmittance in the visible area. Then the band gap energy is above 3.5eV with the lower cut off about 229nm and 247nm, undoped and co-doped L-LGBCAC crystals verify to be a qualified applicant in optoelectronic applications fabrications like communication, data storage.

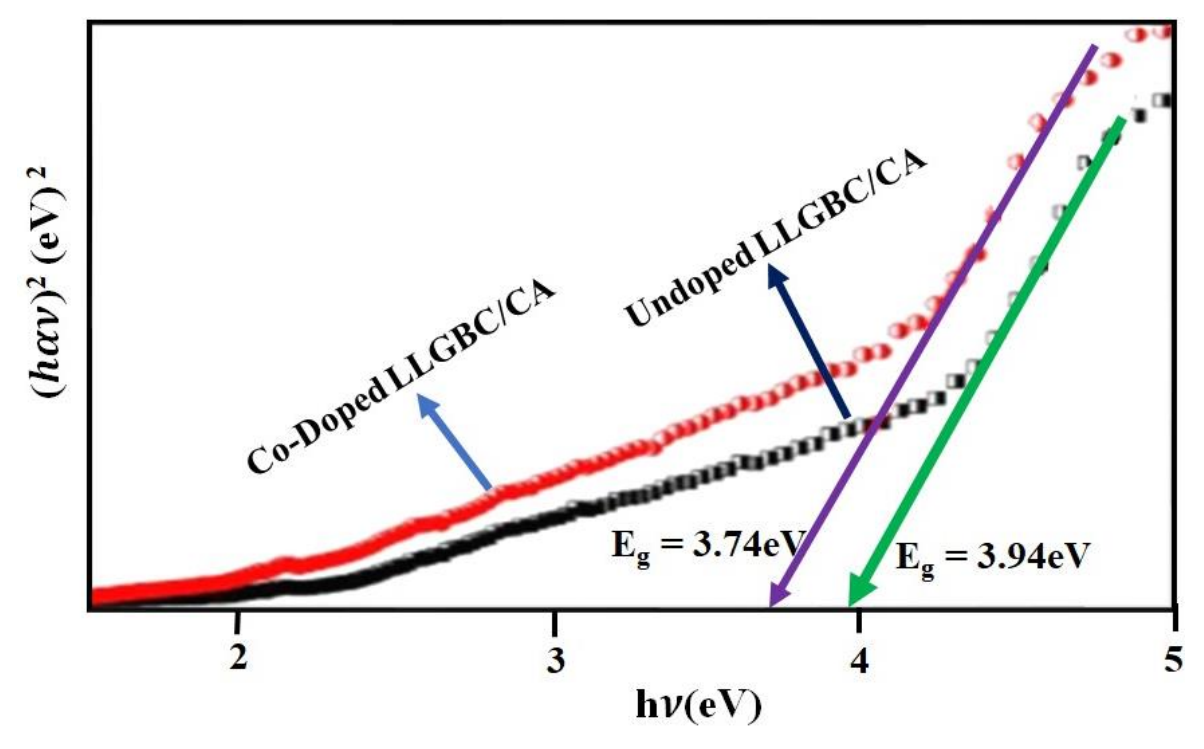


Fig. 6.5 exposed Tauc's scheme of undoped and Co-doped LLGBC/CA crystal.

The Pure L-Lysine and Co-doped $GBC/C_6H_{14}N_2O_2$ of the L-Lysine crystal plates are thickness of 2mm. The crystal plate is refined in without any coating for measure of optical transmission spectra was formed to the form of crystals range of wavelength around 200 to 1000nm. The samples have been used in double beam for UV visible spectra with Pure

L-Lysine and Co-doping GBC/ $C_6H_{14}N_2O_2$ crystals were exposed in Fig.6.6. The sample absorption through the transmission spectra is observed in that pure L-lysine and Co-doping GBC/ $C_6H_{14}N_2O_2$ is confirmed with higher transmission with the whole NIR visible section to a spectrum. At these novel materials have properties of good qualifies for the NLO application.

The pure L-Lysine and Co-doping GBC/ $C_6H_{14}N_2O_2$ crystals to cut off wavelength by UV is formed around 229nm and 247nm respectively. The novel crystals are an enhanced to individual to the production by Optoelectronic systems [19].

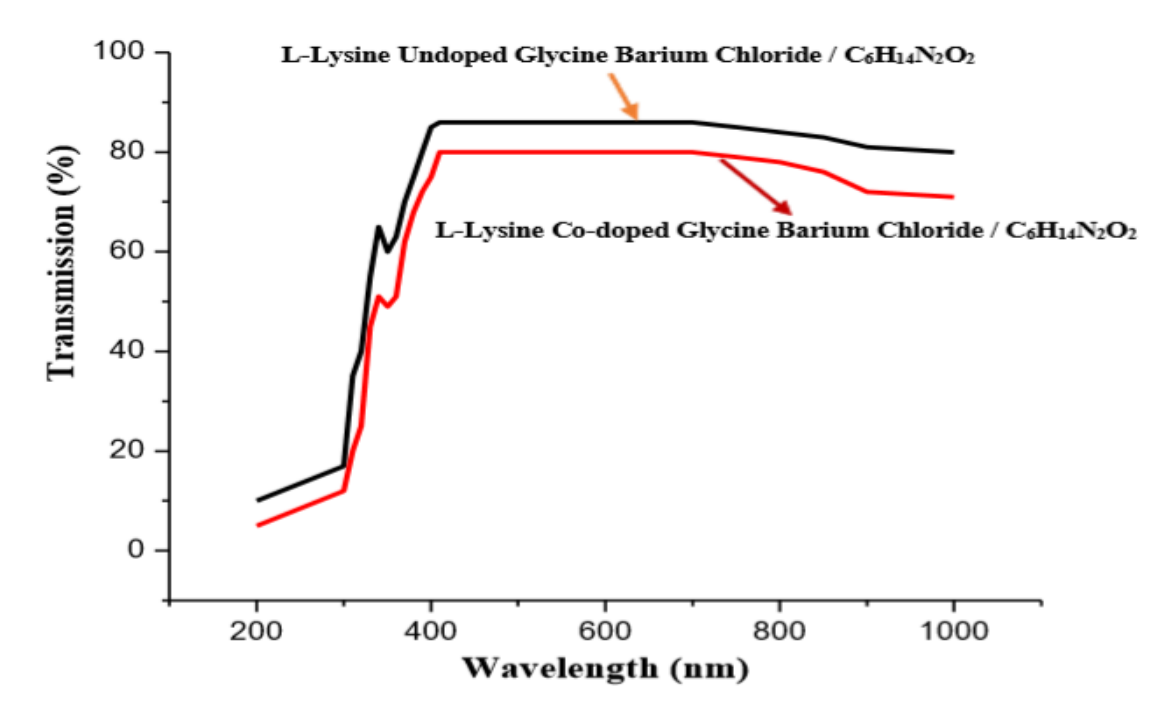


Fig. 6.6. Illustrations Optical transmission of pure and Co-doping L-LGBCAC.

6.3.4 Pure L-Lysine and doped samples analysis of Nonlinear optical studies

The measurements of the samples through the SHG conversion efficiency is used in Kurtz and Perry technique [20]. The wavelength of the beam (Q-switched Nd: YAG) is 1064nm through effort of ray source around 1.5mJ/pulses. Which is the pulses size 15ns in the recurrence proportion of 20Hz is used. The pure L-Lysine and Co-doped GBC/C₆H₁₄N₂O₂ of the L-Lysine Crystal have been developed of the sample with even of the

particle size, the strongly crowded with the micro-capillary for even windbag, showing with laser rays.

A beam of source emission of $\lambda = 532 \text{nm}$ is distinguished, it shows SHG behaviour full developed materials. A qualified of SHG productivity to the pure L-Lysine (11.58 mJ) and Co-doping GBC/C₆H₁₄N₂O₂ (14.57mJ) is virtually 1.27 to 1.79 periods which its KDP (8.71mJ) individually.

6.3.5 Pure L-Lysine and doped samples analysis of TG - DTA studies

The sample analysis of thermal properties has been premeditated by TGA (Thermogravimetric) events the variations to the weight by temperature which can be due to variations in the sample arrangement by a thermal stability. L-LGBCAC compounds have gone on heating the samples from the thermal values the maximum temperature (45°C to 800°C) by which a sample have been applied [21]. Similarly, which is no phase transition experimental in the corresponding area. LLGBC/CA single crystal values for 45% bulk loss experimental in TG curvature. Theoretical and experimental weight loss of the LLGBC/CA is much closed in the samples. The samples of remaining portion are very slowly decomposed form of 780°C and high weight loss designates that the incidence of lysine in LLGBC/CA. which the L-Lysine is stable up to 160°C then it decomposes into two molecules of GBCCA and a molecule of carbon monoxide. L-Lysine is slowly vaporising at 300°C and GBCCA begins to riven to hydrogen sulphide, nitrogen and carbon remainder. The samples accounts for 3.91% weight loss experimental in the TG curve. The TG studies thus approves the establishment of the LLGBC/CA in the stoichiometric ratio and the decomposition design of LLGBC/CA. These protections the appropriateness of the sample for likely request in lasers where the single crystals have been required to withstand higher temperature. DTA (Differential Thermal Analysis) with STA 409C device amid the temperature range of 45°C to 800°C at a heating proportion of 30°C per min in the nitrogen atmosphere. Fig. 6.7 is the pure L-Lysine in GBC/C₆H₁₄N₂O₂ Crystal analysis of TG-DTA curve.

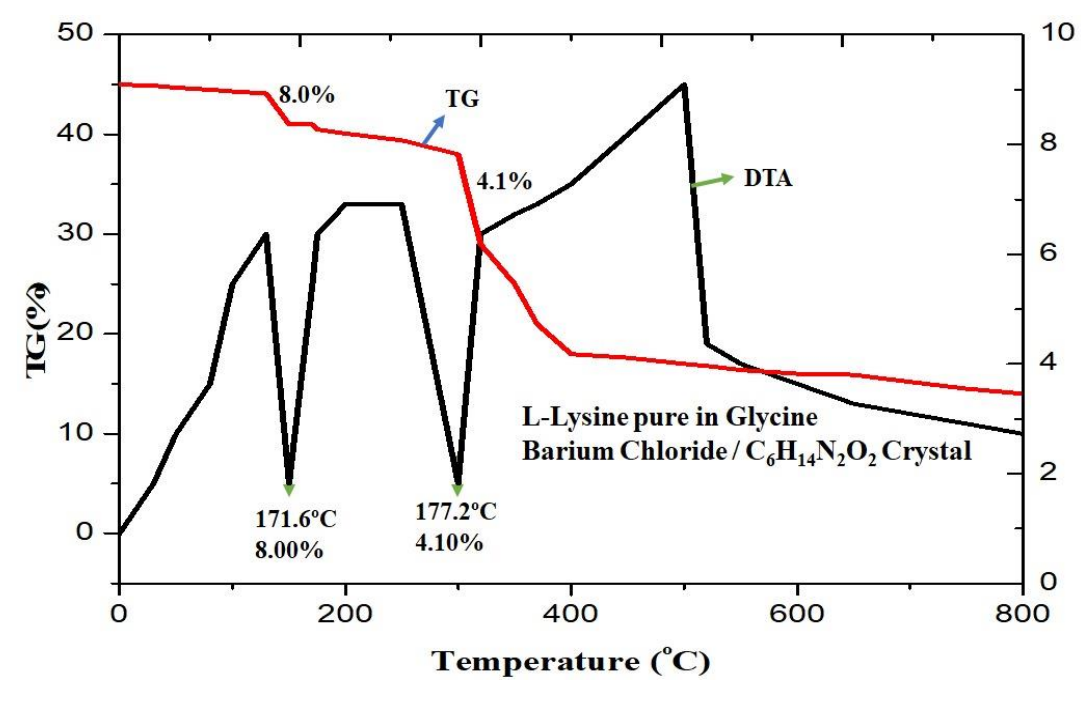


Fig. 6.7. TG and DTA curve of pure and Co-doping L-LGBCAC.

Fig. 6.8 explain the L-Lysine Co-doped GBC/C₆H₁₄N₂O₂ crystals analysis of TG-DTA curve respectively. The water skiving of the molecule in pure L-Lysine and Co-doping GBC/C₆H₁₄N₂O₂ have been observed through skiving of weight injury at 100°C. The pure L-Lysine in GBC/C₆H₁₄N₂O₂ is shows of DTA curve a strident endothermic highest at 171.6°C for pure and 177.2°C for the L-Lysine Co-doped GBC/C₆H₁₄N₂O₂ crystal, which agrees in melting opinion to composite. Henceforth thermal stability with pure L-Lysine and Co-doping GBC/C₆H₁₄N₂O₂ crystal are 171.6°C to 177.2°C. Accumulation in pure L-Lysine and Co-doping GBC/C₆H₁₄N₂O₂ crystal the thermal stability is augmented by approximately 6°C. The mass loss of the cure by TG is taken the place up to reached the temperature of 171.6°C. The mass lost from 171°C to 332°C is found to be 4.10%. Overhead 332°C of the sample is experiences permanent endothermic transition about at 545°C. There are additional to form in damage of 8.00% happening with temperature boundary around 332-545°C, it authorizes with L-Lysine Co-doped GBC/C₆H₁₄N₂O₂ crystal as follows by [22-24].

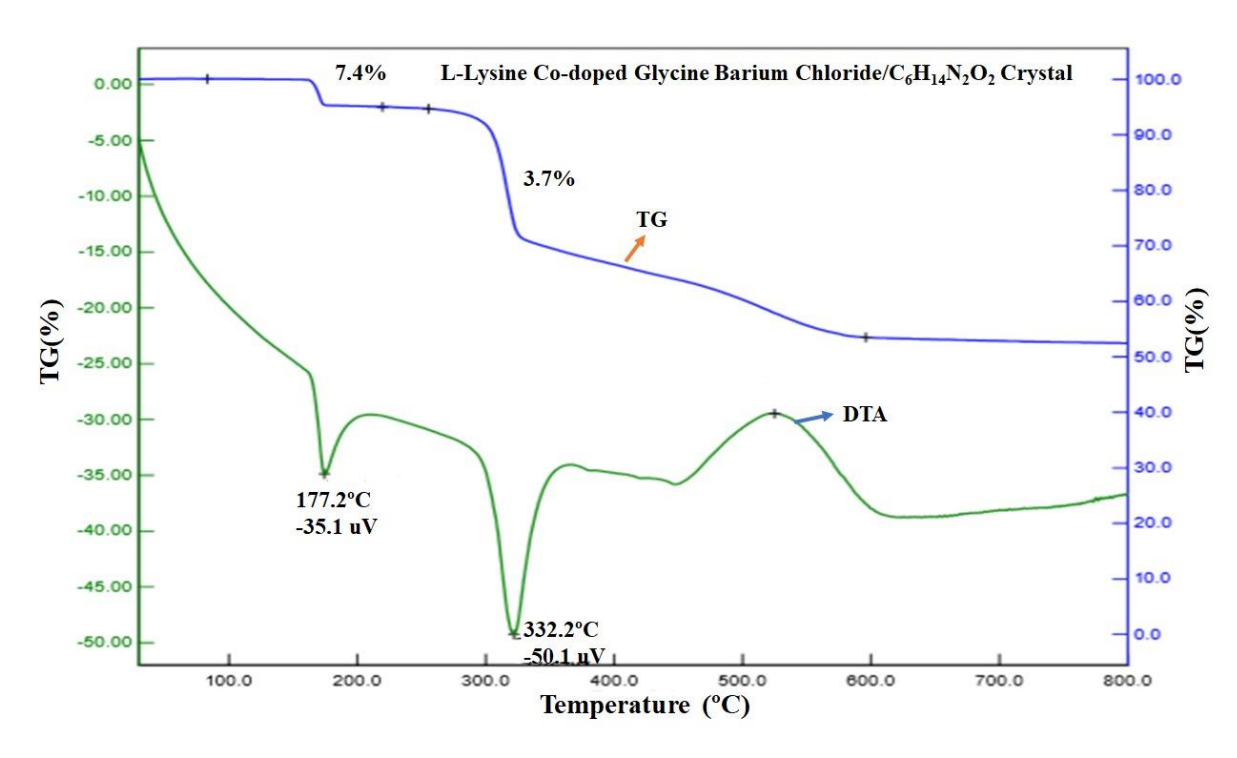


Fig.6. 8. TG and DTA curve of pure and Co-doping L-LGBCAC.

6.4 Conclusion

The slow evaporation technique is used in L-Lysine materials with pure and Co-doped Lithium sulfate - Citric Acid (LLCA) crystal grown on good transparent of the novel crystal. The samples are occupied the unit cell parameters to measure the XRD and Powder XRD illustrations moral crystalline of the grown-on the pure L-Lysine and L-Lysine doped novel crystal. The novel crystal is used in pure L-Lysine and doped with form of in numerous the functional groups are analyzed of FTIR. Pure L-Lysine and doped novel crystal is studied of UV cut off wavelength range of 229nm and 247nm respectively. There are conformed to the potential effect of NLO applications and SHG productivity of pure L-Lysine and co-doped novel crystal are 1.27 to 1.79 periods at that KDP individually. The novel crystal has been studied in thermal properties by TGA and DTA at the melting point of the L-Lysine and co-doped novel crystal is 171.6°C and 177.2°C.

References

- [1] Yuting Wang, et al., Int. J. Electrochem. Sci. 13 (2018) 147 158. DOI: 10.20964/2018.01.20.
- [2] Zhang, Y. Li, H. Xi, B. Che, Y.J. Zheng, Materials Chemistry and Physics 108(2–3) (2008) 192-195. https://doi.org/10.1016/j.matchemphys.2007.09.006.
- [3] D.F. Eaton, Science 253(5017) (1991) 281-287. DOI: 10.1126/science.253.5017.281.
- [4] M. Arivanandhan, K. Sankaranarayanan, K. Ramamoorthy, Sanjeeviraja, P. Ramasamy, Thin Solid Films 477(1–2) (2005) 2-6. https://doi.org/10.1016/j.tsf.2004.08.162.
- [5] B.J. Mc Ardle, J.N. Sherwood, A.C. Damask, Journal of Crystal Growth 22(3)(1974) 193-200. https://doi.org/10.1016/0022-0248(74)90094-3.
- [6] E.M. Hampton, B.S. Shah, J.N. Sherwood, Journal of Crystal Growth 22(1) (1974)22-28. https://doi.org/10.1016/0022-0248(74)90053-0.
- [7] M.D. Aggarwal, R.B. Lal, Simple, Review of Scientific Instruments 54 (1983) 772.https://doi.org/10.1063/1.1137443.
- [8] S. Ayers, M. M. Faktor, D. Marr, J. L. Stevenson, Journal of Materials Science 7(1) (1972) 31–33. DOI: https://doi.org/10.1007/BF00549546.
- [9] J. Martin Sam Gnanaraj, M. Iniya Pratheepa, M. Lawrence, Optics and Laser Technology 107 (2018) 478–483. https://doi.org/10.1016/j.optlastec.2018.05.045.
- [10] S. M. Azhar, S. S. Hussaini, M. D. Shirsat, G. Rabbani, Mohd Shkir, Icon, S. Alfaify,
 H. A. Ghramh, M. I. Baig & Mohd Anis, Journal Materials Research Innovations
 23(3) (2019) 123-128 https://doi.org/10.1080/14328917.2017.1392694.
- [11] B. Sivasankari1 and P. Selvarajan, Journal of Materials Article ID 216732 (2013) 1-7 http://dx.doi.org/10.1155/2013/216732

- [12] P. Saminathan, M. SenthilKumar, S. Shanmugan, V. Chithambaram, Materials

 Today: Proceedings 18(3), (2019) 1256-1262

 https://doi.org/10.1016/j.matpr.2019.06.587.
- [13] Navaneethan Krishnan Srinivasan, Balasubramanian Sridhar R. K. Rajaram, Structure Reports Online 57(9) DOI: 10.1107/S1600536801014040.
- [14] W. Boris, Batterman, Henderson Cole, Reviews of modern physics 36(3) (1964)681. DOI: https://doi.org/10.1103/RevModPhys.36.681.
- [15] S. Udayakumar, V. Renuka, K. Kavitha, J. Chem. Pharm. Res. 4 (2) (2012) 1271–1280.
- [16] K. Ravichandrika, P. Kiranmayi, R.V.S.S.N. Ravikumar, Int. J. Pharm. Pharm. Sci. 4(4) (2012) 336–338.
- [17] X. Liu, J. Zhang, L. Wang, T. Yang, X. Guo, S. Wu, S. Wang, J. Mater. Chem. 21 (2011) 349–356.
- [18] J. Thomas Joseph Prakash, J. Martin Sam Gnanaraj, Spectrochim. Acta A 135(2015)25.
- [19] V. Venkataramanan, S. Maheswaran, J.N. Sherwood, H.L. Bhat, J. Cryst. Growth 179 (1997) 605-610.
- [20] S.K. Kurtz, T.T. Perry, J.Appl. Phys. 39 (1968) 3798.
- [21] M. Fleck, V.V. Ghazaryan, A.M. Petrosyan, J. Mol. Struct. 984 (2010) 63-68.
- [22] C. Sekar, R. Parimaladevi, J. Optoelect. Biomed. Mater. 1 (2009) 215-225.
- [23] T. Balakrishnan, K. Ramamurthi, Materials Letters, 62 (2008) 65-68.
- [24] S.R. Thilagavathy, P. Rajesh, P. Ramasamy, K. Ambujam, Molecular and
 Biomolecular Spectroscopy 127 (2014) 248–255.

 http://dx.doi.org/10.1016/j.saa.2014.01.137

CHAPTER - 7

To summarizes the results obtained from various characterization studies carried out on the grown crystals. It also includes the comparison of these results and discusses the suggestion for future work.

7.1 Overall Conclusions of the thesis - Summarizes

The present work designates the growth and characterization of L-Lysine crystals of MHCl, TAPB, Citric Acid (CA), Malic acid (C₄H₆O₅) /Oxalic acid (C₂H₂O₄)/ lithium sulphate (Li₂SO₄) (LM), L-Lysine with and without Co-Doped Glycine Barium Chloride (GBC)/C₆H₁₄N₂O₂ (Amino acid) (LGBA). Companies operating in the global L-Lysine market are focusing on merger and acquisitions and new product launches to gain competitive advantage. Growth strategies adopted by these companies are studied in detail in the report. The report also includes several valuable information on the L-Lysine market, derived from various industrial sources.

7.2 Comparison of these results and discusses the suggestion for future work.

Order of the L-Lysine simple to complex (building to conclusion); or may state conclusion first. Conclusion should be consistent with study research question. Emphasize what is new, different, or important about your results. Consider alternative explanations for the results.

Limit speculation.

The increasing demand on animal products expected for the next decades requiresanimal production systems to become more efficient in resource use. Most commercial operations feed all pigs the same feed at a determined time depending on the average BW of the batch, but withoutconsidering the variability of the population. However, low body weight (BW) pigs have been related to extra costs as reduced barn utilization, losses

due to the poor carcass grading and inefficiency ofphase feeding strategies. Some studies have previously hypothesized the need to do different phasefeeding strategies to pigs sorted by initial BW. This work aimed to compare the effect of increasing thestandardized ileal digestible L-Lsine to net energy ratio (SID Lys:NE) over the performance of growingpigs sorted by initial BW in 3 categories (small, medium, and large). The results showed that smallpigs could use more efficiently high SID Lys:NE diets compared to the large pigs during the growingphase (28–63 kg). The conclusions imply positive effects of feeding higher dietary L-Lysine to small pigsto compensate for their reduced feed intake capacity. This strategy might improve growth rate andfeed efficiency, without increasing feed costs per kg gain.

BIBLIOGRAPHY

Lysine is a building block for protein. It's an essential amino acid because your body cannot make it, so you need to obtain it from food. It's important for normal growth and muscle turnover and used to form carnitine, a substance found in most cells of your body. The present work designates the growth and characterization of L-Lysine crystals of MHCl, TAPB, Citric Acid (CA), Malic acid ($C_4H_6O_5$) /Oxalic acid ($C_2H_2O_4$)/ lithium sulphate (Li_2SO_4) (LM), L-Lysine with and without Co-Doped Glycine Barium Chloride (GBC)/ $C_6H_14N_2O_2$ (Amino acid) (LGBA).

Proof of the Experimental work photos







A new class single crystal L-lysine hydrogen chloride (LLHC) for optoelectronic applications

S. Varadarajan¹, M. Senthil Kumar¹, S. Shanmugan², A. Arputhalatha³, V. Chithambaram⁴, and Geetha Palani^{5,*}

Received: 10 June 2021 Accepted: 6 September 2021 Published online: 5 October 2021

© The Author(s), under exclusive licence to Springer Science+Business Media, LLC, part of Springer Nature 2021

ABSTRACT

This manuscript is discussing the growth of a new class semi-organic nonlinear crystal L-Lysine hydrogen chloride (LLHC) was grown by slow evaporation method using a mixed solvent of deionized water + ethanol and pure deionized water. The crystal crystallizes in orthorhombic space group of P2₁2₁2₁. Lattice parameters were revealed by single crystal X-ray diffraction analysis. The FT-IR spectral analysis was performed on the grown crystal LLHC to identify its functional groups. The position of protons and carbons was determined by the NMR technique. The grown crystal was characterized by optical transparency through UV-Vis range with a short cutoff wavelength of 212nm. Thermal and physiochemical stability of the title crystal was found out through the TG-DTA analysis, which proves the crystal stability up to 251.4 °C. Brewster's point method was used to find out the refractive index of the grown compound LLHC. Vickers's microhardness test was performed on LLHC to find out its mechanical stability. The second harmonic generation (SHG) of the grown crystal LLHC was confirmed by the Kurtz-perry powder method and the SHG efficiency was compared with the known Potassium Dihydrogen phosphate (KDP) standard. By using a minimal bactericidal concentration (MBC) benchmark, their antibacterial activity was evaluated. The grown crystal shows longterm and outstanding antibacterial activity against E.coli and S.aureus.

Address correspondence to E-mail: kesangee@gmail.com



¹Department of Physics, Government Arts College (Autonomous), Affiliated to Bharathidasan University, Kumbakonam, Tamilnadu 612002, India

² Research for Solar Energy, Department of Physics, Koneru Lakshmaiah Education Foundation, Guntur, Andhra Pradesh 522502, India

³Department of Physics, Arizona State University, 85287 Phoenix, USA

⁴Department of Physics, Peri Institute of Technology, 600048 Chennai, India

⁵Research Centre Physics, Dhanalakshmi College of Engineering, Chennai 601301, India

1 Introduction

The nonlinear optics (NLO) is the phenomena that the characteristics of highly coherent light are modified by the interaction with nonlinear crystals. Modern technical fields like optoelectronics and photonics depend on the NLO crystals as they are the key functional materials in many fields [1]. The large optical nonlinearity is one of the unique and important properties of the grown crystals, because of this property it is being used as the low profile cut off frequency. This unique property of the NLO crystals is used in the photosensitive gadgets. Organic crystals are bonded by feeble van der Waals forces and hydrogen bonds subsequently have a severe level of delocalization. Organic materials are deprived of mechanical and thermal solubility. To overcome these complications, a research is made to combine inorganic and organic materials that leads to a new class of materials called as semi organic materials. Semi organic materials have advanced mechanical and chemical stability [2]. Amino acids are the crucial part of nonlinear optical crystal development. The characteristic feature of amino acids is the presence of NLO property. They have NH₂ (donor), COOH (acceptor) and nearly all the amino acids exist as zwitterions [3]. Some regular amino acids are aspartic, glutamic, arginine, lysine, and L-alanine [4]. The γ glycine [5] is clearly exhibiting NLO efficiency. Unlike other amino acids, there is no asymmetric carbon, and it is optically inactive. The dopants added to amino acids [6-8] enhance their optical, mechanical, thermal, ferroelectric, and nonlinear optical properties and it opens the way to more applications. Semi organic single crystals of L-histidine tetrafluoroborate and L-arginine diphosphate are well known [9, 10] for their high mechanical and chemical solidness.

Semi organic single crystals of L-Lysine monohydrochloride doped with rubidium chloride were studied and analyzed earlier [11, 12]. They were characterized by good optical, mechanical and antifungal properties. When compared with the pure crystal, the doped one has good optical transparency and bandgap increased from 5.30 to 5.94 eV. The pure L-lysine and Co-doped GBC/C₆H₁₄N₂O₂ are identified as good NLO single crystals [13, 14] with remarkable optical properties and the observed UV cutoff wavelength are 229 nm and 247 nm, respectively. The SHG signals of these novel crystals are

found to be 1.27, 1.79 times that of KDP and they are stable up to 171.6 and 177.2 °C, respectively, which prove their thermal stability.

This paper delineates the synthesis, crystal growth and characterization studies of LLHC single crystal. The title compound is subjected to X-ray diffraction, NLO studies, thermal analysis, Micro hardness, NMR spectroscopy, and Antimicrobial activity and the results are discussed briefly.

2 Experimental procedure

2.1 Solubility test

The slow evaporation technique based on the solubility of the substance and it depends on the choice of the solvent, i.e., water, ethanol, methanol and combined solvents. To synthesize the LLHC crystal, the solvents used are deionized water or deionized water + ethanol at the ratio of 1:1. The solubility curves of LLHC with different concentrations at temperatures 30, 35, 45 and 55 °C for the two different solvents are shown in Fig. 1. As evidenced from Fig. 1, the temperature analysis of solubility results is consistent with an accuracy of \pm 0.01 K. The slow evaporation growth of the LLHC crystals was achieved with the utilization of deionized water, homogenized solvents and with the account of the solubility curves.

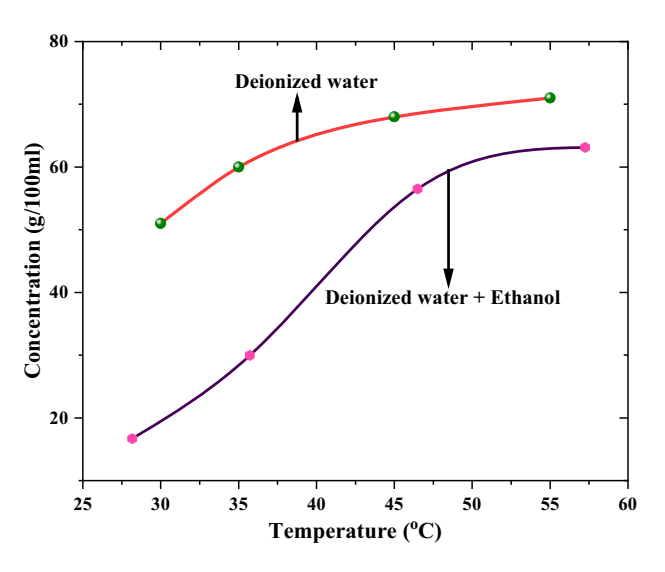


Fig. 1 Solubility curve of LLHC



2.2 Crystal growth

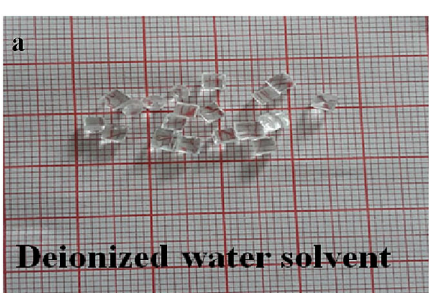
Single crystal of LLHC was grown by slow evaporation growth technique. The saturated solution of LLHC was prepared using 100 ml of deionized water at 35 °C. The prepared solution was filtered using a micro filter paper of 10 μ m thickness. The beaker containing the solution was closed with a perforated skinny polyethylene sheet and kept at a constant temperature bath of 35 °C. The temperature is slowly reduced at a rate of 0.1 to 0.3 K/day. After attaining the super saturation condition, tiny crystals were formed. Appropriate seed crystals were accumulated at the room temperature. Good quality colorless single crystals were obtained after 34 days with the dimensions of 19 \times 13 \times 4mm³. The photographs of the grown LLHC crystal are shown in Fig. 2.

3 Results and discussion

3.1 Single crystal and powder X-ray diffraction analysis

To know the cell parameters, the grown LLHC crystal was subjected to single crystal X-Ray diffraction study using an ENRAF NONIUS CAD4 XRD device. The obtained cell parameters are a = 4.7531 Å, b = 12.2467 Å, c = 6.6134 Å, $\alpha = 90.12^{\circ}$, $\beta = 96.54^{\circ}$,

Fig. 2 Growth process of LLHC a deionized water as solvent, b deionized water + ethanol as solvent, c Grown single crystal of LLHC







 γ = 91.12°, and V = 614.376 Å3, which are in good agreement with the literature survey. Cell parameters should be supplied by possible error ranges. Please add the citations for related papers from "the literature survey". The powder X-ray diffraction (PXRD) patterns were collected using a Rich Seifert X-ray diffractometer with CuKα radiation (λ = 1.6329 Å) and with the scan rate of 0.3°/sec. To determine the unit cell parameters, the analysis was carried out from 20° to 80° 2θ with the use of Proszki software [15]. If the structure of LLHC crystal is known, it is topical, for comparison, to show the theoretical XRD pattern in Fig. 3. The sample is pure crystalline in nature which is established from the sharp peaks obtained at the diffraction 2θ angles.

3.2 FT-IR and Raman spectral analysis

Fourier Transform Infrared Spectroscopy is used to study the molecular structure and identification of expected functional groups. The grown crystal was subjected to FT-IR analysis using a BRUKER 66 V FT-IR spectrometer in the range of 400–4000/cm. The FT-IR spectrum is shown in Fig. 4. FT-RAMAN spectroscopy is a chemical analysis technique used to give the detailed chemical structure and vibrational frequencies. The FT-RAMAN spectrum of the grown crystal was obtained using a Bruker FRA 106 FT RAMAN Spectrometer in the range of 50–3500/

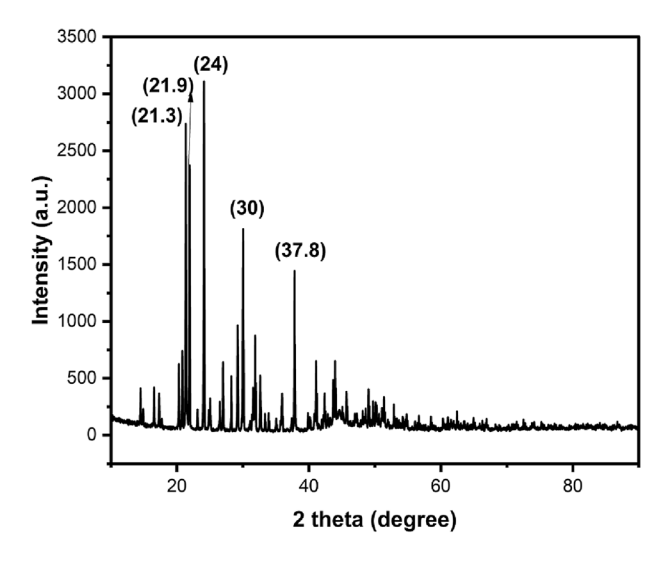


Fig. 3 Powder XRD pattern analysis of LLHC

cm and the obtained data are shown in Fig. 5. The torsional NH₃ vibrations are found in both Raman and FT-IR spectrum at the wavenumber 621/cm [16]. The vibrations at 811/cm in the Raman spectrum are attributed to the CO2 stretching mode. C–O–H state of the composite is shown at 811/cm in the IR spectrum and it is at 872/cm in the Raman spectrum. The intense band in Raman spectrum at 931/cm shows the C–C–N stretching and the same is at 1001/cm in the IR spectrum. It identifies that these functional groups belong to the amino acid L-Lysine [17]. The C–C stretching vibrations are observed at 1114 and 1248/cm. The nitrogen of the amino group has been identified from the bands appeared at the wave

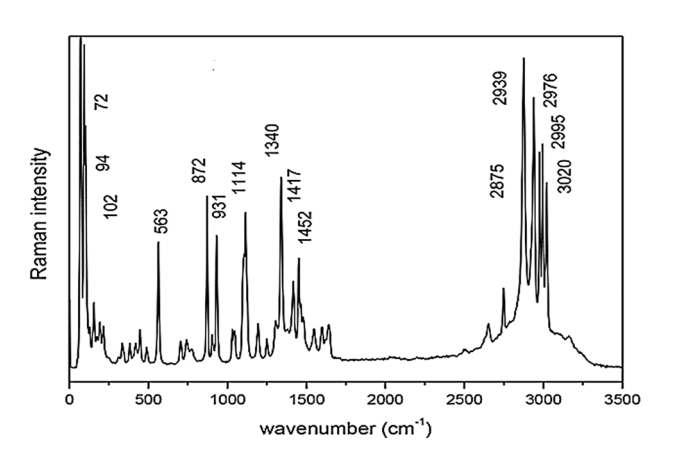
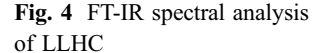
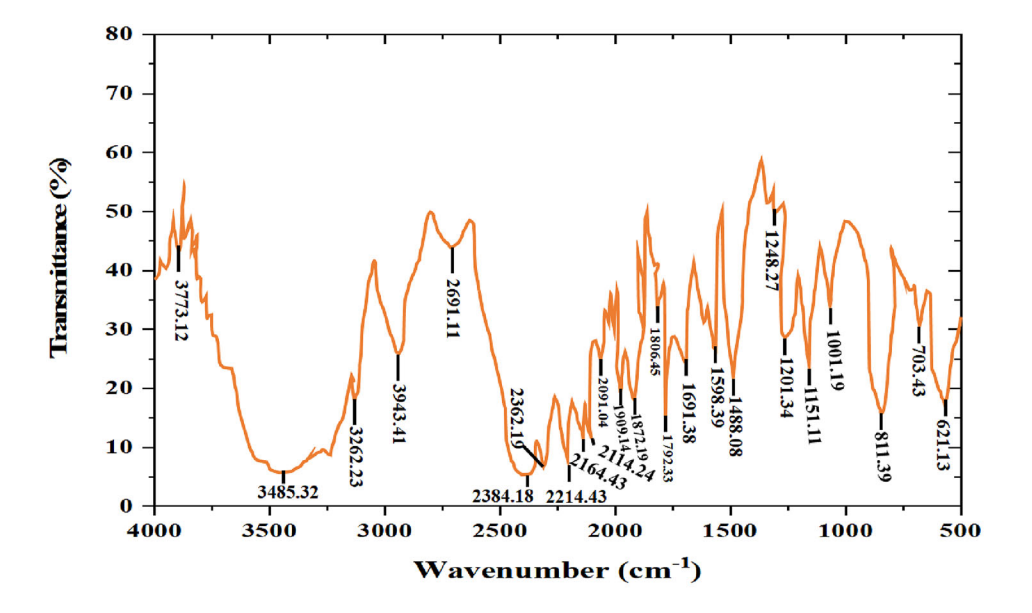


Fig. 5 FT-RAMAN spectrum of LLHC

number 1806/cm, Diem et al., [18] identified that the band appeared at 1872/cm within the IR-spectra range is due to the C-C-N asymmetric stretching vibration. The bands of C-H group were identified at 1909, 2114 and 2164/cm in the IR range and the band of vibrations of the CH₃ group is at 1417/cm. The vibration band of NH₃ group in LLHC crystal are at 1488 and 1452/cm in the IR and Raman spectra, respectively. The functional group assessment of LLHC crystal through FT-IR and FT-RAMAN has been distinguished and compared. These studies confirmed the presence of LLHC functional groups.







3.3 NMR spectroscopy studies

The grown single crystal of LLHC was subjected to NMR spectroscopy analysis using a JOEL GSX 400 NB FT NMR spectrometer in the range of 500 MHz, ¹H NMR and the NMR spectrum is shown in Fig. 6. According to the 1 H NMR spectra obtained from the reaction mixture of LLHC, after a few minutes three singulets of the mono-, di-, and tri- N-CH₂OH protons can be observed at 4.1, 4.2 and 4.35 ppm. The signal at 3.38 ppm affirms the carbon conveying the terminal NH₂ group. The signals at 3.29 and 2.24 ppm show that it is for the methylene carbon. The new crystals developed from the carbon intuitive of the NMR valuable demonstrate the use of ¹³C NMR and it is shown in Fig. 7. The carboxylic group carbon signal at 158.6 ppm, proves that the substance consists of six kinds of carbons and this affirms that the material is a kind of virtue materials [19].

3.4 Thermal analysis

The thermal behavior of the LLHC was studied by Thermo gravimetric analysis (TG) and differential thermal analysis (DTA). NETSZCH STA 409 C is the apparatus used for this analysis. A thermal analyzer was employed at a heating rate of 12 K/min in nitrogen atmosphere. The DTA and TG thermal analysis were made in the temperature range of 40–800 °C. There is a 17.3% heat reduction at 100 °C and it is due to water loss. The recorded thermo grams are shown in Fig. 8. There is a significant weight loss of about 51.13% in between 250 and

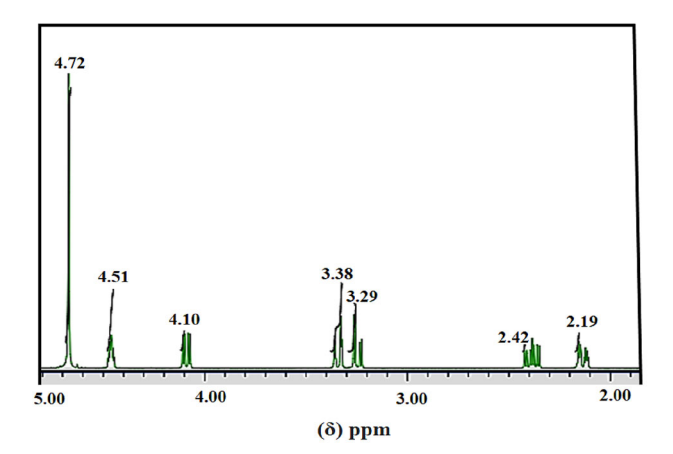


Fig. 6 LLHC crystal analysis of ¹H NMR spectra

360 °C. There is one more weight loss in the range of 430–540 °C and weight reduction of about 18.3% which corresponds to the significant deterioration. This effect was attributed to the loss of two water molecules from LLHC crystal structure. Endothermic changes of LLHC crystal were analyzed from the DTA curve and it describes that the crystal decays after the melting point. It is concluded that the crystal has a high melting point and exhibits high thermal stability.

3.5 Microhardness properties

Microhardness study was performed on the grown crystal using a Vicker's microhardness tester to evaluate the mechanical stability of the crystal [20]. By using an optical microscope Vicker's microhardness was carried out. This test was performed on the sample at various loads from 5 to 25 g. The chosen surface of the crystal was cleaned by a velvet cloth to get a smooth surface and then the loads were applied. The Vicker's microhardness value is calculated from the relation, $H_v=1.8627 P/d^2$ (kg/mm³), where H_v is the Vickers hardness number (VHN), P is the indentation load in kg and d is the diagonal length of the impression in mm. 1.8544 is a constant of a geometrical fraction for the diamond pyramid [21]. The dependence of hardness on load is presented in Fig. 9. This curve shows that the hardness increases gradually with the applied load increase and decreases after a particular point. The hardness number was found to increase with the load up to 50 g and after a load of 50 g, H_{v} suddenly decreases as cracks developed in the material. This may be due to the release of internal stresses generated locally by indentation.

3.6 UV-Vis spectrum analysis

The grown crystal is analyzed for its optical transparency using the UV–Vis spectrometer in the frequency range of 200-800nm and the spectrum is shown in Fig. 10 (i), (ii). The grown crystals were analyzed for its optical transparency with the use of a UV–Vis spectrometer in the wave number range of 200-800nm and the spectra are shown in Fig. 10. It is proven that the crystal grown from deionized water as the solvent is highly transparent and has good



Fig. 7 ¹³C NMR spectrum of LLHC

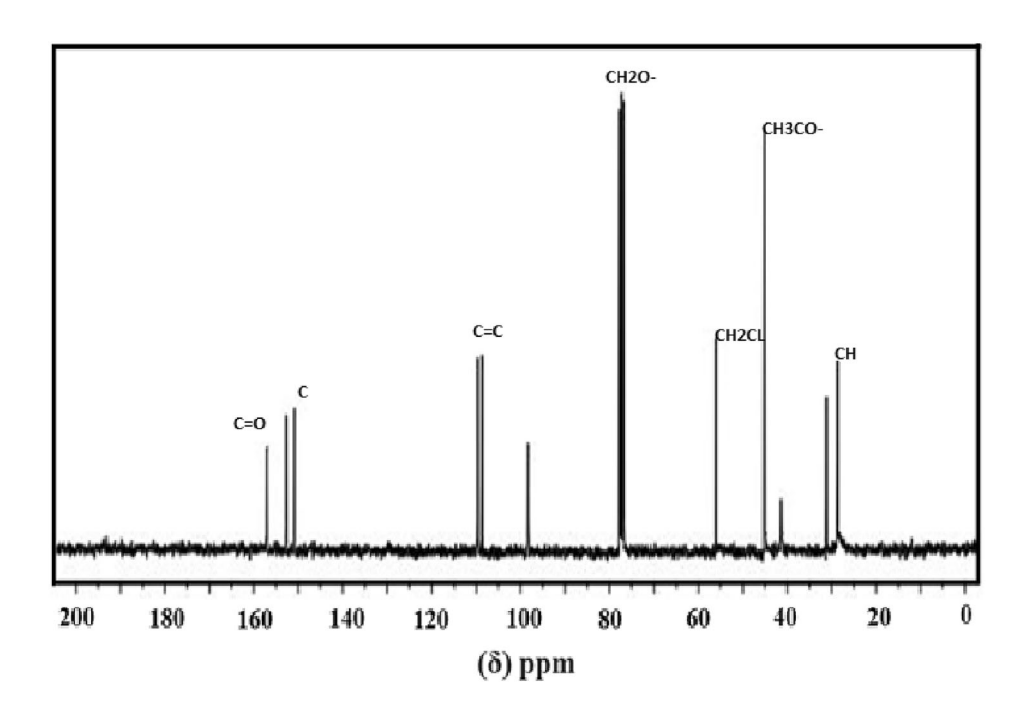
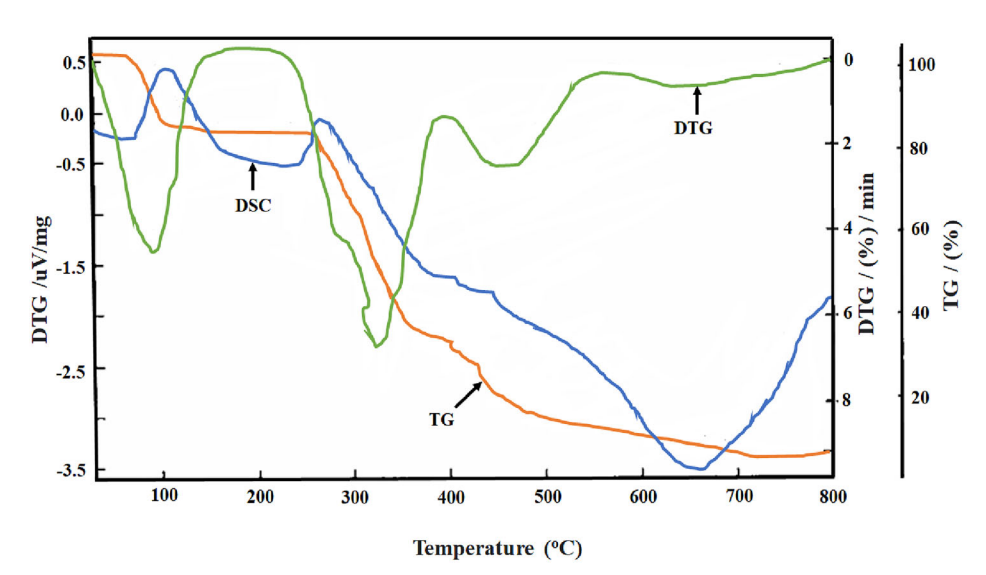


Fig. 8 Thermal analysis of LLHC



optical properties [22]. This new material is precious for NLO applications.

3.7 Nonlinear optical study

The SHG efficiency of LLHC powdered sample was determined using the Kurtz and perry technique. A Q-switched Nd: YAG laser operating at 1064 nm and energy 5.4 mJ/pulse was used for this study. The SHG signal generated from the tested sample was confirmed by the emission of green light at 532nm. The SHG signal of 60.6mV was obtained from the

sample and it is compared with the standard KDP crystal.

3.8 Antibacterial study

For biological assays, the grown sample was prepared in Dimethyl sulfoxide and final Dimethyl sulfoxide concentration did not exceed 0.1%. The antibacterial properties were tested towards standard pathogens specifically against Gram positive, Gram negative bacteria and against representative strains: *S.Aureus, E.coli.* The species are fastidious microorganism, which is absolutely safe for experiment



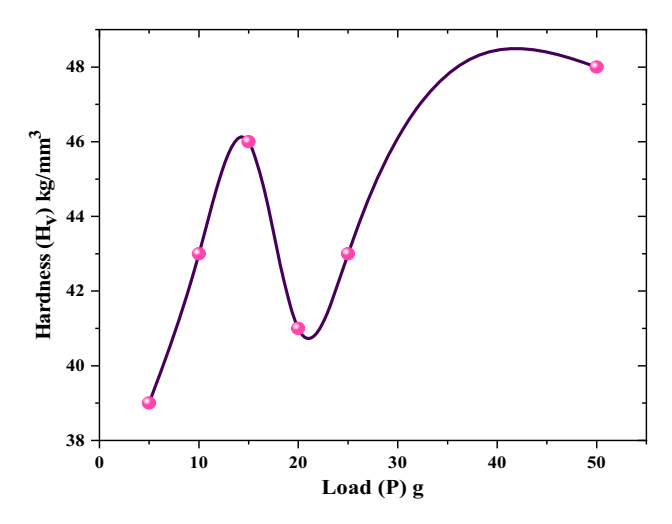


Fig. 9 Vicker's microhardness analysis - hardness vs. load

purpose. The in vitro antibacterial activity was found using minimum inhibitory concentration tests (MIC). The petriplates utilized for antibacterial activities were incubated at 37 °C for one day. After incubation, the resulting zones of inhibition around the disks were measured. Each assay was repeated twice and the most accurate readings were noted. When there is no growth of microorganisms was observed in the medium contains the lowest concentration of the tested sample, the tested material the MIC was concluded at this point of dilution [23]. In general, when tested with both Gram positive and Gram negative bacteria, all compound exhibited higher activity than the standard one.

Fig. 10 (i) and (ii) shows optical transmittance spectra of

LLHC crystal

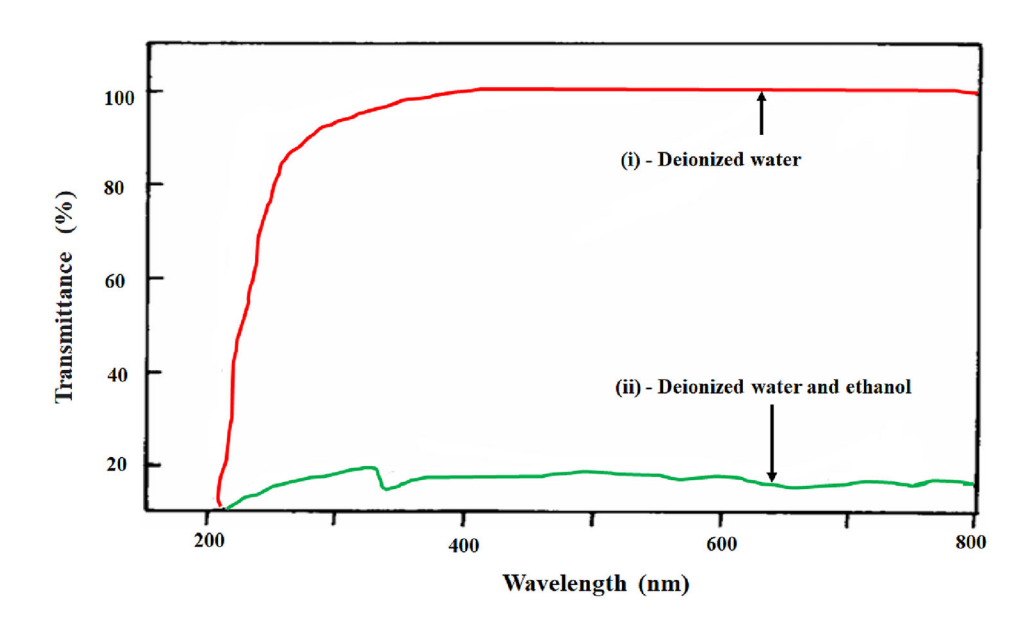


Table 1 Antibacterial activity of LLHC

LLHC (µl)	S.Aureus (mm)	E. coli (mm)
25	7	7
50	7.5	8
100	12	13

4 Conclusions

Semi-organic LLHC crystals were grown using the slow evaporation solution technique. Deionized water and (deionized water + ethanol) were used as solvents. The cell parameters and crystal system were identified from the Single crystal X-ray diffraction and the Powder X-ray diffraction confirms the crystalline nature of LLHC. Good transparency window was observed through UV-Vis analysis and FT-IR, FT-RAMAN, NMR spectroscopy were used to identify the functional groups and chemical structure of LLHC. The thermal and mechanical stabilities of LLHC were found through the TG/DTA and Vickers microhardness tests, respectively. Finally, nonlinear optical property of the grown crystal was confirmed using the Kurtz and Perry powder technique and the emission of green light was clearly observed (see Table 1).

References

- D.S. Chemla, J. Zyss (eds.), Nonlinear optical properties of organic molecule and crystalemclose, vol. 1 and 2 (Academic Press, New York, 1987)
- C. Pravallika et al., Crystal growth, spectroscopic and antimicrobial investigations on glycine-doped ZnSO 4–(NH 4) 2 SO 4 single crystal. J Mater Sci Mater Electron 32, 1–9 (2021)
- C. Razzetti, M. Ardoino, L. Zanotti, M. Zha, C. Paorici, Cryst. Res. Technol. 37, 456–465 (2002)
- A. Arputhalatha, Synthesis, growth, physio-chemical and Hirshfeld surface analysis of guanidinium l-glutamate single crystal. J. Mater. Sci. Mater. Electron. (2021). https://doi.org/ 10.1007/s10854-021-05884-9
- S. Shanmugan et al., Investigation on single crystal by tartaric acid-barium chloride: growth and characterization of novel NLO materials. Bull. Mater. Sci. 43(1), 1–8 (2020)
- S. Rajeswari et al., Growth and investigations of 3rd order NLO properties of novel semi organic tartaric acid lithium sulfate single crystal for photonics application. Opt. Quantum Electron. 52(8), 1–10 (2020)
- R. Mohan Kumar, R. Muralidharan, D. Rajan Babu, K.V. Rajendran, R. Jayavel, D. Jayaraman, P. Ramasamy, J. Cryst. Growth 229, 568–573 (2001)
- J.H. Joshi et al., Growth and characterization of pure and picric acid doped ADP single crystals. Chin. J. Phys. 64, 138–162 (2020)
- R. Vivekanandhan et al., Investigation on novel bulk size single crystal of glycine with metal ions grown by solution growth method for photonic applications. Mater. Lett. 257, 126674 (2019)
- M.D. Aggarwal, J. Choi, W.S. Wang, K. Bhat, R.B. Lal, A.D. Shields, B.G. Penn, D.O. Frazier, J. Cryst. Growth 204, 179–182 (1999)
- J.H. Joshi et al., Crystal growth, spectroscopic, second and third order nonlinear optical spectroscopic studies of L-phenylalanine doped ammonium dihydrogen phosphate single crystals. Arab. J. Chem. 13, 5018–5026 (2020)
- Geetha Palani et al., Growth and characterization of semi organic nonlinear optical l-valine ferric chloride single crystal by solution growth technique. Curr. Appl. Phys. 15(3), 201–207 (2015)

- Daixi Li, Xiaonan Lian, Yi. Xu, Qingli Dong, Baolin Liu, Dong-Qing. Wei, Baisong Guo, Chem. Phys. 538, 110889 (2020)
- P. Saminathan, M. SenthilKumar, S. Shanmugan, P. Selvaraju,
 B. Janarthanan, Kishor KumarSadasivuni, Mater. Today Proc. 30(1), 57–61 (2020)
- 15. E. Appleman, H.T. Evans Jr., D. Handwerker, *PROSZKI* (Jagiellonian University, Krakow, 1989)
- J.H. Joshi et al., Crystal growth, A.C. electrical and nonlinear optical studies of pure and DL-methonine doped ammonium dihydrogen phosphate single crystal. J. Mater. Sci. Mater. Elect. 29(7), 5837–5852 (2018)
- V. Revathi, K. Karthik, Physico-chemical properties and antibacterial activity of Hexakis (Thiocarbamide) Nickel (II) nitrate single crystal. Chem. Data Collect. 21, 100229 (2019)
- J.H. Joshi et al., Influence of L-serine on micro structural, spectroscopic, electrical and non-linear optical performance of ammonium dihydrogen phosphate single crystal. J. Mater. Sci. Mater. Electron. 30(15), 14243–14255 (2019)
- J.H. Joshi et al., Dielectric relaxation, protonic defect, conductivity mechanisms, complex impedance and modulus spectroscopic studies of pure and L-threonine-doped ammonium dihydrogen phosphate. Ionics 24(7), 1995–2016 (2018)
- V. Revathi, Growth, spectral, optical, thermal, electrical, mechanical and etching studies of organic single crystal: L-histidinium L-tartrate hemihydrates. J. Mater. Sci. Mater. Electron. 29, 17323–17332 (2018)
- J.H. Joshi et al., Raman, photoluminescence, and ac electrical studies of pure and 1-serine doped ammonium dihydrogen phosphate single crystals: an understanding of defect chemistry in hydrogen bonding. New J. Chem. 42, 17227–17249 (2018)
- 22. G. Palani et al., Growth, characterisation and antibacterial activity of LHCdBr single crystal. Mater. Res. Innov. **25**, 1–7 (2020)
- S. Sakthy Priya et al., Crystal growth and characterization of benzimidazolium salicylate single crystal for nonlinear optical studies and antibacterial activity. Phys. Chem. Solid State 21, 377–389 (2020)

Publisher's Note Springer Nature remains neutral with regard to jurisdictional claims in published maps and institutional affiliations.



Terms and Conditions

Springer Nature journal content, brought to you courtesy of Springer Nature Customer Service Center GmbH ("Springer Nature").

Springer Nature supports a reasonable amount of sharing of research papers by authors, subscribers and authorised users ("Users"), for small-scale personal, non-commercial use provided that all copyright, trade and service marks and other proprietary notices are maintained. By accessing, sharing, receiving or otherwise using the Springer Nature journal content you agree to these terms of use ("Terms"). For these purposes, Springer Nature considers academic use (by researchers and students) to be non-commercial.

These Terms are supplementary and will apply in addition to any applicable website terms and conditions, a relevant site licence or a personal subscription. These Terms will prevail over any conflict or ambiguity with regards to the relevant terms, a site licence or a personal subscription (to the extent of the conflict or ambiguity only). For Creative Commons-licensed articles, the terms of the Creative Commons license used will apply.

We collect and use personal data to provide access to the Springer Nature journal content. We may also use these personal data internally within ResearchGate and Springer Nature and as agreed share it, in an anonymised way, for purposes of tracking, analysis and reporting. We will not otherwise disclose your personal data outside the ResearchGate or the Springer Nature group of companies unless we have your permission as detailed in the Privacy Policy.

While Users may use the Springer Nature journal content for small scale, personal non-commercial use, it is important to note that Users may not:

- 1. use such content for the purpose of providing other users with access on a regular or large scale basis or as a means to circumvent access control:
- 2. use such content where to do so would be considered a criminal or statutory offence in any jurisdiction, or gives rise to civil liability, or is otherwise unlawful:
- 3. falsely or misleadingly imply or suggest endorsement, approval, sponsorship, or association unless explicitly agreed to by Springer Nature in writing:
- 4. use bots or other automated methods to access the content or redirect messages
- 5. override any security feature or exclusionary protocol; or
- 6. share the content in order to create substitute for Springer Nature products or services or a systematic database of Springer Nature journal content

In line with the restriction against commercial use, Springer Nature does not permit the creation of a product or service that creates revenue, royalties, rent or income from our content or its inclusion as part of a paid for service or for other commercial gain. Springer Nature journal content cannot be used for inter-library loans and librarians may not upload Springer Nature journal content on a large scale into their, or any other, institutional repository.

These terms of use are reviewed regularly and may be amended at any time. Springer Nature is not obligated to publish any information or content on this website and may remove it or features or functionality at our sole discretion, at any time with or without notice. Springer Nature may revoke this licence to you at any time and remove access to any copies of the Springer Nature journal content which have been saved.

To the fullest extent permitted by law, Springer Nature makes no warranties, representations or guarantees to Users, either express or implied with respect to the Springer nature journal content and all parties disclaim and waive any implied warranties or warranties imposed by law, including merchantability or fitness for any particular purpose.

Please note that these rights do not automatically extend to content, data or other material published by Springer Nature that may be licensed from third parties.

If you would like to use or distribute our Springer Nature journal content to a wider audience or on a regular basis or in any other manner not expressly permitted by these Terms, please contact Springer Nature at

 $\underline{onlineservice@springernature.com}$



Contents lists available at ScienceDirect

Materials Today: Proceedings

journal homepage: www.elsevier.com/locate/matpr



Growth and investigation on novel single crystal of β -cyclodextrin 2, 4-dinitrophenylhydrazine for optical sensors applications

S. Varadarajan ^{a,*}, P. Saminathan ^a, M. Senthil Kumar ^a, S. Shanmugan ^b, V. Chithambaram ^{c,*}, V. Gandhimathi ^c

ARTICLE INFO

Article history:
Received 30 January 2020
Received in revised form 17 March 2020
Accepted 7 April 2020
Available online 29 April 2020

Keywords: Crystal growth X-ray diffraction Optical properties

ABSTRACT

Nonlinear optical (NLO) 2, 4-Dinitrophenylhydrazine (DNPH) single crystal was grown by slow evaporation solution growth method at ambient temperature. The characterization of Powder X – Ray diffraction peaks was confirmed the new crystalline system. Fourier transform infrared spectroscopic analysis (FTIR) was used to the identification of various functional groups present in the grown crystal. The range of optical transmittance exhibited by the grown βCD -DNPH crystal was investigated by UV Visible – NIR spectral analysis. The lower cut off wavelength of the grown crystal is observed at 270 nm. The SEM figures are recorded in different magnification. It is clear that the surface of the grown crystal appears very smooth although it has pots and microcrystal on the surface. The grain boundaries are clearly seen which shows the perfect growth of the crystal. The weight percentage (wt %) of C, N and O as obtained from EDAX analysis is in concurrent with the theoretical values. The SHG efficiency of the grown crystal was determined.

© 2020 Elsevier Ltd. All rights reserved.

Selection and Peer-review under responsibility of the scientific committee of the International Conference on Advancement in Nanoelectronics and Communication Technologies

1. Introduction

Second order non-linear optical materials find different role of applications like optical communication, sensing, signal processing, data storages, optical logic gates, laser radiation protection and THz-wave generation [1–5]. In recent years the broad investigation is performed for the growth of nonlinear optical materials because it has wide applications in photonic and optoelectronic fields. Most of the organic materials have large nonlinear optical coefficient but poor mechanical and thermal properties. The growth of large size single crystal is very difficult for the device fabrication. Inorganic materials have excellent mechanical and thermal properties but less optical nonlinearity due to the lack of π -electron delocalization [6–10]. In the view of these problems,

E-mail addresses: varadanphy@gmail.com, vagish2009@gmail.com (S. Varadarajan), msenthilprof@gmail.com (M. Senthil Kumar), s.shanmugam1982@gmail.com (S. Shanmugan), chithambaramv@gmail.com (V. Chithambaram).

interest has been made to grow the semi organic crystals because it has less delinquency, high damage threshold, exceptional mechanical and nonlinear optical property, low angular sensitivity, wide optical transparency range which make them comfortable for device fabrications [11–19]. Therefore, it is essential to grow novel semi organic crystals having consistent phantasy of both organic and inorganic materials.

In the present work the title compound was successfully synthesized by combining β -Cyclodextrin and 2, 4-dinitrophenylhydrazine in equimolar ratio. The single crystals have been grown by solution growth slow evaporation technique using water as the solvent. A transparent good quality crystal was obtained within 4 weeks as shown in Fig. 1. The photograph was taken by using high megapixel camera. To have a full understanding about the structure and its properties for the grown crystals Powder XRD, FTIR, Nonlinear Optical Property (Second Harmonic Generation) measurements were also been carried out.

^a Dept of Physics, Govt. Arts College, Kumbakonam 612002, Tamilnadu, India

^b R&D for Solar Energy, Department of Physics, Koneru Lakshmaiah Education Foundation, Guntur 522502, Andhra Pradesh, India

^c Research Center Physics, Dhanalakshmi College of Engineering, Chennai 601301, India

^{*} Corresponding author.

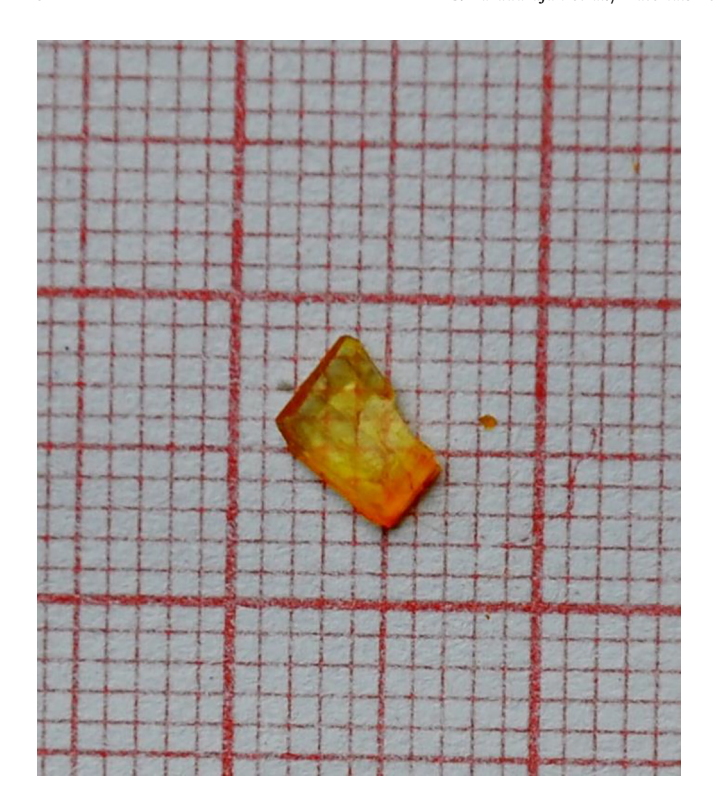


Fig. 1. Photograph of crystal formed by inclusion complex of DNPH:β-CD.

2. Results and Discussion:

2.1. Single crystal x-ray diffraction

The good quality DNPH: β -CD grown crystal was subjected to single crystal X-ray diffraction analysis to collect the data using BRUKER KAPPA APEX II CCD. The grown crystals have their triclinic non-centrosymmetric space group P2. The cell parameters were

measured to be a = 14.03 Å, b = 13.39 Å, C = 14.49 Å, α = 103°. β = 113°, γ = 98° and V = 3651 ų.

2.2. Powder X-Ray diffraction analysis

Powder X-Ray diffraction study was used for the identification of crystallinity of the grown crystal. The $K\alpha$ radiations from a copper target were used. The sample was scanned in the range between 10 and 100°C. Fig. 2(a), (b) and (c) represents the indexed powder diffractogram for the grown crystal of DNPH, β -CD and DNPH: β -CD. The sharp intensity peaks found in spectra shows good crystalline nature and purity of the grown crystal.

2.3. FTIR analysis

The infrared (FTIR) spectra of wave number from 4000 to $400~cm^{-1}$ of DNPH, β -CD and the solid inclusion complex of DNPH with β -CD are registered by FTIR spectrometer and the complete band assignments can be found in Fig. 3. We can see that there are apparent differences between the FTIR spectra of β -CD (Fig. 3a), DNPH (Fig. 3b) and DNPH: β -CD (Fig. 3c) solid crystal which infers the formation of DNPH: β -CD complex.

The infrared (FTIR) spectra of wave number from 4000 to 400 cm $^{-1}$ of DNPH. β -CD and the crystal of DNPH with β -CD are registered by FTIR spectrometer and the complete band assignments can be found in Fig. 3. We can see that there are apparent differences between the FTIR spectra of β-CD (Fig. 3a), DNPH (Fig. 3b) and DNPH: β-CD (Fig. 3c) solid crystal. The IR spectrum of DNPH (Fig. 3b) exhibits a strong peak at 3092 cm⁻¹ for stretching vibration of C-H from aromatic ring. IR peak at 1135 cm⁻¹is noted for the bending vibration of C-H from aromatic ring. 1637 and 1496 were noted for stretching vibration of C=C in benzene ring. However, in the IR spectrum of DNPH:β-CD crystal (Fig. 3c), absorption band due to the stretching (at 2926 cm⁻¹) and bending (at 1411 cm⁻¹) vibrations are shifted. The stretching vibration of C=C (at 1643 and 1411 cm⁻¹) also shifted. In the IR spectrum of DNPH the intensity of N-H stretching is very high (3326 cm⁻¹) and there is slightly increased in the IR spectrum

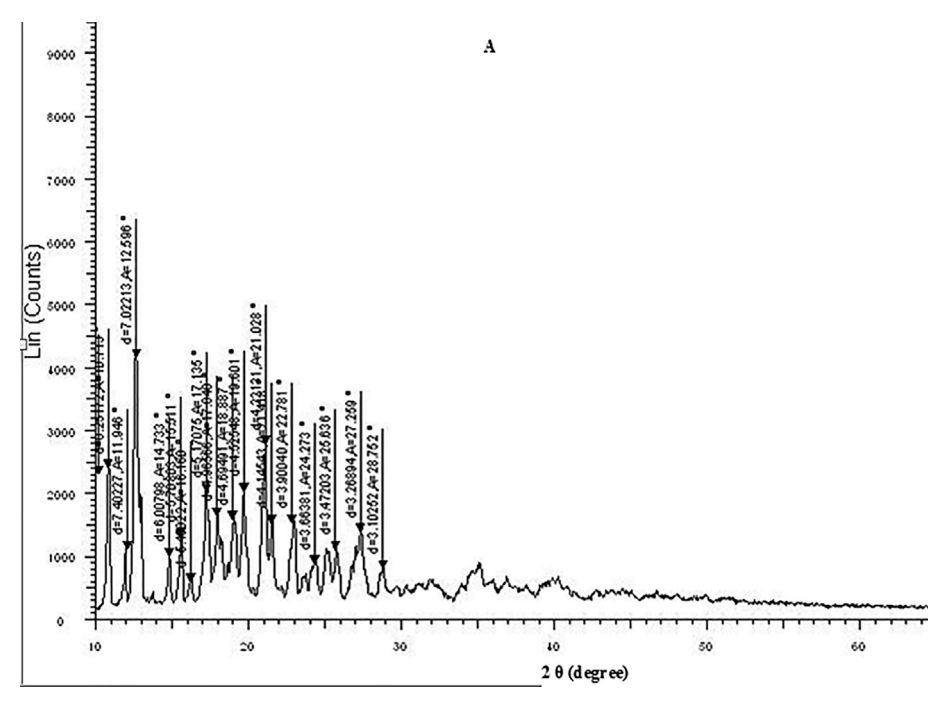


Fig. 2. The Powder XRD pattern of β-CD, DNPH and grown crystal by DNPH:β-CD.

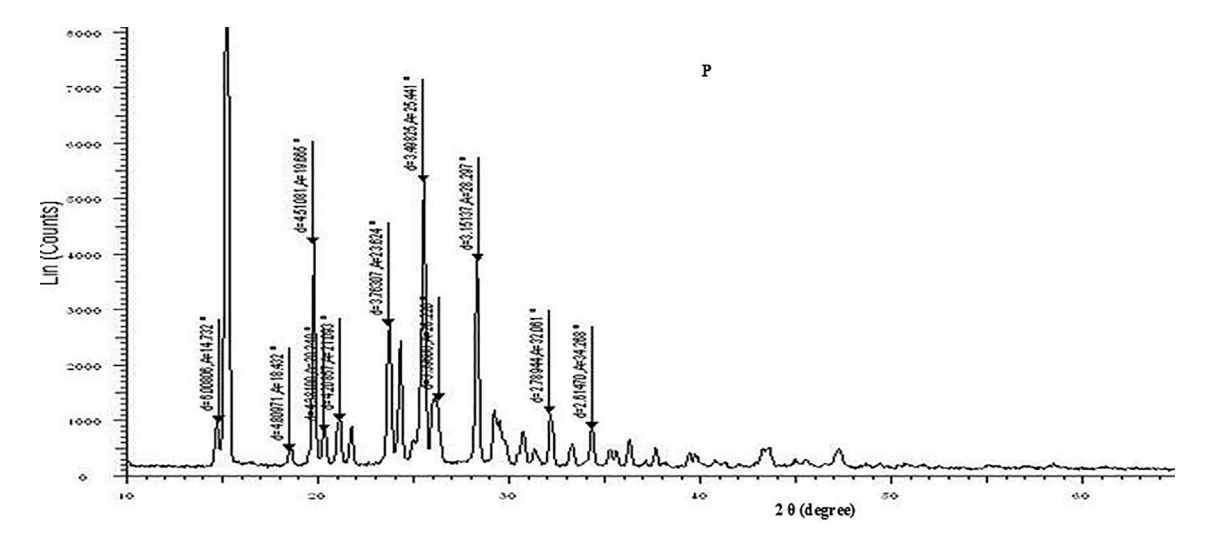


Fig. 2 (continued)

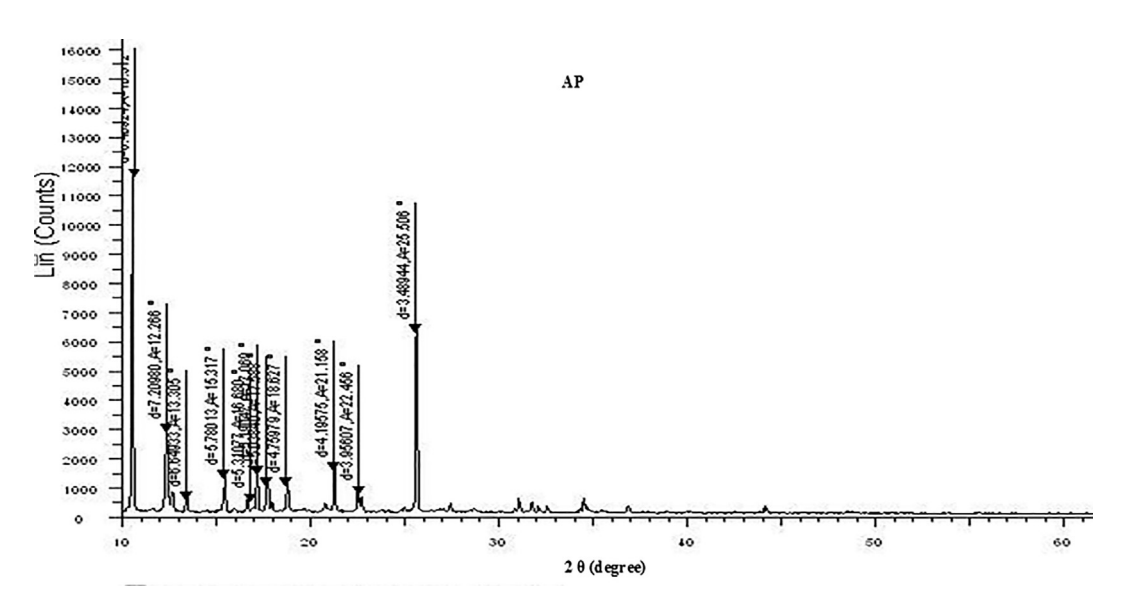


Fig. 2 (continued)

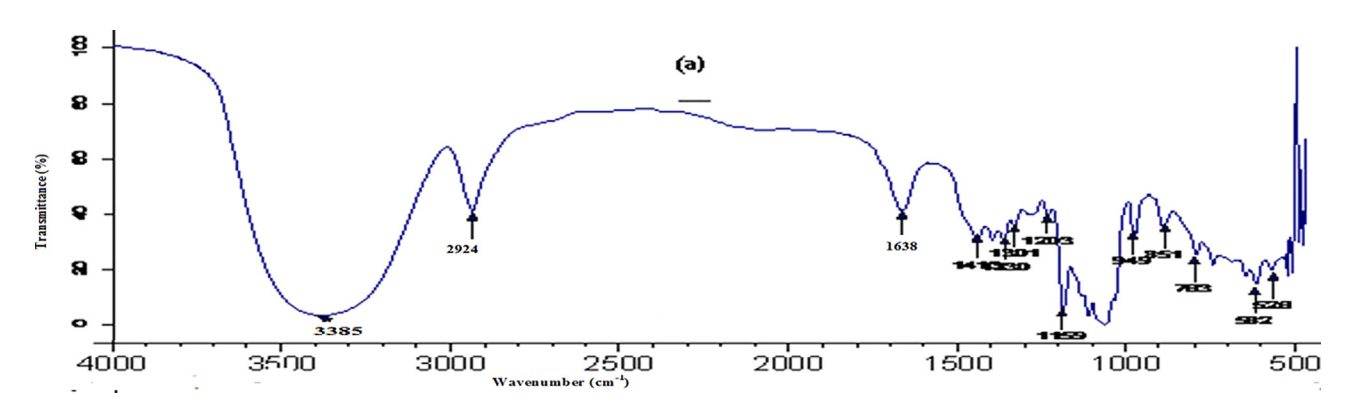


Fig. 3. FTIR Spectrum of (a) β -CD, (b) DNPH, (c) as grown crystal of DNPH: β -CD.

of DNPH: β -CD complex (3302 cm $^{-1}$). IR peak at 1219 cm $^{-1}$ is noted for the symmetric strectching vibration of N-O in DNPH and there is increased in IR spectrum of DNPH: β -CD complex (1151 cm $^{-1}$).

2.4. Scanning electron Microscope studies

The Scanning electron microscopy (SEM) image of the grown crystal was recorded using FEI Quanta FEG 200 - High resolu-

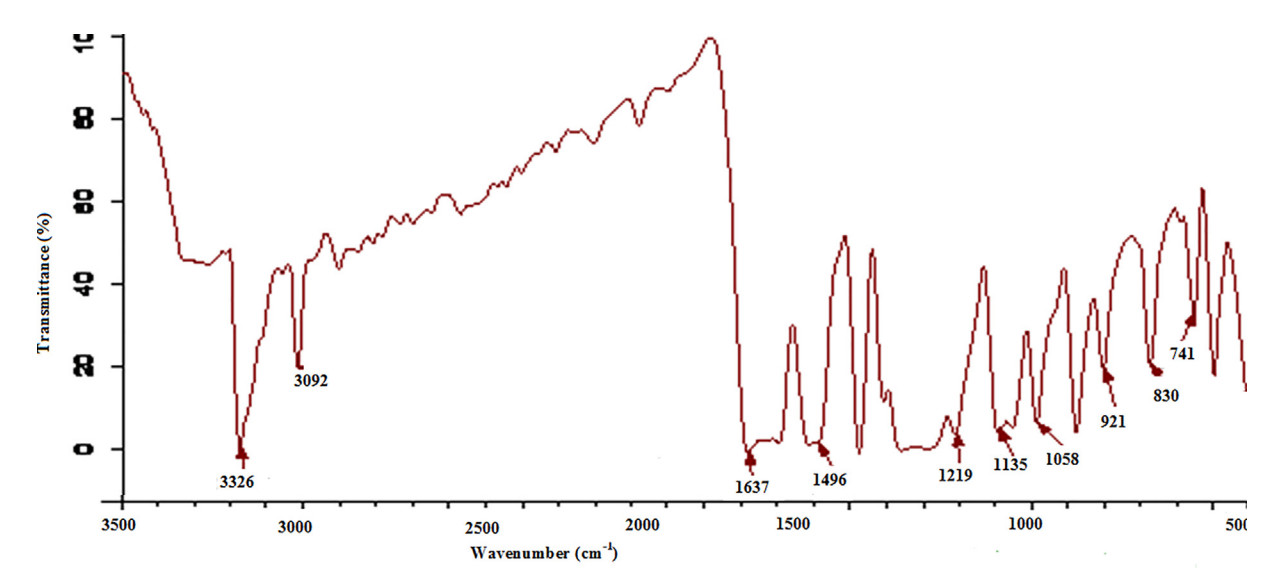
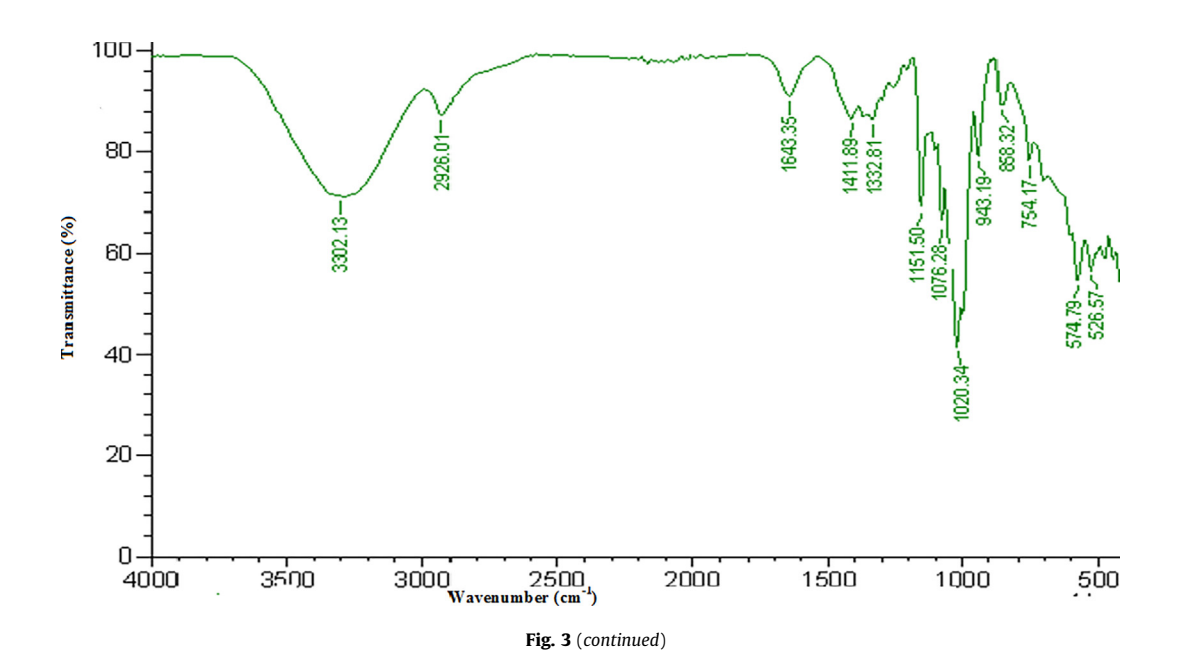


Fig. 3 (continued)



tion Scanning Electron Microscope to study the surface morphology of DNPH: $\beta\text{-}CD$ crystal. A two dimensional image was generated over a selected area of the sample. Since DNPH: $\beta\text{-}CD$ is a single crystal, which is poor conducing in nature so the sample was subjected to gold/carbon coating. THE SEM figures are recorded in different magnification. From the Fig. 4, it is clear that the surface of the grown crystal appears very smooth though it has pots and microcrystal on the surface. The grain boundaries are clearly seen which shows the perfect growth of the crystal.

Energy dispersive X-ray analysis (EDAX) is a micro-analytical technique, used to obtain information about the chemical composition of the grown crystal. In this work, the grown crystal was subjected to EDAX analysis using the instrument FEI QUANTA 200F energy dispersive X-ray micro analyzer. The EDAX spectrum of the crystal is shown in Fig. 5. The weight percentage (wt %) of C, N and O as obtained from EDAX analysis is in concurrent with the theoretical values.

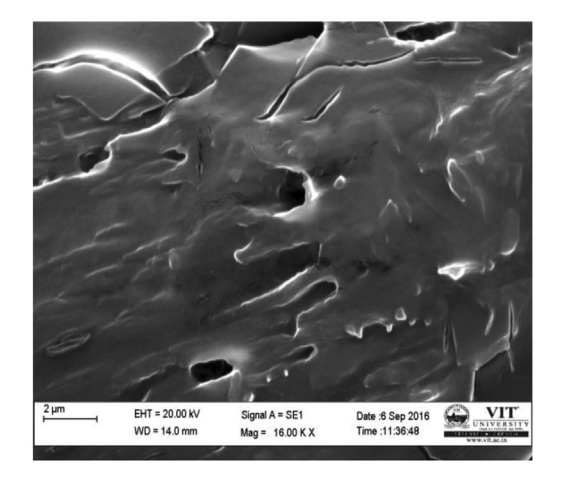
2.5. Nonlinear optical studies

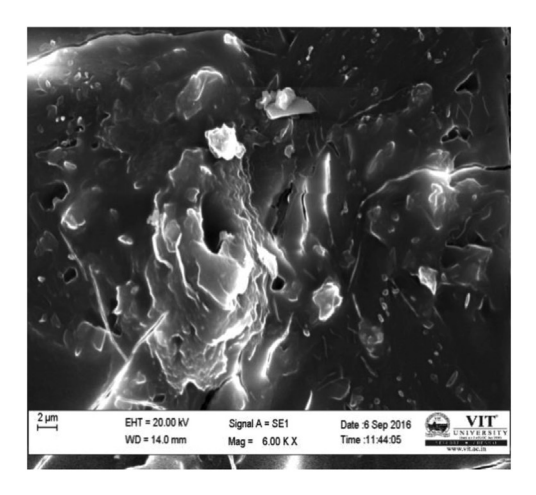
'The second harmonic generation efficiency measurement was carried out to the grown crystal using the Kurtz–Perry powder technique. The crystal was well grinded into a homogenous powder and densely packed between two transparent glass plates. The powder sample with average particle size $100{\text -}115\mu$ was illuminated using Q-switched Nd: YAG laser emitting a fundamental wavelength of 1064 nm with the pulse width of 8 ns. The value of SHG for the grown crystal is found to be 42.32 mV as in comparison with that of pure KDP crystal's value of 26.4 mV which asserts that the grown crystal has the efficiency of 0.62 times greater than that of KDP assuring itself to be a potential candidate for photonic applications.

3. Conclusion

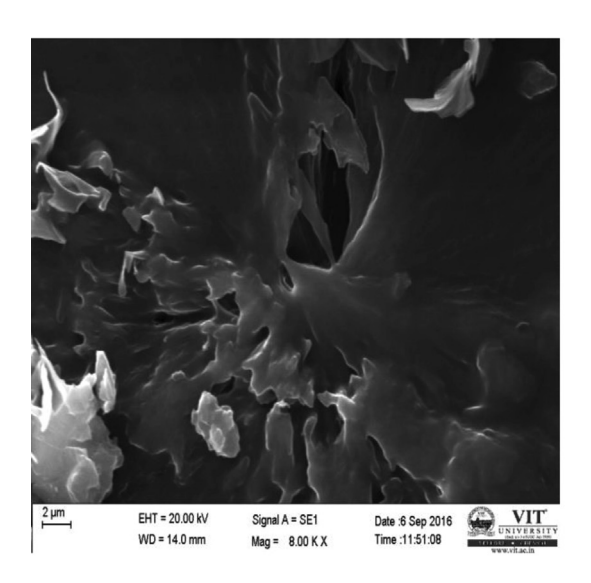
Nonlinear optical (NLO) 2, 4-Dinitrophenylhydrazine (DNPH) single crystal was grown by slow evaporation solution growth

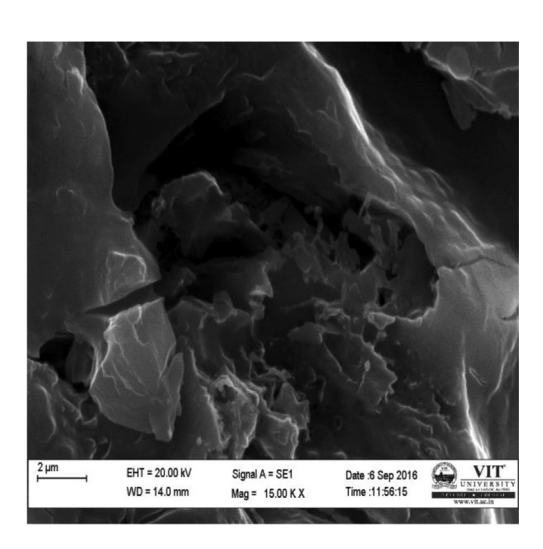
4a 4b





4c 4d





4e

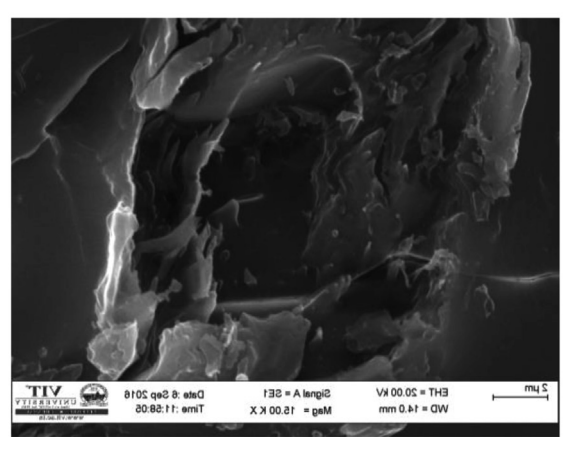
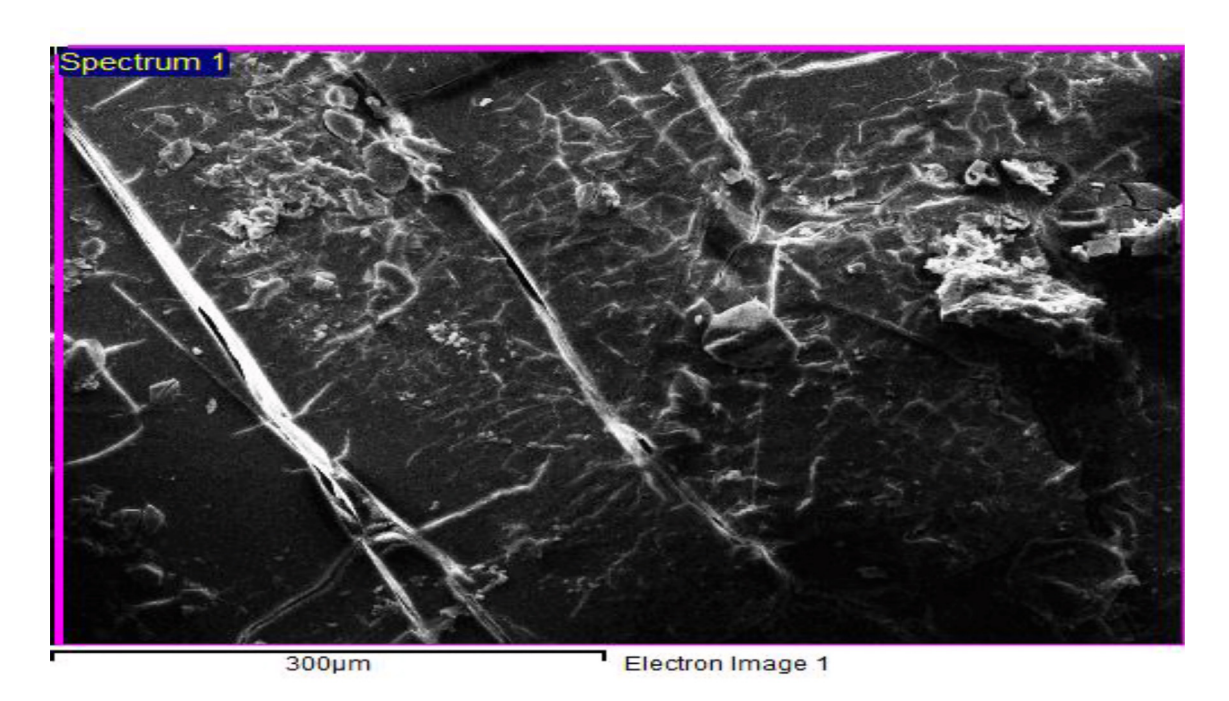


Fig. 4. SEM images of grown crystal of DNPH: β -CD.

method at ambient temperature. The characterization of Powder X – Ray diffraction peaks was confirmed the new crystalline system. Fourier transform infrared spectroscopic analysis (FTIR)

was used to the identification of various functional groups present in the grown crystal. The range of optical transmittance exhibited by the grown β CD-DNPH crystal was investigated by UV Visible –



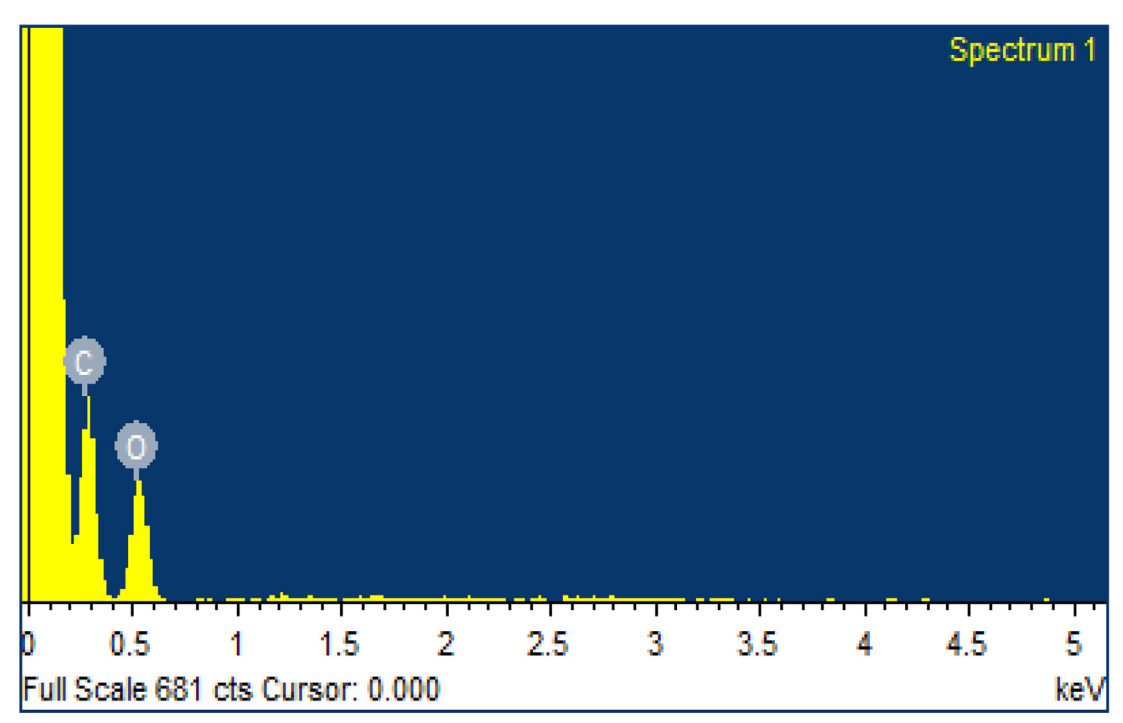


Fig. 5. EDAX spectrum of inclusion complex crystal of DNPH:β-CD.

NIR spectral analysis. The lower cut off wavelength of the grown crystal is observed at 270 nm. The SEM figures are recorded in different magnification. It is clear that the surface of the grown crystal appears very smooth although it has pots and microcrystal on the surface. The grain boundaries are clearly seen which shows the perfect growth of the crystal. The weight percentage (wt %) of C, N and O as obtained from EDAX analysis is in concurrent with the theoretical values. The SHG efficiency of the grown crystal was determined. The grown crystal has the SHG efficiency was 0.62 times greater than that of KDP assuring itself to be a potential candidate for photonic applications.

CRediT authorship contribution statement

S. Varadharajan: Methodology. P. Saminathan: Data curation. M. Senthil Kumar: Investigation. S. Shanmugan: . V. Chithambaram: Supervision. V. Gandhimathi: Investigation.

Declaration of Competing Interest

The authors declare that they have no known competing financial interests or personal relationships that could have appeared to influence the work reported in this paper.

References

- [1] C. Zhang, Z. Li, H. Cong, J. Wang, H. Zhang, R.I. Boughton, J. Alloy. Compd. 507 (2010) 335–340.
- [2] S. Arjunan, A. Bhaskaran, R. Mohan Kumar, R. Mohan, R. Jayavel, J. Alloy.
- [2] 3. Algunia, A. Bhasakani, R. Mohair Ruhiar, R. Mohair, R. Jayaver, J. Alloy. Compd. 506 (2010) 784–787.
 [3] R. Uthrakumar, C. Vesta, G. Bhagavannarayana, R. Robert, S. Jerome Das, J. Alloy. Compd. 509 (2011) 2343–2347.
- [4] V. Chithambaram, S. Krishnan, Opt. Laser Tech. 55 (2014) 18–20. [5] P.V. Dhanaraj, N.P. Rajesh, G. Bhagavannarayana, Phys. B Conden. Matter. 405 (2010) 3441-3445.
- [6] B. Mohd Shakir, K.K. Riscob, V. Ganesh Maurya, M.A. Wahab, G. Bhagavannarayana, J. Cryst. Growth 312 (2010) 3171–3177.
 [7] D. Sonal, S. Gupta Ranjith, A. Pardhan, D. Maeano, Noureddine Melikechi, C.F.
- Desai, J. Appl. Phys. 91 (5) (2012) 3125–3128.
- [8] M.H. Jiang, Q. Fang, Adv. Mater. 11 (1999) 1147–1151.
- [9] S.A. Oliver, App. Phys. Lett. 76 (2000) 3612.

- [10] J. Ramajothi, S. Dhanuskodi, K. Nagarajan, Cryst. Res. Technol. 39 (2004) 414-
- [11] S. Ariponnammal, S. Radhika, R. Selva, N. Victor Jeya, Cryst. Res. Technol. 40 (2005) 786-788.
- [12] J.M. Linet, S. Dinakaran, S.J. Das, J. Alloy. Comp., in press.
- [13] J. Dennis, H.K. Henisch, J. Electrochem. Soc. U.S.A 114 (1967) 263.
 [14] V. Chithambaram, S. Jerome Das, R. Arivudai Nambi, K. Srinivasan, S. Krishnan, Phys. B 405 (2010) 2605-2609.
- [15] P. Jayaprakash, M. Peer Mohamed, P. Krishnan, M. Nageshwari, G. Mani, M. Lydia Caroline, Phys. B 503 (2016) 25-31.
- [16] R. Vivekanandhan, K. Raju, V. Ravisankar, V. Chithambaram, J. Pure Appl. Mathemat. 115 (2017) 281–285.
- [17] S.K. Kurtz, T.T. Perry, J. Appl. Phys. 39 (1968) 3798.
- [18] V. Chithambaram S. Jerome Das S. Krishnan J. Synthes. Alloy. Comp. 509 2011 4543 4546
- [19] N. Saravanan, V. Chithambaram, V. Ravisankar, J. Mater. Sci. 29 (2018) 5009-5013.